INFORMATION TO USERS

This manuscript has been reproduced from the microfilm master. UMI films the text directly from the original or copy submitted. Thus, some thesis and dissertation copies are in typewriter face, while others may be from any type of computer printer.

The quality of this reproduction is dependent upon the quality of the copy submitted. Broken or indistinct print, colored or poor quality illustrations and photographs, print bleedthrough, substandard margins, and improper alignment can adversely affect reproduction.

In the unlikely event that the author did not send UMI a complete manuscript and there are missing pages, these will be noted. Also, if unauthorized copyright material had to be removed, a note will indicate the deletion.

Oversize materials (e.g., maps, drawings, charts) are reproduced by sectioning the original, beginning at the upper left-hand corner and continuing from left to right in equal sections with small overlaps.

ProQuest Information and Learning
300 North Zeeb Road, Ann Arbor, MI 48106-1346 USA
800-521-0600

The Design and Synthesis of Platinum-Based DNA Intercalators

By

Michel Paradis
Department of Chemistry
McGill University, Montréal

A thesis submitted to the Faculty of Graduate Studies and Research of McGill University
in partial fulfillment of the degree of Master of Science

Submitted October, 2000

National Library of Canada
Acquisitions and Bibliographic Services
395 Wellington Street
Ottawa ON K1A 0N4
Canada

Bibliothèque nationale du Canada
Acquisitions et services bibliographiques
395, rue Wellington
Ottawa ON K1A 0N4
Canada

Your file Votre référence

Our file Notre référence

0-612-70482-3

Canada

Abstract

Over the past years, considerable attention has focused on the synthesis of small complexes that can bind and react at specific DNA sequences. This understanding of how to target DNA sites with specificity becomes important for nucleotide probing and novel chemotherapeutics.

Inert and stable transition-metal complexes are already being used for this purpose. Square planar platinum (II) complexes containing an aromatic heterocyclic ligand can insert and stack between the double helix base pairs. Two known ligands, DPPZ and phi, do intercalate DNA when chelating ruthenium, rhodium, or osmium.

Here are presented the syntheses of $[Pt(NH_3)_2DPPZ](CF_3SO_3)_2$, $[Pt(en)DPPZ](CF_3SO_3)_2$, $[Pt(phen)DPPZ](CF_3SO_3)_2$, $[Pt(Me_2bpy)DPPZ](CF_3SO_3)_2$, and $[Pt(phendione)DPPZ](CF_3SO_3)_2$, and the attempted syntheses of $[Pt(en)phi](PF_6)_2$ and $[Pt(phen)phi](PF_6)_2$. The binding constants of $[Pt(NH_3)_2DPPZ](CF_3SO_3)_2$ and $[Pt(en)DPPZ](CF_3SO_3)_2$ to calf thymus DNA have been determined. The knowledge coming from the synthetic strategy to obtain monomers has allowed the synthesis of a platinum-based dimer, $[(DPPZ)Pt\{DPPZ(11\text{-}11')DPPZ\}Pt(DPPZ)](CF_3SO_3)_4$, having two intercalative DPPZ ends. We hope that this bis-intercalator will bring into close proximity two DNA strands.

Résumé

Au cours des dernières années, la synthèse de complexes pouvant interagir avec des séquences spécifiques d'ADN a soulevé un grand intérêt. Une meilleure compréhension du ciblage précis de sites d'ADN devient important pour le développement de sondes nucléotidiques et le traitement du cancer

Les complexes stables et inertes formés de métaux de transition sont déjà utilisés à cet effet. Les complexes de platine (II) carré plan formés d'un ligand aromatique hétérocyclique peuvent s'insérer et s'empiler entre les bases de l'ADN. Deux de ces ligands, DPPZ et phi, s'intercalent avec une grande affinité en présence d'ADN bicathénaire lorsque coordinés au ruthénium, au rhodium et à l'osmium.

Le projet présenté ici vise la synthèse de $[Pt(NH_3)_2DPPZ](CF_3SO_3)_2$, $[Pt(en)DPPZ](CF_3SO_3)_2$, $[Pt(phen)DPPZ](CF_3SO_3)_2$, $[Pt(Me_2bpy)DPPZ](CF_3SO_3)_2$ et $[Pt(phendione)DPPZ](CF_3SO_3)_2$, ainsi que les tentatives d'obtention de $[Pt(en)phi](PF_6)_2$ et de $[Pt(phen)phi](PF_6)_2$. Les constantes de liaison de $[Pt(NH_3)_2DPPZ](CF_3SO_3)_2$ et de $[Pt(en)DPPZ](CF_3SO_3)_2$ avec une séquence aléatoire d'ADN (thymus de veau) ont été déterminées. Ces expériences ont permis la synthèse d'un dimère de platine, $[(DPPZ)Pt\{DPPZ(11\text{-}11')DPPZ\}Pt(DPPZ)](CF_3SO_3)_4$, ayant deux extrémités intercalatrices DPPZ. Nous espérons que ce double intercalateur permettra le rapprochement de deux brins d'ADN.

Acknowledgements

I would like to sincerely and gratefully acknowledge the invaluable support and help of Professor Hanadi Sleiman who directed this research. I would also like to thank Antisar R. Hlil for MALDI-TOF mass spectrometry, Nadim Saade for FAB mass spectrometry, and Kimberly Yach for mathematical equation best fitting.

I would particularly like to acknowledge my labmates, Hassan S. Bazzi, Felaniaina Rakotondradany, Dr. Bouchra El Mouatassim, Dr. Bertrand Dabiens, Dr. Kumaravel Selvakumar, and especially Dr. Ignacio Vargas-Baca for his tremendous help. Thank you all for the interesting discussions about Chemistry, Politics, History, Geography, and Sports.

Glossary of Symbols and Abbreviations

bpy	2,2'-bipyridine
°C	Degree Celsius
chrysi	5,6-chrysenequinone diimine
dicnq	6,7-dicyanodipyridoquinoxaline
DPPZ	Dipyrido[3,2-a:2'-3'-c]phenazine
dpqC	Dipyrido[3,2-a:2',3'-c](6,7,8,9-tetrahydro)phenazine
en	Ethylenediamine
HOAc	Acetic acid
IR	Infrared
Me_2bpy	4,4'-dimethyl-2,2'-bipyridine
MeCN	Acetonitrile
Meim-1	1-methylimidazole
MeOH	Methanol
MGP	4-(guanidylmethyl)-1,10-phenanthroline
NH_2py-4	4-aminopyridine
NMR	Nuclear Magnetic Resonance
Ph	Phenyl
phen	1,10-phenanthroline
phen'	5-(glutaric acid monoamide)-1,10-phenanthroline
phendione	1,10-phenanthroline-5,6-dione
phi	Phenanthrenequinone diimine

py	Pyridine
qdppz	Naphtho[2,3-a]dipyrido[3,2-h:2',3'-f]phenazine-5,18-dione
quaterpy	2,2':6',2'':6'', 2'''-quaterpyridine
terpy	2,2':6',2''-terpyridine
*t*N^C	4-*tert*-butyl-2-phenylpyridine
tpphz	Tetrapyrido[3,2-a:2',3'-c:3'',2''-h:2'',3''-j]phenazine
UV-Vis	Ultraviolet-visible

Table of Contents

Abstract ii
Résumé iii
Acknowledgements iv
Table of contents v
Glossary of symbols and abbreviations vii

Chapter 1. Introduction 1

1.1- Demonstration DNA Intercalation 2
1.2- Application of Platinum Chemistry to DNA 8
1.3- Dipyrido[3,2-a:2'-3'-c]phenazine as a DNA Intercalator 16
1.4- Phenanthrenequinone Diimine as a DNA Photocleaving Agent 23
1.5- Metal-Based Dimers 27

Chapter 2. Purpose of the research 35

2.1- Goals and Experiments 35
2.2- Target Monomers 36
2.3- Synthetic Strategy 37
2.4- Pt(II)-Based Molecular Architectures 39
2.5- Target Dimer 41
2.6- Synthetic Strategy 42

Chapter 3. Experimental section 44

3.1- Materials and Apparatus 44
3.2- Successful Syntheses 44
3.3- Synthesis of Pt(II) Dimers 59
3.4- Purification of Calf Thymus DNA 61
3.5- Attempted Syntheses 61

Chapter 4. Results and discussion 68

4.1- Synthesis of 1,10-phenanthroline-5.6-dione and DPPZ 68
4.2- Synthesis of $[Pt(L\text{-}L)DPPZ]^{2+}$ complexes starting from $[Pt(L\text{-}L)Cl_2]$ or $[Pt(DPPZ)Cl_2]$ (L-L = 2 NH_3, en, phen, Me_2bpy, DPPZ) 69
4.3- Synthesis of $[Pt(L\text{-}L)DPPZ](CF_3SO_3)_2$ complexes starting from $[Pt(L\text{-}L)I_2]$ (L-L = 2 NH_3, en, phen, Me_2bpy, phendione) 75
4.4- Attempted synthesis of $[Pt(en)phi](PF_6)_2$ and $[Pt(phen)phi](PF_6)_2$ 79
4.5- Synthesis of Pt(II) dimers 81

4.6- Absorption spectrum of $[Ru(phen)_2DPPZ](PF_6)_2$ with calf thymus DNA. 85
4.7- $[Pt(NH_3)_2DPPZ](CF_3SO_3)_2$ and $[Pt(en)DPPZ](CF_3SO_3)_2$: binding constants to calf thymus DNA 91
4.8- $[(DPPZ)Pt\{DPPZ(11\text{-}11')DPPZ\}Pt(DPPZ)](CF_3SO_3)_4$: binding constants to calf thymus DNA 96

Conclusion 102
References 104

Chapter 1. Introduction

The design of small complexes that bind and react at specific sequences of DNA becomes important as we begin to delineate, on a molecular level, how genetic information is expressed.[1] A more complete understanding of how to target DNA sites with specificity will lead not only to novel chemotherapeutics but also to a greatly expanded ability for chemists to probe DNA and to develop highly sensitive diagnostic agents.

Transition-metal complexes are being used at the forefront of many of these efforts.[1] Inert, stable, and water-soluble complexes containing spectroscopically active metal centers are extremely valuable as probes of biological systems. Following the discovery of antitumor activity of cisplatin,[2,3] it was established that square planar platinum (II) complexes containing an aromatic heterocyclic ligand could bind to DNA by intercalation.[4] These metallointercalators insert and stack between the base pairs of double-helical DNA,[1] causing a disruption in the duplex and thus modifying its properties.[5]

DPPZ[6] and phi[7] are known to intercalate within the DNA major groove. Here are presented the successfull syntheses of five DPPZ complexes of platinum and the attempts to obtain two phi complexes with the same metal center. Binding constants to calf thymus DNA for some DPPZ complexes have been determined and the knowledge coming from the synthetic strategy has been used to design a platinum-based dimer with

two intercalative ends. We hope that the latter molecular architecture will allow the study of packaged DNA and to bring into close proximity two DNA duplexes.

1.1- Demonstrating DNA Intercalation

1.1.1- What is an intercalative interaction?

DNA binding agents tend to interact noncovalently with the host molecule through two general modes: (i) in a groove-bound fashion stabilized by a mixture of hydrophobic, electrostatic, and hydrogen-bonding interactions and (ii) through an intercalative association in which a planar, heteroaromatic moiety interacts through π-stacking with the DNA base pairs.[5]

Intercalative binding is a noncovalent π-stacking interaction resulting from the insertion of a planar heterocyclic aromatic moiety between the base pairs of the DNA helix.[8,9] It is the most common mode of binding of small probes such as ethidium bromide (scheme 1).[10] The flat intercalator is held rigidly in a well-defined orientation perpendicular to the axes of the helix.[9]

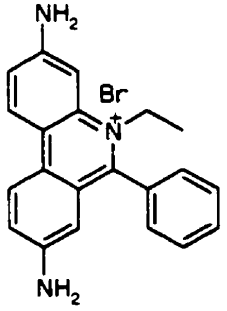

Scheme 1: Structure of ethidium bromide.

1.1.2- General experimental criteria for assessing intercalation

Numerous methods to probe the interaction of a DNA-binding molecule with its host in solution are available.[11,12] However, considering the fact that new three-dimensional intercalators in which the DNA-binding molecule is not wholly described by a classical planar, aromatic structure, criteria constituting strong evidence for an intercalative interaction have been established.[1]

-Unwinding and lengthening of the DNA helix:

Intercalation produces extension, unwinding, and stiffening of the DNA helix (scheme 2).[1] These changes are a consequence of the untwisting of the base pairs and helical backbone needed to accomodate the intercalator. Because of this structural change, a modification in the solution viscosity, in the sedimentation coefficient, and in the electrophoretic mobility of DNA can be observed.[12,13] In the latter case, linear and closed circular DNA will migrate more slowly than the free duplex. Moreover, unwinding

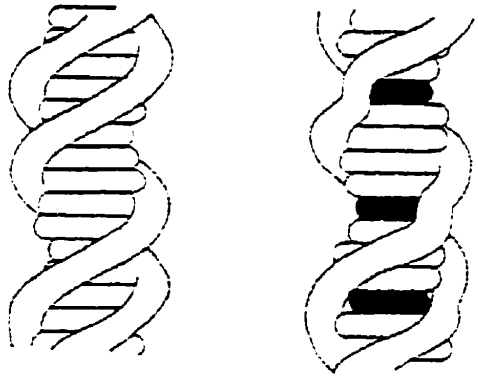

Scheme 2: The intercalation process.

at the site of intercalation indicates formation of positive supercoils in circular DNA.[14] Downfield shifts in the ^{31}P NMR spectrum of the phosphodiester backbone of DNA are also indicative of structural perturbations.[15]

-Electronic interactions:

Intercalation results in an ordered stacking of the bound species between base pairs at 3.4Å separation.[1] The intercalating surface is sandwiched tightly between the aromatic, heterocyclic base pairs and stabilized electronically in the helix by π-π stacking and dipole-dipole interactions.[5]

Binding commonly results in hypochromism and a shift to longer wavelengh of the metal-to-ligand charge-transfer and intraligand (π-π^*) transitions of the intercalated chromophore.[5] Moreover, for luminescent molecules, emission enhancements, or in some cases quenching, are also observed. Also applicable are ^1H NMR upfield shifts in the aromatic protons of the intercalator which result from ring currents from the stacked aromatic bases.[15]

-Rigidity and orientation of the intercalator:

Upon intercalation at the unwound site, there is a substantial structural association between the base pairs and the intercalator.[1] The intercalator becomes rigidly held and oriented with the planar moiety perpendicular to the helical axis. This can be measured experimentally through the use of different dichroic techniques (linear flow[16] or electric[17]) where the bound orientation of the intercalator is evaluated relative to the oriented helical axis. Moreover, luminescence polarization experiments that establish the time during which the molecule is rigidly bound within the helix can be carried out.[18]

1.1.3- Binding constant determination

-The Scatchard equation:

A convenient method to determine the affinity of an intercalator for its host is to establish its intrinsic binding constant (equation 1).[19,20] The first step in the analysis of a binding problem is to determine experimentally the amount of a bound complex as a function of free ligand concentration by luminescence enhancement or quenching for example (equation 2).[19] The total number of moles of intercalator bounded to DNA and of free intercalator can be evaluated using the luminescence intensity of an intercalator at complete DNA saturation and establishing the amount of intercalator bounded to DNA corresponding to the luminescence intensity obtained for a particular intercalator concentration. The substraction between these two values gives the number of moles of free intercalator. The slope and x intercept of this kind of plot are used to obtain estimates of binding constant and site size. Any deviation of the plot from linearity is taken to indicate more than one type of binding sites (cooperative binding), a ligand-ligand interaction, or both.

Equation 1: $K = \frac{[\text{DNA-intercalator}]}{[\text{DNA}][\text{intercalator}]}$

K = intrinsic binding constant

[DNA-intercalator] = concentration of bound intercalator to DNA

[DNA] = concentration of free DNA

[intercalator] = concentration of free intercalator

Equation 2: r/c = Kn - Kr

$$r = \frac{\text{moles of intercalator bounded to DNA}}{\text{moles of free intercalator}}$$

c = total number of moles of intercalator

n = number of binding sites on DNA (x intercept)

K = intrinsic binding constant (slope = -K)

-The McGhee and von Hippel equation:

Unfortunately, the Scatchard approach is valid if the ligand binds to only one repeating unit of a lattice, e.g. to one base or base-pair.[20] Thus, when a bound ligand covers two or more lattice residues, complications enter into the analysis which cannot be treated by the simple Scatchard relation. For such ligand, potential binding sites overlap. Therefore, at any degree of binding saturation the number of free ligand binding sites depends not only on the number of ligands already bound, but also on the distribution of these bound ligands on the lattice. The result is a curved Scatchard plot, but here the curvature arises solely as a consequence of the overlap of potential ligand sites (intercalator is not equally distributed along the DNA) and cannot be attributed to binding site heterogeneity or ligand binding co-operativity. The McGhee and von Hippel mathematical approach is thus based on simple conditional probabilities where almost every lattice residue can potentially start a ligand binding site (equation 3). The concentration of free intercalator is determined once again with differences in the luminescence intensities. The slope is equal to -K and n is given by the x intercept.

Equation 3: $r/C_f = K(1-nr)\{(1-nr)/[1-(n-1)r]\}^{n-1}$

$r = (C_t-C_f)/[DNA]$

C_f = concentration of free intercalator = $C_t[(I/I_o)-P]/(1-P)$

C_t = total concentration of the intercalator

P = y intercept of the plot of I/I_o vs. $1/[DNA]$

I = emission at actual intercalation ratio

I_o = emission at full intercalation saturation

n = binding site size in base pairs

K = intrinsic binding constant

-Non luminescent probes:

It is also possible to determine binding constants to DNA for non luminescent probes by hypochromic changes of its absorption (equation 4).[21] The equation leads to a double-reciprocal plot of the change in the apparent extinction coefficient of the ligand $D/\Delta\varepsilon_{AP}$ vs. DNA concentration D where the slope equals $1/\Delta\varepsilon$ and the y intercept gives $1/(\Delta\varepsilon \times K)$. K is then given by the ratio of the slope to the y intercept.

Equation 4: $D/\Delta\varepsilon_{AP} = D/\Delta\varepsilon + 1/(\Delta\varepsilon \times K)$

D = [DNA] in base pairs

$\Delta\varepsilon_{AP} = |\varepsilon_A - \varepsilon_F|$

$\Delta\varepsilon = |\varepsilon_B - \varepsilon_F|$

$\varepsilon_A = A_{obs}/[intercalator]$

ε_B = extinction coefficient of bound intercalator

ε_F = extinction coefficient of free intercalator

K = intrinsic binding constant

1.2- Application of Platinum Chemistry to DNA

1.2.1- Cisplatin and Cisplatin Derivatives Anticancer Activity

In the course of examining the effect of electric fields in the growth of *Escherichia coli* cells, biological activity of platinum compounds was uncovered that led to the development of some of the most widely used anticancer drugs today.[2,22] Compounds formed by reaction of platinum from the electrodes with ammonium chloride in the buffer stopped cell division and induced filamentous growth in the bacteria. After subsequent testing of these compounds, a complex known since 1845,[23] *cis*-diamminedichloroplatinum (II), or cisplatin (scheme 3), was shown in 1970 to possess remarkable successful antitumor activity.[2,3]

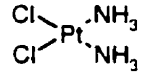

Scheme 3: Structure of cisplatin.

Platinum complexes offer many advantages: they are moderately soluble in water, are kinetically stable, and do not form insoluble hydrated oxides at neutral pH.[24] Early clinical trials with cisplatin showed a cure rate greater than 90% for testicular cancer and

the drug was approved by the FDA in 1978.[25] It is also used to treat other kinds of malignancies, including ovarian, esophageal, cervical, head and neck, and nonsmall cell lung cancer.[26]

Much research has been conducted over the years following the discovery of biological activity for cisplatin in an attempt to elucidate its mechanism of action.[26] A major focus of this work has been elucidating the biological target of this drug within the DNA molecule and examining the effects of cisplatin adduct formation on DNA-dependent cellular functions. According to the generally accepted mechanism, cisplatin binds preferentially at the N(7) position of purines[27], mostly guanines and to a smaller extent to adenines, replacing the two Cl ligands and thereby forming inter-[28] and intrastrand[29] cross-links (scheme 4). The 1,2-intrastrand cross-link is most likely the critical lesion.[29,30]

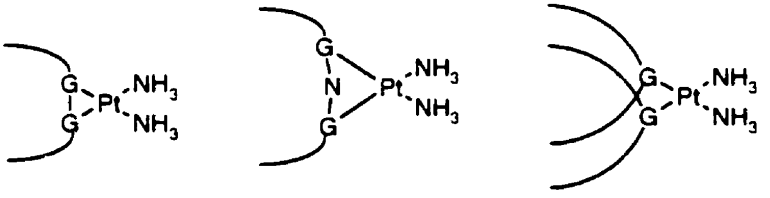

Scheme 4: 1,2-, 1,3-, and interstrand cross-links.

Following injection into the bloodstream, cisplatin encounters a relatively high concentration of chloride ions (100 mM), which suppresses hydrolysis and maintains the compound in a neutral state.[26] Once inside the cell, the diminished chloride ion concentration (~20 mM) facilitates hydrolysis (equation 5). The result is an activated, aquated form, *cis*-$[Pt(NH_3)_2Cl(OH_2)]^+$, which can react more readily with cellular targets.

This hydrolysis reaction is the rate-limiting step for DNA binding, the half-life being ~2h.[31] Aquated cisplatin subsequently binds to an N(7) atom of a guanine base in DNA scheme 5), which displaces the water molecule in a relatively fast reaction step ($t_{1/2}$ ~0.1h), forming a monofunctional adduct. Formation of a bifunctional adduct involves hydrolysis of the second chloride ligand by a similar process ($t_{1/2}$ ~2h) where coordination with N(7) of a second purine occurs.

Equation 5: *cis*-$Pt(NH_3)_2Cl_2 + H_2O \rightarrow$ *cis*-[$Pt(NH_3)_2Cl(OH_2)]^+ + Cl^-$

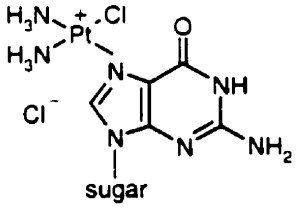

Scheme 5: Monofunctional binding to guanine.

Enzymatic digestion of cisplatin-treated salmon sperm DNA and characterization of the products allowed the identification of the major DNA adducts formed by cisplatin.[32] The major products were 1,2-intrastrand cross-links involving adjacent bases,with *cis*-[$Pt(NH_3)_2${d(GpG)}] comprising 47-50% of the adducts formed and *cis*-[$Pt(NH_3)_2${d(ApG)}] comprising another 23-28%. In addition, 8-10% of the digested products contained 1,3-intrastrand cross-links involving non-adjacent guanines and interstrand adducts, and another 2-3% was the result of monofunctional binding to guanine.

These results vary for non-biological conditions (scheme 6). At pH=10.5, N(1)-coordinated platinum adducts are also formed, and a migration of the platinum moiety from N(1) to N(7) is observed with a pH decrease.[33] Moreover, a different and unexpected adduct has also been observed, where one cisplatin binds to the N(7) position and another one to the N(1) position, both in a monofractional fashion.[34]

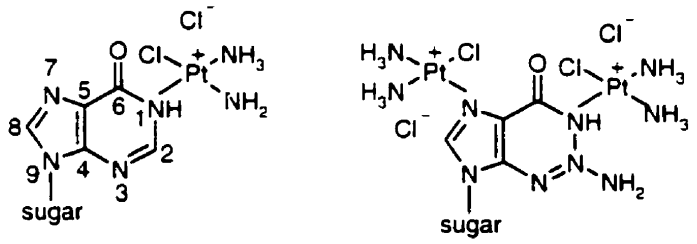

Scheme 6: N(1)-coordination to guanine and N(1) and N(7) monofunctional coordination to guanine.

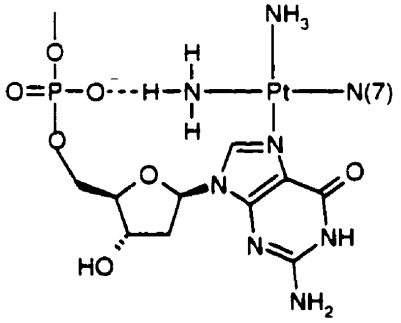

Scheme 7: Suggested hydrogen-bonding between ammine ligand and 5'-phosphate group.

The formation of cisplatin-DNA cross-links structurally distorts the DNA.[26] Its binding can unwind DNA and, at saturation levels, shorten the duplex by up to 50%.[35] The formation of these adducts also results in a loss of the helix stability.[36] The 5'-end-coordinated guanine tilts out of the base stack, resulting in loss of one of the amino hydrogen bonds involved in GC base pairing, and forming a weak bifurcated hydrogen

bond at this position.[37] Moreover, a hydrogen bond is suggested to occur between one ammine ligand on platinum and the 5'-phosphate group of the d(pGpG) unit (scheme 7).

The ability of cisplatin to bind to DNA and distort its structure suggests that it can interfere with the normal functioning of the helix.[26] Inhibition of DNA synthesis has been observed with different DNA sequences and DNA polymerases[38] and transcription elongation was blocked.[39] In the latter case, cells treated with cisplatin were temporarily or permanently arrested in the G_2 phase.[40] Thus mitosis could not occur and cell death followed.

Unfortunately, the applicability of cisplatin is still limited to a relatively narrow range of tumors.[41] Some tumors have natural resistance to cisplatin, while others develop resistance after the initial treatment. Cisplatin also has limited solubility in aqueous solution and is administrated intravenously, another inconvenience to outpatient treatment. Coupled with the severe renal toxicity associated with cisplatin,[42] these drawbacks have been the impetus for the development of improved platinum antitumor drugs. Currently, over 28 platinum compounds are in the human clinical trials phase[41,43] and some more detailed research has been carried out on different amine-based platinum complexes.[44]

1.2.2- Pt(II) intercalating complexes

A new class of platinum complexes with a different kind of interaction with DNA has been developed in the last two decades.[45-48] These complexes possess aromatic nitrogen-based ligands instead of labile chloride ions like cisplatin and its derivatives. This imparts different properties to these nucleic acid probes, as they cannot coordinate to

DNA. Double helix DNA would inhibit the reactions between cationic complexes and anionic nucleophiles, avoiding ligand substitution.[49] Instead, a reversible interaction occurs where a planar aromatic ligand intercalates between DNA base pairs.

Some of the most efficient platinum intercalating complexes have 2,2'-bipyridine or one of its derivatives as a chelating intercalator, and pyridine, pyridine-like, or other chelators as ancillary ligands.[45-48] In the case of non-aromatic chelating ancillary ligands, the binding affinity to DNA has been established using ethylenediamine, as in the case of $[Pt(bpy)(en)](ClO_4)_2$ (scheme 8).[45] The process gave rise to a large bathochromic shift and substantial hypochromicity of the absorption band of the complex as expected from intercalation.[5] Moreover, with an increasing Na^+ concentration, the binding constant decreases from 152.4 x 10^3 M^{-1} for $[Na^+]$ = 0.011M to 14.5 x 10^3 M^{-1} for $[Na^+]$ = 0.100M.[45]

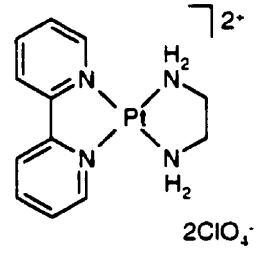

Scheme 8: Structure of $[Pt(bpy)(en)](ClO_4)_2$.

According to similar studies with palladium complexes, the binding constants values are larger for substrates containing a greater number of aromatic rings.[45] The presence of methyl substituents on the bipyridine ring enhances the binding strength. A first example of this phenomenon was given by $[Pt(5,5'\text{-}Me_2bpy)(4\text{-}ampy)_2](CF_3SO_3)_2$ (scheme 9).[46] This complex showed hypochromism in the presence of DNA and also a

small red shift of its absorption bands. The binding constant obtained was 1.7 x 10^4 M^{-1} which is higher than the one obtained for $[Pt(bpy)(en)](ClO_4)_2$.

Some other complexes have been studied and do fulfill the requirements mentionned previously to enhance binding strength (scheme 10).[47] For example, $[Pt(bpy)(py)_2](PF_6)_2$ gave a binding constant to DNA of 16.2 x 10^4 M^{-1}. Substitution of the hydrogen in para position of the pyridine led to binding constants different than that for $[Pt(bpy)(py)_2](PF_6)_2$. The binding constant increases from 1.5 x 10^4 M^{-1} to 116.7 x 10^4 M^{-1} going from R = CNpy to Phpy, py, Mepy, and NH_2Py. Using 4,4'-diphenyl-2,2'-bipyridine and the same ancillary ligands, the binding constants are greatly enhanced from 4.0 x 10^6 M^{-1} to 140.0 x 10^6 M^{-1} going from R = CNpy to NH_2Py.

A different method to observe the effect of an increase in the number or aromatic rings on DNA affinity is to study the ring-coplanarity effect.[48] Extended planarity of the intercalating ligand allows a better stacking surface effect as shown by $[Pt(bpy)(py)_2](PF_6)_2$, $[Pt(terpy)(py)](PF_6)_2$, and $[Pt(quaterpy)](PF_6)_2$ (scheme 11).

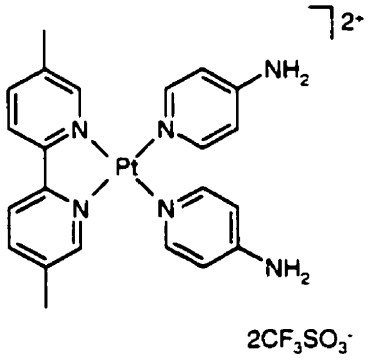

Scheme 9: Structure of by $[Pt(5,5'\text{-}Me_2bpy)(4\text{-}ampy)_2](CF_3SO_3)_2$.

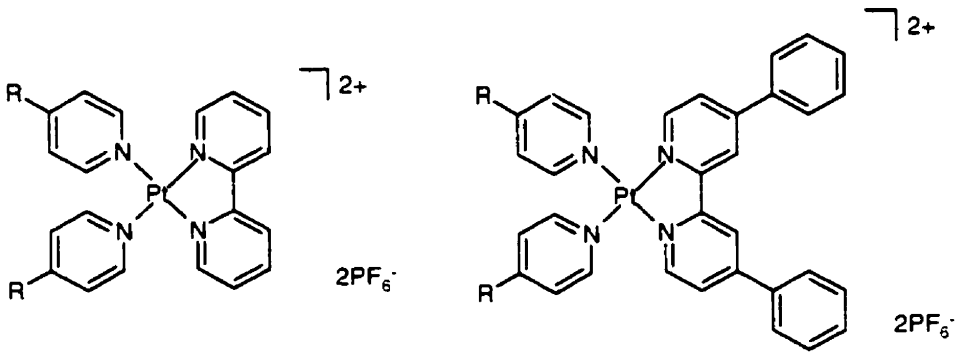

Scheme 10: Structure of $[Pt(bpy)(4\text{-}Rpy)_2](PF_6)_2$ and $[Pt(4,4'\text{-}Ph_2bpy)(4\text{-}Rpy)_2](PF_6)_2$.

The binding constant to DNA increases from 1.0 x 10^4 M^{-1} for $[Pt(bpy)(py)_2]^{2+}$ to 3.4 x 10^4 M^{-1} for $[Pt(terpy)(py)]^{2+}$, and to 2.2 x 10^5 M^{-1} for $[Pt(quaterpy)]^{2+}$. In this particular case, the differences in affinity result from the ancillary pyridine ligands which are perpendicular to the plane of the intercalator. The strength of the interaction depends on the surface that can slide between the nucleobases. $[Pt(bpy)(py)_2]^{2+}$ and $[Pt(terpy)(py)]^{2+}$ both have a perpendicular pyridine ligand that clashes directly with the DNA bases, thus decreasing their intercalative strength. This explains why the binding constant value increases more on going from $[Pt(terpy)(py)]^{2+}$ to $[Pt(quaterpy)]^{2+}$ because the latter does not have a pyridine ligand, than on going from $[Pt(bpy)(py)_2]^{2+}$ to $[Pt(terpy)(py)]^{2+}$.

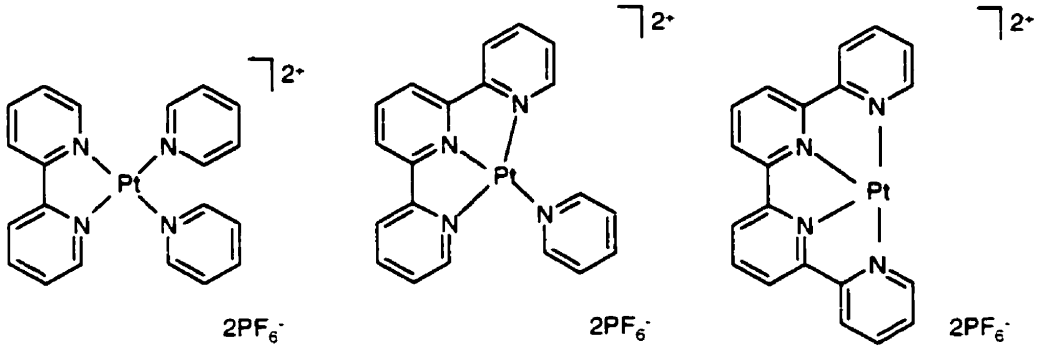

Scheme 11: Structure of $[Pt(bpy)(py)_2](PF_6)_2$, $[Pt(terpy)(py)](PF_6)_2$, and $[Pt(quaterpy)](PF_6)_2$ (all complexes are square planar).

1.3- Dipyrido[3,2-a:2'-3'-c]phenazine as a DNA Intercalator

1.3.1- Introduction

It is known that 2,2'-bipyridine and 1,10-phenanthroline are poor DNA intercalators.[50] 1,10-phenanthroline and especially 2,2'-bipyridine appear to surface-bind to DNA to a quite lage extent when chelating a metal center. A new intercalating ligand, DPPZ, was synthesized from 1,10-phenanthroline-5,6-dione and 1,2-diaminobenzene which showed useful features.[6] DPPZ consists of a 2,2'-bipyridine chelating subunit connected to a phenazine fragment acting as an electron acceptor (scheme 12).[51]

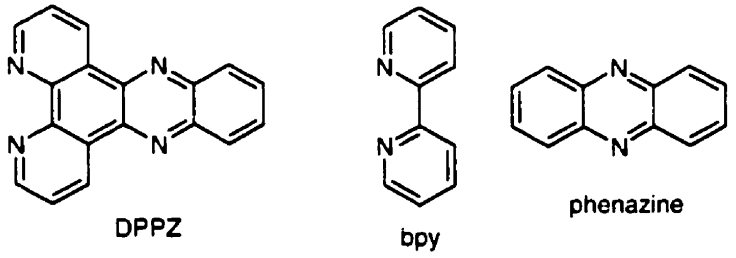

Scheme 12: Structures of DPPZ, bpy, and phenazine.

1.3.2- Preliminary studies with ruthenium and osmium

Ruthenium complexes of the DPPZ ligand provide very sensitive reporters of DNA in aqueous solution.[52] $[Ru(bpy)_2DPPZ](PF_6)_2$ and $[Ru(phen)_2DPPZ](PF_6)_2$ were the first complexes studied for photophysical properties (scheme 13).[51-53] For $[Ru(bpy)_2DPPZ]^{2+}$, the charge transfer excited state is directed from the ruthenium atom to the phenazine part of DPPZ because of differences in $DPPZ^{-\bullet}$ and $bpy^{-\bullet}$ UV-Vis absorption profiles.[51] However, according to similarities in Ru^{III}/Ru^{II} redox potentials, the back donation of Ru is localized on the π^* orbitals having a bpy character and does not

involve the phenazine fragment of DPPZ. This suggests that $[Ru(bpy)_2DPPZ]^{2+}$ is made up of two electronically independent units, one behaving as a chromophore, the other as an electron acceptor.[53]

$[Ru(bpy)_2DPPZ]^{2+}$ and $[Ru(phen)_2DPPZ]^{2+}$ are true molecular light switches for DNA.[52] They show no photoluminescence in aqueous solution at ambient temperatures but display intense photoluminescence in the presence of double-helical DNA. These complexes bind through intercalation, owing to the increased stacking area of the DPPZ ligand; groove binding thus becomes negligible. Moreover, large luminescent enhancements are observed for these DPPZ complexes compared to their parent $[Ru(bpy)_3]^{2+}$ and $[Ru(phen)_3]^{2+}$ complexes.[52,54]

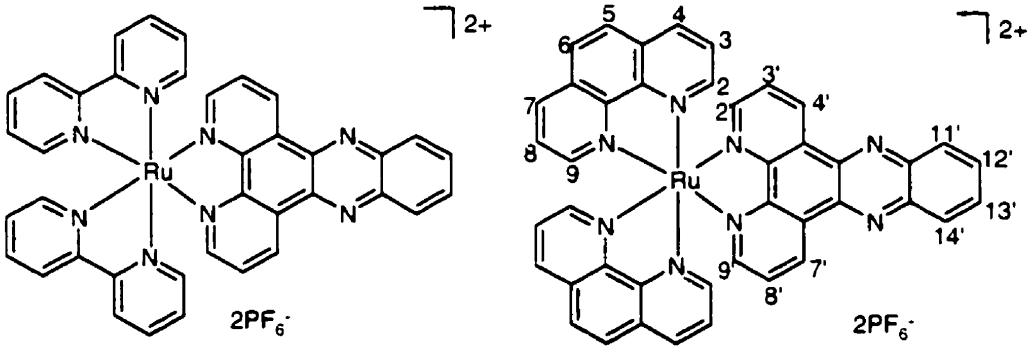

Scheme 13: Structure of $[Ru(bpy)_2DPPZ](PF_6)_2$ and $[Ru(phen)_2DPPZ](PF_6)_2$.

Because of the octahedral coordination of ruthenium, two enantiomers, Δ and Λ, are obtained when synthesizing $[Ru(bpy)_2DPPZ]^{2+}$ and $[Ru(phen)_2DPPZ]^{2+}$ (scheme 14).[55-57] Unfortunately, these previous studies on $[RuL_2DPPZ]^{2+}$ complexes have been on racemates, although it is known that interaction of DNA with chiral metal complexes is in general enantioselective.[55,58] Similar studies with pure enantiomers of

$[Ru(phen)_2DPPZ]^{2+}$ led to complexes showing luminescence in the presence of DNA with different intensities.[55] The relative luminescence quantum yield of the bound Δ enantiomer is 6-10 times larger than that of the bound Λ enantiomer. The two enantiomers also show two different binding constants to DNA, 3.2 x 10^6 M^{-1} for the Δ isomer and 1.7 x 10^6 M^{-1} for the Λ isomer.[56] Moreover, a binding stoichiometry of 0.7 mol of base pair/mol of ligand was obtained for the Δ enantiomer compared to 3 mol of base pair/mol of ligand for the Λ enantiomer.

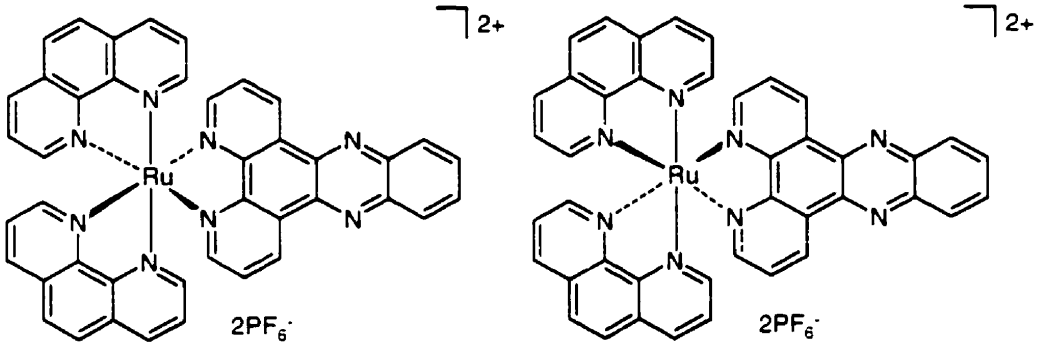

Scheme 14: Structure of Δ- and Λ-$[Ru(phen)_2DPPZ](PF_6)_2$.

These differences in binding affinities and enantioselective interactions have also been demonstrated by ^1H and ^{31}P NMR spectroscopies.[57] The first aspect is a characteristic downfield change in the ^{31}P chemical shifts for the DNA duplex bound to the metal complex which has become criterium of intercalation.[8] More substantial information can be obtained from the ^1H NMR spectral studies.[57] Differences in intercalative geometries are clearly manifested through chiral shifts in racemic mixtures and distinct resonance patterns for the 4'-7'-DPPZ ligand protons (scheme 13) of Λ- and Δ-$[Ru(phen\text{-}d_8)_2DPPZ]^{2+}$. All protons undergo upfield chemical shifts but, because of

substantially broader lines obtained for the Λ enantiomer reflecting a faster exchange rate between intercalated and free states, two populations of intercalative geometries are thought to be present, one providing asymmetric protection of the DPPZ ligand from aqueous solvent for the Λ enantiomer.

Considering the above results, two binding modes have been proposed for Λ- and Δ-$[Ru(phen)_2DPPZ]^{2+}$.[52,55-57] The quenching phenomenon in aqueous buffer results from an interaction of the phenazine nitrogens with water.[59] Thus, with full intercalation into DNA, both phenazine nitrogens are fully protected from the buffer by the bases and this would explain the higher photoluminescence observed for Δ-$[Ru(phen)_2DPPZ]^{2+}$.[52,55,57] For Λ-$[Ru(phen)_2DPPZ]^{2+}$, the lower photoluminescence would result from a partial protection of phenazine, i.e. only one nitrogen being protected. Two models were thus proposed for intercalation of these enantiomers[52] considering the above conclusions, one which is a side-on interaction for Λ-$[Ru(phen)_2DPPZ]^{2+}$, the other being for Δ-$[Ru(phen)_2DPPZ]^{2+}$ a complete intercalation.[55-57]

Emission of $[Ru(phen)_2DPPZ]^{2+}$ and its derivatives bound to nucleic acid polymers of different sequence has also been investigated.[60,61] In the presence of a 1:1 mixture of poly d(AT) and poly d(GC), ~85% of Δ-$[Ru(phen)_2DPPZ]^{2+}$complexes are bound to poly d(AT).[60] The metallointercalator thus preferentially occupies AT sites in mixed-sequence polymers. Moreover, an oligonucleotide containing the ruthenium complex tethered to its terminus has been prepared by the coupling of a 15-mer functionalized with a hexylamine at its 5'-terminus to $[Ru(phen')_2DPPZ]^{2+}$ (phen' = 5-(glutaric acid monoamide)-1,10-phenanthroline).[61] This sequence-specific light switch

targets single-stranded DNAs and gives the approximate position of mismatches as luminescence is decreased substantially with a mismatch near the 3'-terminus.

There has been a controversy about the DNA groove where intercalation occurs.[60,62,63] A first study established that $[Ru(phen)_2DPPZ]^{2+}$ intercalates via the major groove because of results obtained from ^1H NMR spectroscopy.[62] NOE crosspeaks have been detected between an adenine H(8) resonance and upfield-shifted DPPZ protons 4' and 7'. However, another study led to photophysical evidence that Λ- and Δ-$[Ru(phen)_2DPPZ]^{2+}$ intercalate DNA from the minor groove.[63] Because of similar results obtained for titrations experiments with both the Λ and Δ enantiomers, it was concluded that, having the non-intercalated part of the metal complex confined in the minor groove, it would be difficult to envisage two distinct orientations of $[Ru(phen)_2DPPZ]^{2+}$ in the intercalation pocket. To solve this controversy, competition titration experiments were carried out with known major and minor groove intercalators (scheme 15).[60] In the presence of major groove intercalator Δ-α-$[Rh[(R,R)\text{-}Me_2trien]phi]^{3+}$, the ruthenium emission yield decreases while its absorption increases. In contrast, addition of minor groove binding agent distamycin produces an increase in ruthenium emission, a result consistent with the double helix being able to accomodate major and minor groove binders simultaneously. Thus, these results are probably the strongest evidence that $[Ru(phen)_2DPPZ]^{2+}$ intercalates DNA in the major groove.

$[Ru(bpy)_2DPPZ]^{2+}$ and $[Ru(phen)_2DPPZ]^{2+}$ have not been the only complexes synthesized. For example, $[Ru(NH_3)_4DPPZ](PF_6)_2$ showed no photoluminescence and its binding constant to DNA was determined to be $1.24 \times 10^5\ M^{-1}$ (scheme 16).[64] Moreover, some DPPZ complexes of platinum have already been synthesized by Che et al.[65]

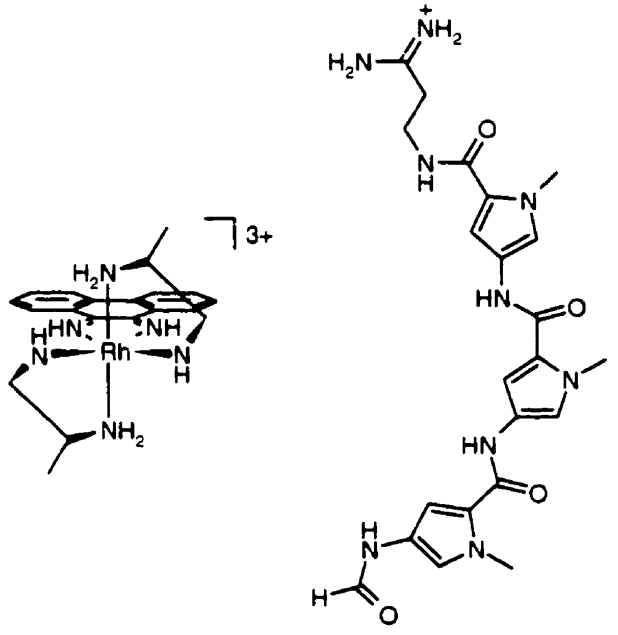

Scheme 15: Structure of Δ-α-[Rh[(R,R)-Me_2trien]phi]$^{3+}$ and distamycin.

[Pt(DPPZ)(tN^C)](CF_3SO_3), [Pt(DPPZ)(Meim-1)](CF_3SO_3)$_2$, and [Pt(DPPZ)(NH_2py-4)$_2$](CF_3SO_3)$_2$ (scheme 17) showed respective binding constants to DNA of 1.3 x 10^4 M^{-1}, 1.1 x 10^4 M^{-1}, and 1.2 x 10^4 M^{-1}. Hypochromism was observed for all three complexes in the presence of calf thymus DNA. [Pt(DPPZ)(Meim-1)](CF_3SO_3)$_2$ and [Pt(DPPZ)(NH_2py-4)$_2$](CF_3SO_3)$_2$ showed no photoluminescence even in the presence of DNA. On the other end, [Pt(DPPZ)(tN^C)](CF_3SO_3), containing a Pt(I) metal center, was not emissive in solution but displayed intense photoluminescence with λ_{max}=650 nm. This complex also showed cytotoxic activity against KB-3-1 and KB-V1 cell lines.

All these discoveries led to synthesis and studies of ruthenium complexes with some modified DPPZ ligands such as [Ru(phen)$_2$(qdppz)]$^{2+}$,[66] [Ru(phen)$_2$(dicnq)]$^{2+}$,[66] [Ru(phen)$_2$(dpqC)]$^{2+}$,[67] and [Ru(phen)$_2$(tpphz)]$^{2+}$ (scheme 18).[68] Moreover, a family of

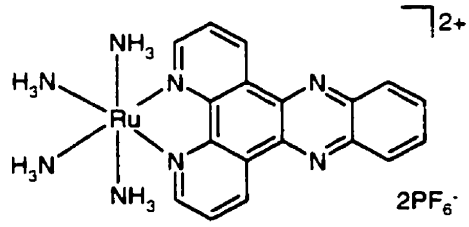

Scheme 16: Structure of $[Ru(NH_3)_4DPPZ](PF_6)_2$.

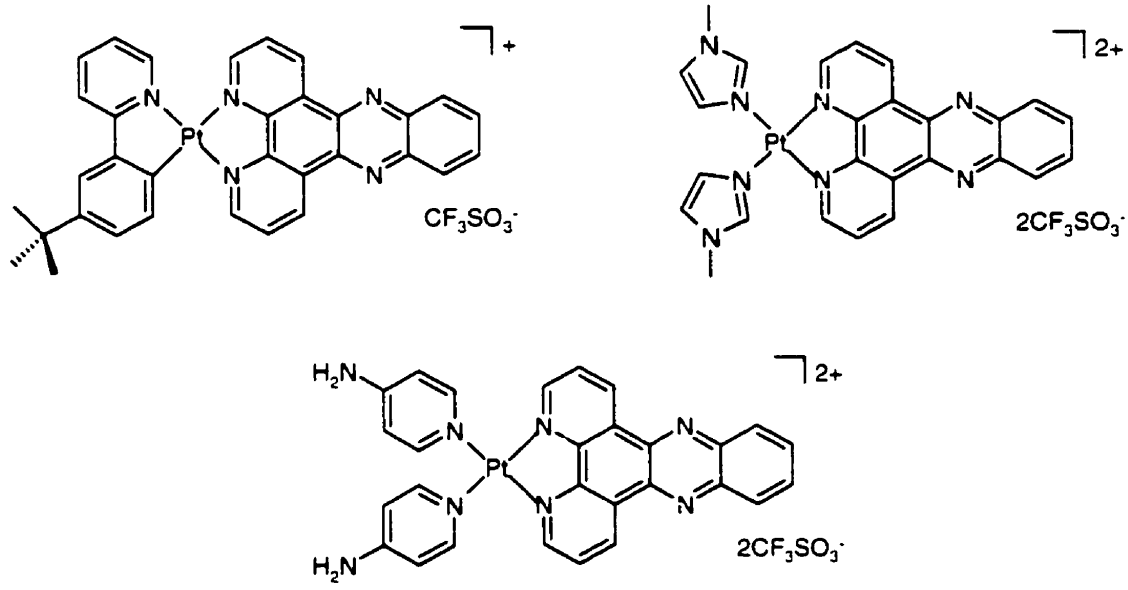

Scheme 17: Structure of $[Pt(DPPZ)(tN^C)](CF_3SO_3)$, $[Pt(DPPZ)(Meim\text{-}1)](CF_3SO_3)_2$, and $[Pt(DPPZ)(NH_2py\text{-}4)_2](CF_3SO_3)_2$.

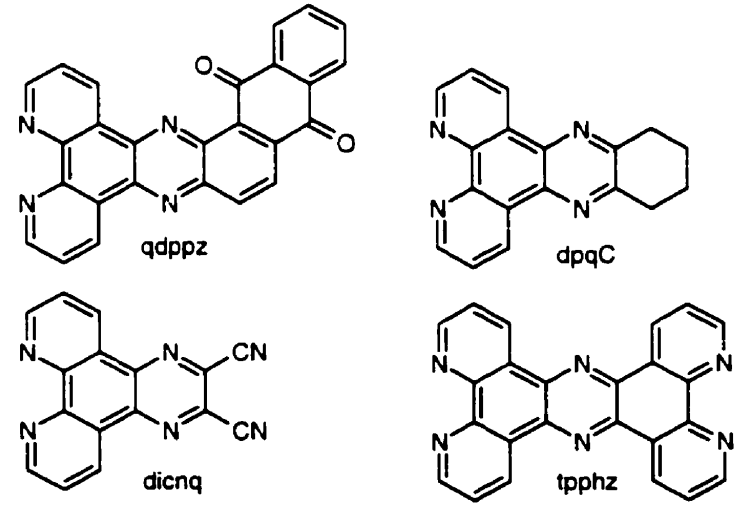

Scheme 18: Modified DPPZ ligands.

osmium complexes with simple modifications in the ancillary phen or bpy ligands indicated intercalative binding to DNA with high affinity ($K_B \sim 10^6\ M^{-1}$).[69]

1.4- Phenanthrenequinone Diimine as a DNA Photocleaving Agent

The intense coloration and stability of the ruthenium (II) diimine complexes provide uniquely sensitive photophysical probes for solids, for surfaces, and for biopolymers.[3,70] Metal complexes containing the phenanthrenequinone diimine (phi) ligand are relatively rare (scheme 19).[71] Owing to the substantial π-acidity and extended aromaticity of the ligand, intense charge-transfer transitions are observed. The ligand is planar with a large hydrophobic surface that extends far away from the metal. At the same time, imine protons on the ligand can hydrogen-bond with Lewis base substrates or templates. The phi ligand therefore provides a rich proton source near the metal center in addition to the substantial π-electron-acceptor capability and is well suited to the study of biological molecules.

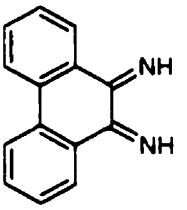

Scheme 19: Structure of 9,10-phenanthrenequinone diimine.

Different ruthenium-phi complexes have been synthesized, for example $[Ru(phi)_3]Cl_2$, $[Ru(bpy)_2(phi)]Cl_2$, $[Ru(phen)_2(phi)]Cl_2$, and $[Ru(phi)_2(bpy)]Cl_2$ (scheme 20).[50,71,72] A crystal structure of $[Ru(bpy)_2(phi)]^{2+}$ indicates substantial π-donation to the

metal center of the phi ligand.[73] Moreover, with increasing phi substitution, mixed-ligand complexes of ruthenium (II) containing phi and bpy exhibit charge-transfer transitions at progressively lower energies, suggesting the possibility of a unique delocalized excited state with coordinated phi ligands.

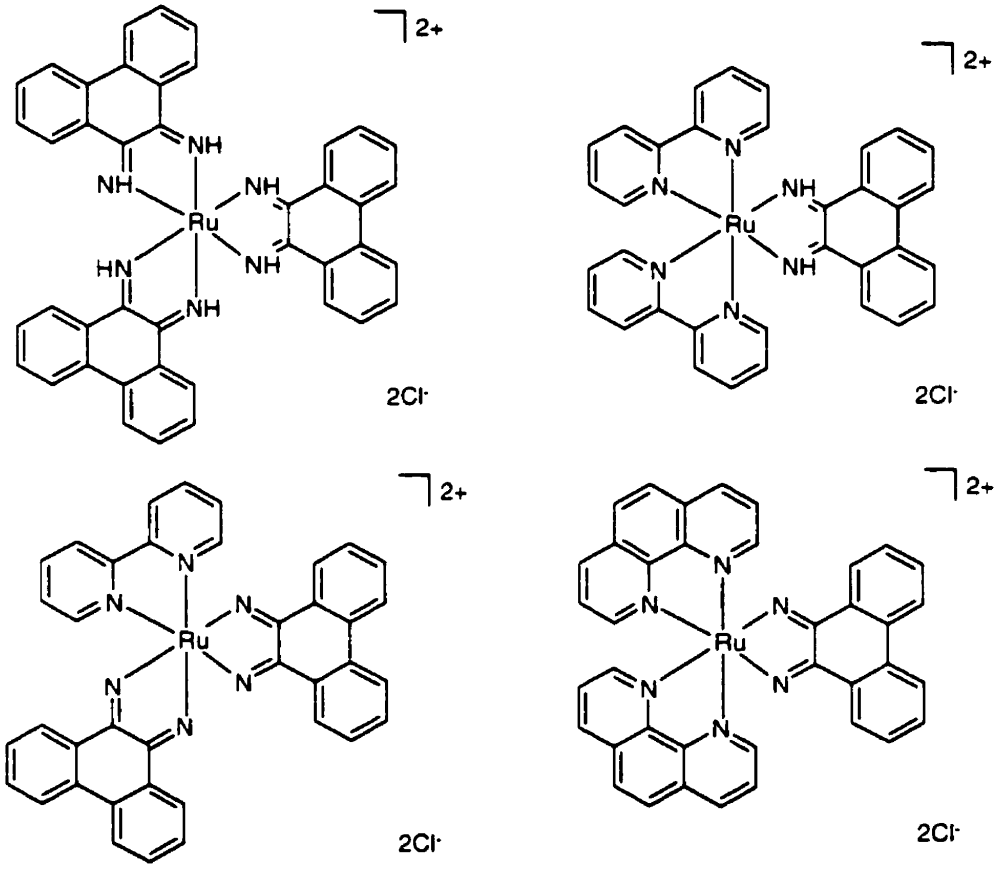

Scheme 20: Structure of $[Ru(phi)_3]Cl_2$, $[Ru(bpy)_2(phi)]Cl_2$, $[Ru(phen)_2(phi)]Cl_2$, and $[Ru(phi)_2(bpy)]Cl_2$.

However, coordination of the phi ligand to a more positive transition metal, rhodium (III), led to the discovery of complexes with very interesting properties (scheme 21). Phi complexes of rhodium (III) undergo photodecomposition with

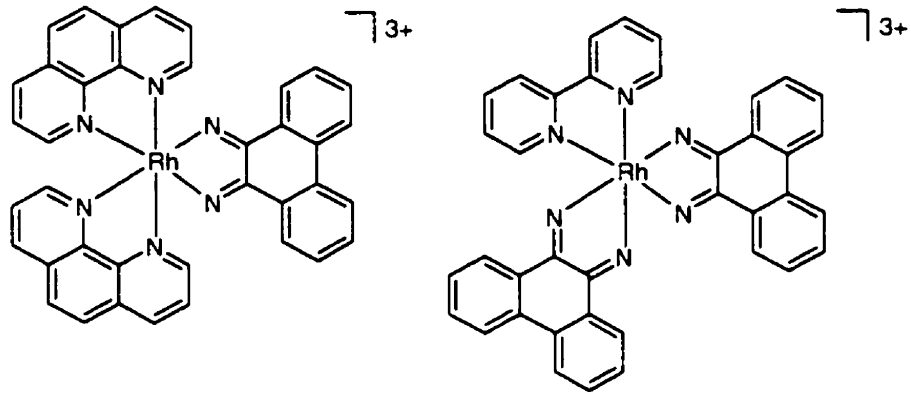

Scheme 21: Structure of $[Rh(phen)_2(phi)]Cl_2$ and $[Rh(phi)_2(bpy)]Cl_2$.

preferential loss of the phi ligand in mixed-ligand complexes.[73] Upon photoactivation, $[Rh(phen)_2phi]^{3+}$ cleaves $[Rh(phen)_2phi]^{3+}$ cleaves double-stranded DNA selectively at 5'-pyrimidine-pyrimidine-purine-3' steps with 5'-asymmetry[74] and in particular at the consensus sequence 5'-CCAG-3'.[75] Its analogue, $[Rh(phi)_2(bpy)]^{3+}$, despite containing ancillary imine for potential hydrogen bonding, cleaves DNA efficiently but in a generally sequence-neutral fashion.[74,75] Moreover, RNA cleavage follows the same patterns of recognition, matching the shape of the metal center to the nucleic structure, and subsequent chemical strand scission.[76]

The design of a small metallointercalator, Δ-α-$[Rh[(R,R)\text{-}Me_2trien]phi]^{3+}$ (scheme 14), targeting 5'-TGAC-3', allowed a more proper understanding of elements of DNA recognition.[77,78] Hydrogen bonding between the axial amines of the metal complex and the O(6) of guanine occurs in addition to axially disposed methyl groups to contact with thymine methyl groups two bases in the 5' direction from the intercalation site.[77] Because of these interactions, Δ-α-$[Rh[(R,R)\text{-}Me_2trien]phi]^{3+}$ is positionned within the major groove.[77,78]

A number of rhodium intercalators were synthesized to target precise DNA sequences.[79] Nonintercalating bipyridyl or phenanthroline ligands containing guanidinium, amido, or amino groups arranged with defined stereochemistry gave DNA cleaving agents with different properties. The most efficients complexes, Λ-1-$[Rh(MGP)_2phi]^{5+}$ and Δ-1-$[Rh(MGP)_2phi]^{5+}$, site-specifically target the 6-base pair sequence 5'-CATATG-3' with binding affinities of 1×10^8 M^{-1} and 5×10^7 M^{-1} respectively (scheme 22). This strong affinity results from the interaction of the guanidinium with guanines in the 3' direction from the intercalation site.[80]

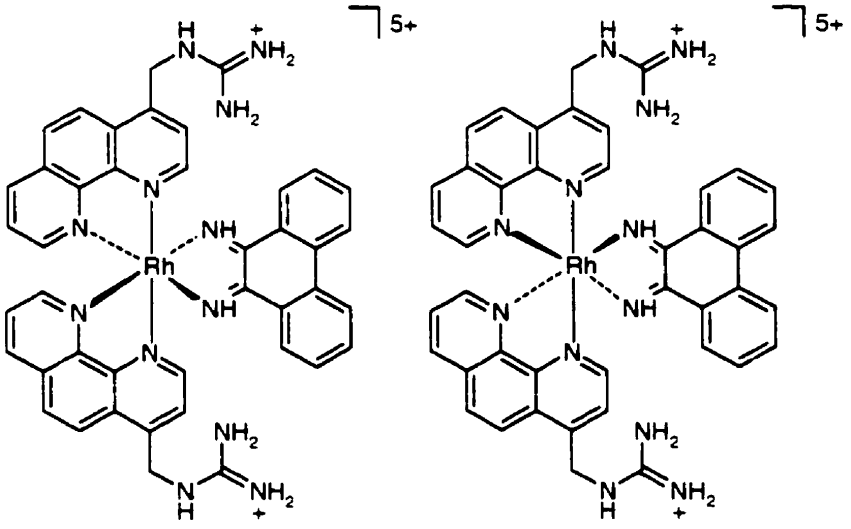

Scheme 22: Structure of Λ-1- and Δ-1-$[Rh(MGP)_2phi]^{5+}$.

The rhodium-phi area is still quite new as only few transition metal derivatives of phi have been reported. An interesting one is $[Rh(bpy)_2(chrysi)]^{3+}$ which recognizes DNA base mismatches and promotes strand scission upon photoactivation (scheme 23).[81]

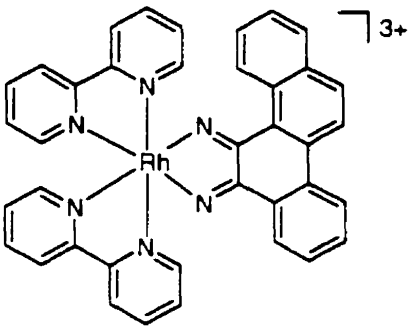

Scheme 23: Structure of $[Rh(bpy)_2(chrysi)]^{3+}$.

1.5- Metal-Based Dimers

Among the attempts to develop drugs that form strong DNA complexes with slow dissociation rates, one approach is to link several DNA-intercalating subunits together to form multi-intercalating ligands.[82] A bifunctional intercalator may interact with DNA in at least two ways (scheme 24).[83] Both intercalating moieties may intercalate with the same DNA molecule (intramolecular cross-linking) or with two separate DNA molecules (intermolecular cross-linking). Bis-intercalating dyes allow basic aspects of the intercalation process to be studied experimentally.[84] The construction of dimers from two DNA binding monomers usually enhances the dye-DNA complex stability considerably, as exemplified by ethidium bromide, where the dimer (scheme 25) binding constant is $\sim 10^{11}$ M^{-1} compared with 10^5 M^{-1} for the monomer.[85]

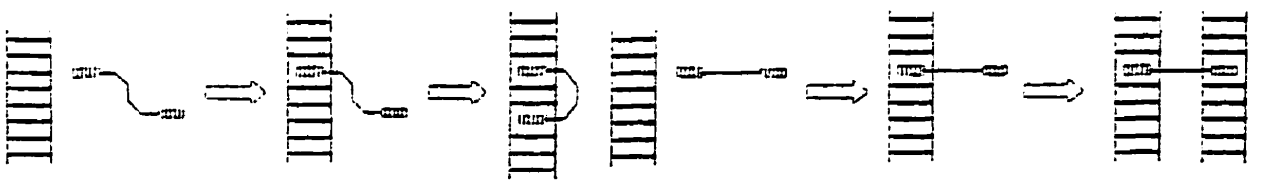

Scheme 24: Intramolecular and intermolecular cross-linking.

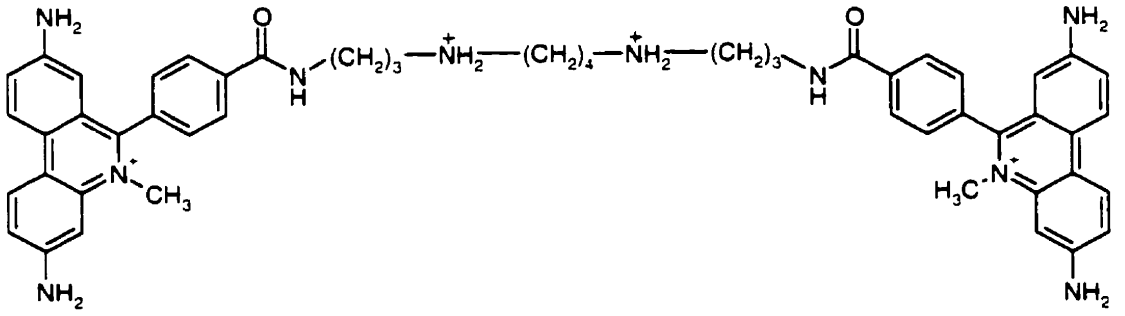

Scheme 25: Structure of ethidium bromide dimer.

Although a large number of DNA bis-intercalators are known, the two intercalating moieties usually bind to the same DNA duplex because they can rotate freely about the connecting linker.[86] Binding of one intercalating moiety inevitably leaves the other in close proximity to the other binding sites in the same duplex, leading to intramolecular cross-linking. However, if the linker is rigid with an extended configuration, binding of both intercalators into the same duplex will be impossible, unless the DNA duplex is long enough to fold back on itself. Therefore, bis-intercalators with rigid and extended linkers should cross-link DNA duplexes, forming intermolecular links.

Many intramolecular cross-linking intercalators have been designed over the past years.[86] Of particular interest are Flexi-Di and ditercalinium (scheme 26) which cause cell death in prokaryotes from futile and abortive repair of DNA,[87] TOTO (scheme 27) which site-selectively intercalates in symmetrical pyrimidine-pyrimidine-purine-purine DNA sequence CTGA:TCAG,[88] and POPO-1 (scheme 28) which is used for high-sensitivity DNA detection.[89]

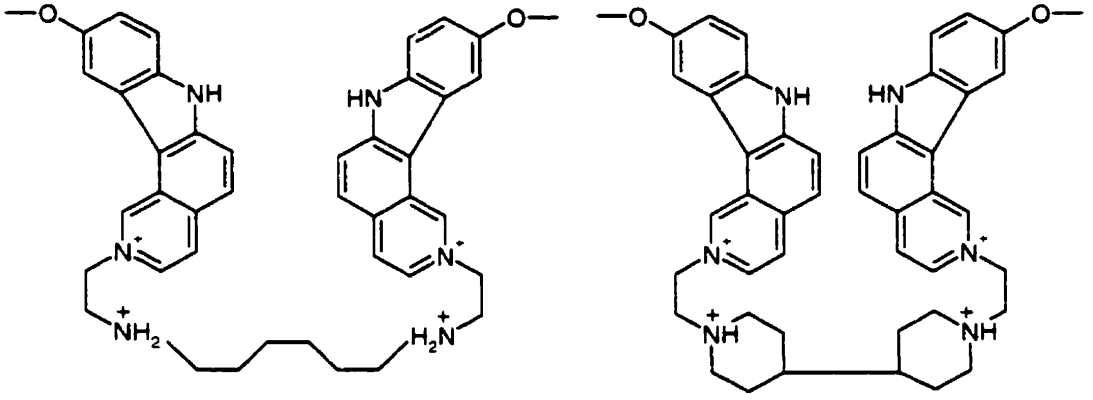

Scheme 26: Structure of Flexi-Di and ditercalinium.

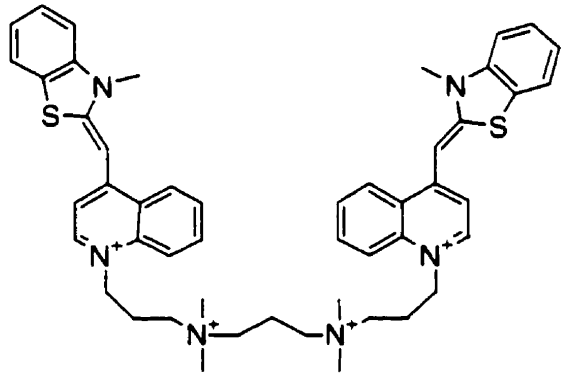

Scheme 27: Structure of TOTO.

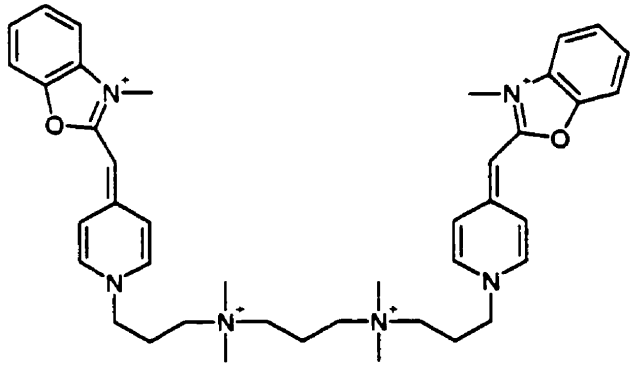

Scheme 28: Structure of POPO-1.

Many bis-intercalating dyes used for fluorescence detection of DNA in electrophoresis have been reported to give band-splitting and band-broadening.[85] Dyes are well-known to affect the position and width of existing bands by affecting the DNA charge, length, and /or flexibility, but the dimeric dyes tend to give rise to more bands than expected from the number of DNA components present.[90] For YOYO-1 (scheme 29), band splitting has been observed by electrophoresis with b/d values (added dye/DNA bases) below 0.10.[84] One faster component continues the trend of increasing migration distance as the amount of dye added decreases while the slower component has a velocity that is independent of dye loading, and which is close to the velocity observed for single bands obtained at higher b/d ratios. However, the possibility of unspecific intermolecular cross-links was excluded as digestion of DNA-dye complex with restriction enzyme λ/*Hin*dIII led to a smaller number of electrophoretic bands as would be expected considering the various possible size-combinations. Moreover, prolonged incubation of the samples resulted in a gradual decrease in the separation between the two bands until they finally merge into one band.

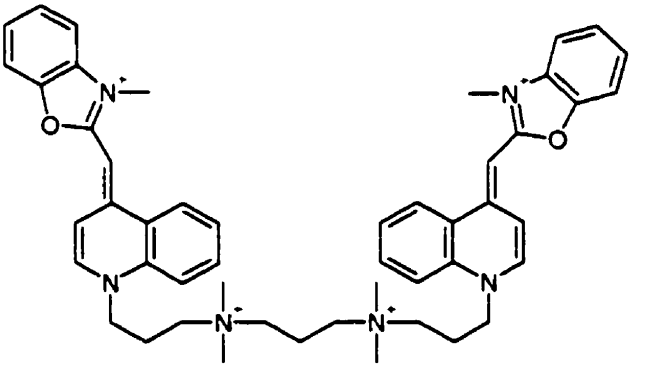

Scheme 29: Structure of YOYO-1.

However, these arguments cannot be used to exclude intramolecular cross-links where the two YO chromophores in YOYO-1 intercalate in different parts of the same DNA molecule so that an internal loop is formed.[84] However, such a mechanism would be expected to give rise to a wide distribution of conformations and hence electrophoretic velocities, which has not been observed.

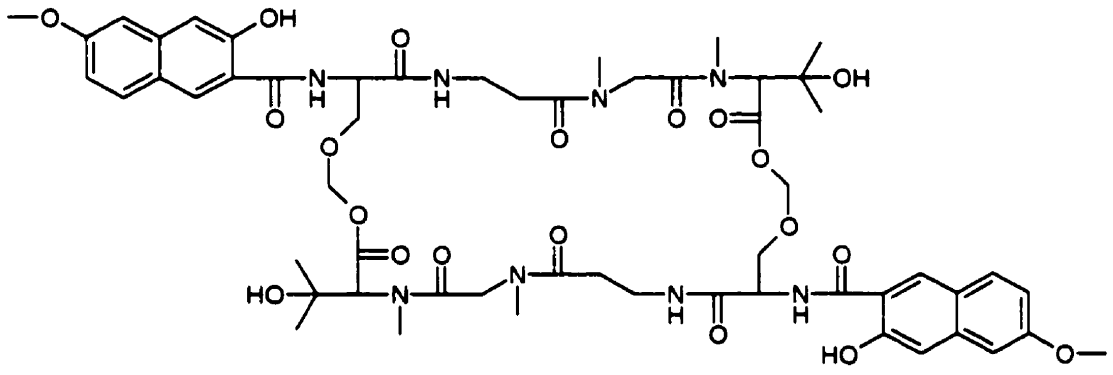

Scheme 30: Structure of luzopeptin A.

Intermolecular cross-linking of DNA has been observed with bis-intercalator luzopeptin A (scheme 30).[83] Additional bands were obtained by electrophoresis as seen in the previous cases but they were this time due to intermolecular cross-links. The maximal production occured at a drug/DNA concentration ratio range of 0.14-0.18 which approximates the theoretical value of 0.125 required for a bis-intercalator to saturate sites on linear DNA molecules.[91]

To support these conclusions, an enzymatic digestion with *Hin*dIII was carried out on PM2DNA.[83] Three fragments were obtained and isolated from agarose gels. Each type of fragment alone or the various combinations of these purified fragments were then treated with luzopeptin A and analyzed by gel electrophoresis. Bands migrating more

slowly than free fragments were observed but, as there is a linear relationship between the gel mobility and the log of the molecular weight, the number of base pairs has thus been evaluated and showed products with molecular weights close to those expected for the intermolecular cross-linking products. However, these intermolecular products gradually disappeared upon longer incubation times. This intermolecular intercalation was made possible probably because of the remarkably high affinity constant of luzopeptin A for DNA ($1.93 \times 10^7\ M^{-1}$).

Polymetallic molecular architectures can be designed for energy and electron transfer purposes[92-94] and in order to study the topology of packaged DNA.[95] In the latter case, these reagents could cross-link two DNA duplexes in close spacial proximity. Thus, varying the linker length should allow different sites in the packaged DNA to be cross-linked, meaning that cross-linking should occur between two duplexes whose spatial relationship best matches the geometry of the linker since this will provide the greatest binding energy. Moreover, by connecting two chiral centers into a dimeric complex, one could hope to amplify the chiral discrimination.[96]

Some ruthenium molecular architectures have already been synthesized, for example $[Pd\{LRu(phen)_2\}_2](PF_6)_6$ where L = 9,11,20,22-tetraazatetrapyrido[3,2-a:2',3'-c:3'',2''-l:2''',3'''-n]-pentacene (scheme 31).[93] Considering DNA studies, linear dichroism experiments have shown that $\Lambda\Lambda$-$[(bpy)_2Ru\{DPPZ(11\text{-}11')DPPZ\}Ru(bpy)_2]^{4+}$, $\Delta\Delta$-$[(bpy)_2Ru\{DPPZ(11\text{-}11')DPPZ\}Ru(bpy)_2]^{4+}$, and $\Lambda\Lambda$-$[(phen)_2Ru\{DPPZ(11\text{-}11')DPPZ\}Ru(phen)_2]^{4+}$ complexes bind with a geometry in which concave DPPZ(11-11')DPPZ ligand embraces the sugar-phosphate backbone, placing one RuL_2 moiety in each groove.[96] However, $\Delta\Delta$-$[(phen)_2Ru\{DPPZ(11\text{-}11')DPPZ\}Ru(phen)_2]^{4+}$ allows both

metal centers to be placed in the same groove. In contrast to this nonintercalative binding, bis-intercalating $[\mu\text{-c4(cpDPPZ)}_2\text{-(phen)}_4\text{Ru}_2]^{4+}$ showed an arrangement of the DPPZ moieties between nucleobases, with a two base pairs separation for all three stereoisomers (scheme 32).[82]

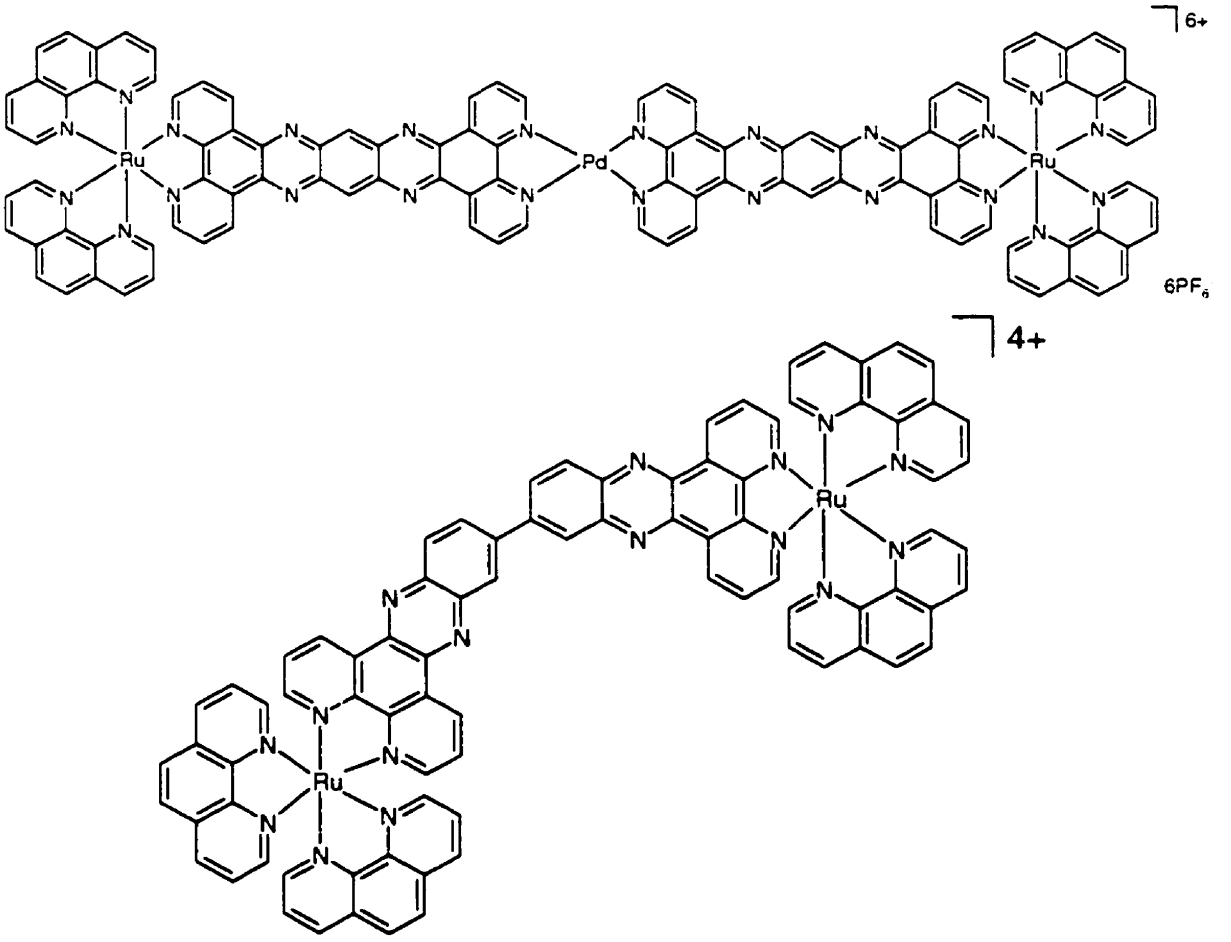

Scheme 31: Structure of $[Pd\{LRu(phen)_2\}_2](PF_6)_6$ and $[(phen)_2Ru\{DPPZ(11\text{-}11')DPPZ\}Ru(phen)_2]^{4+}$.

These complexes represent novel types of DNA-threading compounds that can provide new possibilities for the design of gene-targeting drugs.[82] Numerous molecular architectures using different metal centers, including platinum (II), can thus be designed.

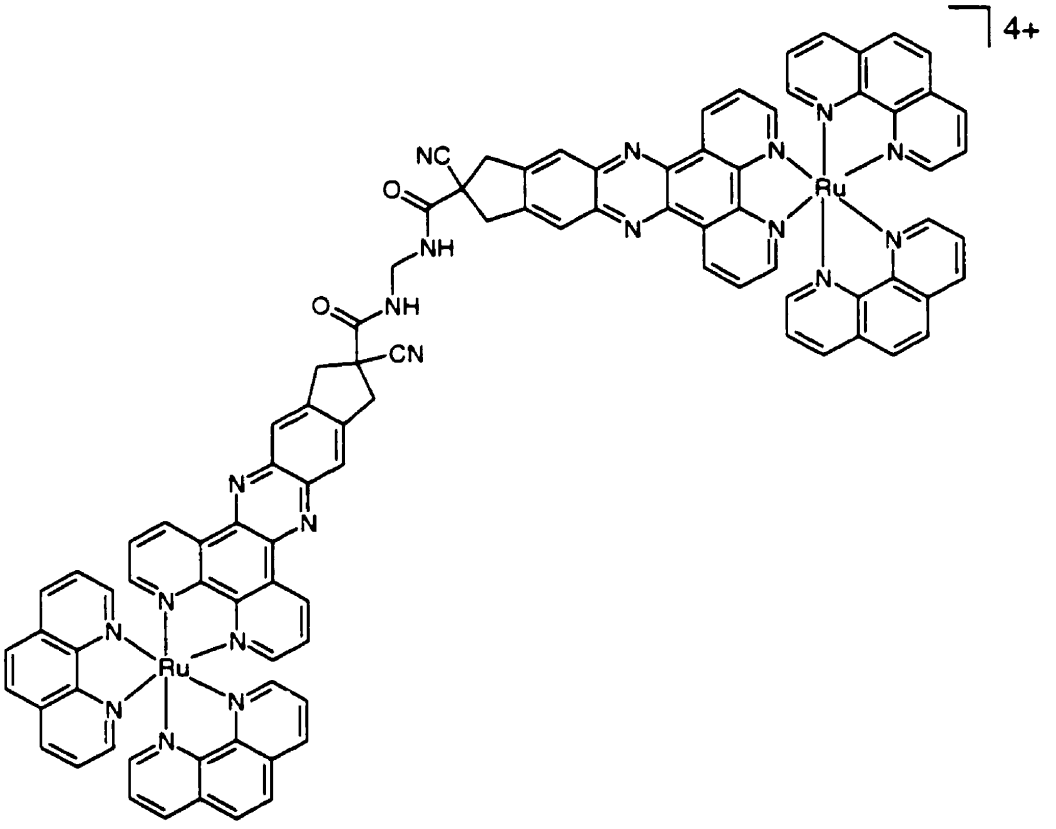

Scheme 32: Structure of $[\mu\text{-c4(cpDPPZ)}_2\text{-(phen)}_4\text{Ru}_2]^{4+}$.

Chapter 2. Purpose of the Research

2.1- Goals and Experiments

As previously mentioned, when using octahedrally coordinated metal centers to synthesize probes for DNA, two enantiomers will result from the synthesis leading to complexes with different affinities toward the double helix.[55-57] The Λ enantiomer of $[Ru(bpy)_2DPPZ]^{2+}$ and $[Ru(phen)_2DPPZ]^{2+}$ show a lower affinity for DNA compared to their respective Δ enantiomers as their ancillary ligands directly clash with the phosphate backbone, preventing complete intercalation. The square planar geometry of platinum (II) complexes prevents this synthetic problem because the d_z^2 orbital is not filled. Such complexes where the ancillary ligand(s) stands within the DNA groove should show no strong repulsive interaction with the phosphate backbone.

Our research objective is to synthesize platinum (II) complexes of dipyrido[3,2-a:2'-3'-c]phenazine and phenanthrenequinone diimine and to study their behaviour in the presence of calf thymus DNA. Characterization and experiments include ^{1}H, ^{13}C, and ^{19}F NMR spectroscopy, MALDI-TOF mass spectrometry, elemental analysis, infrared spectroscopy, UV-visible spectrophotometry, and binding constant determination to calf thymus DNA. These complexes are predicted to show high binding constants to DNA and can potentially be used as chemotherapeutics agents. Moreover, they are a good source of information for the design and synthesis of platinum-based dimers as will be discussed later.

2.2- Target Monomers

Five dipyrido[3,2-a:2'-3'-c]phenazine complexes and two phenanthrenequinone diimine complexes of platinum (II) have been designed (scheme 33). They have different ancillary ligands, which are designed to allow hydrogen-bonding interactions with the phosphate backbone, or to increase the hydrophobicity of the complexes. Moreover, [Pt(phendione)DPPZ]$(CF_3SO_3)_2$ has been designed to allow formation of a Schiff base by reacting the ketones with proper amine molecules. This complex has shown to be extremely useful for the synthesis of dimers.

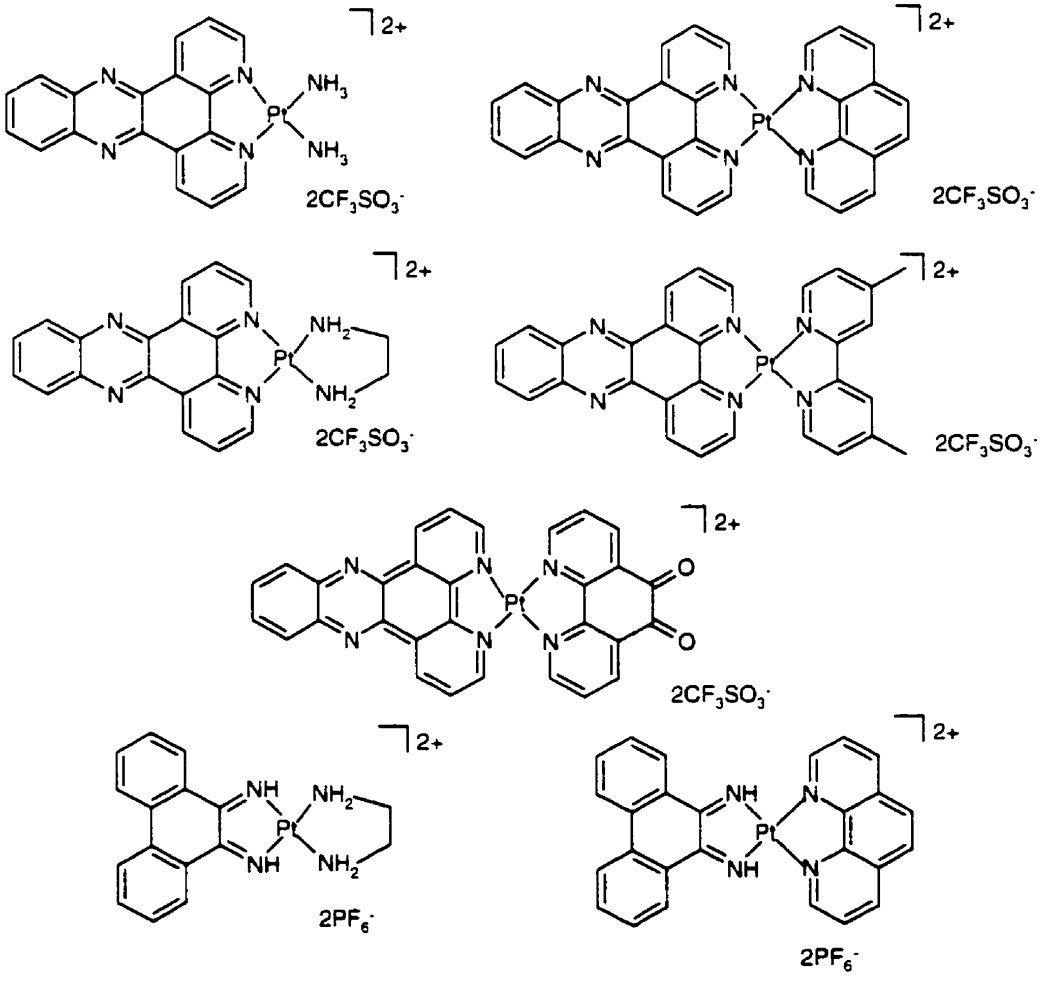

Scheme 33: Target monomers.

2.3- Synthetic Strategy

2.3.1- Synthesis of dipyrido[3,2-a:2'-3'-c]phenazine:

The intercalating DPPZ ligand is synthesized stepwise, first by oxidation of 1,10-phenanthroline to 1,10-phenanthroline-5,6-dione using a highly acidic medium[97] and then by formation of a Schiff base using 1,2-phenylenediamine[6] (scheme 34).

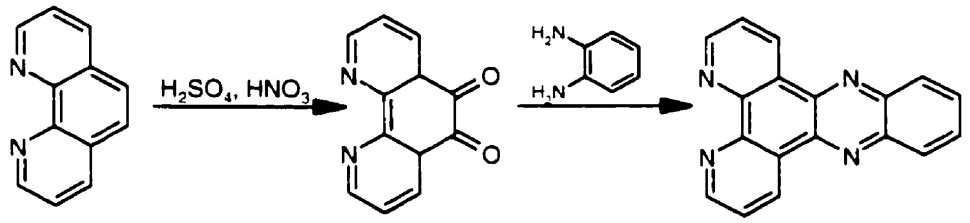

Scheme 34: Synthesis of DPPZ.

2.3.2- Synthesis of DPPZ complexes via removal of chlorides:

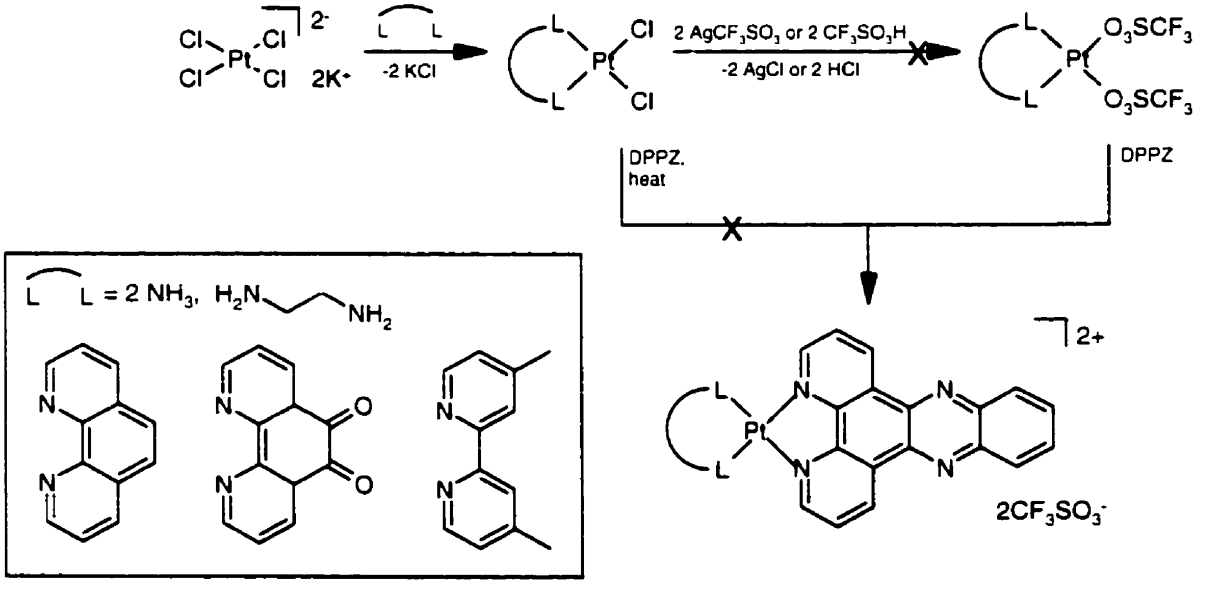

Scheme 35: Synthesis of DPPZ monomers via removal of chlorides.

Our first attempts to synthesize DPPZ complexes of platinum were done converting $K_2[PtCl_4]$ into the proper dichloro precursor (scheme 35).[98-100] This strategy involved displacement of the remaining two chloride ligands either by direct replacement with DPPZ[42,101] or by substitution with more labile $CF_3SO_3^-$ ligands and then by adding DPPZ to the reaction mixture.[102-104,109]

2.3.3- Synthesis of DPPZ complexes via removal of iodides:

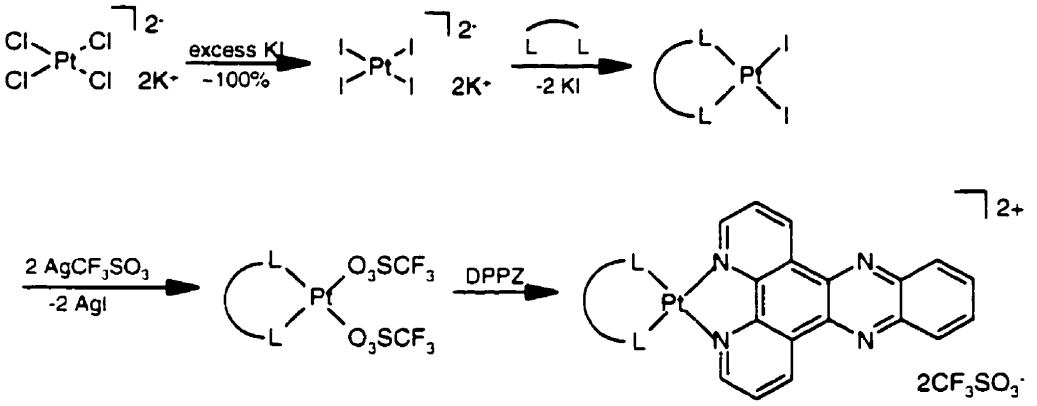

Scheme 36: Synthesis of DPPZ monomers via removal of iodides.

The previous synthetic route using dichloro precursors was modified due to the unsuccessful complete removal of the chloride ligands. Instead, $K_2[PtCl_4]$ was converted to $K_2[PtL_4]$ (scheme 36), and then into the corresponding diiodo precursor.[105-108] The following step involves as mentioned previously substitution of the remaining iodide ligands by labile $CF_3SO_3^-$ ligands followed by chelation with DPPZ.[108-109] This approach was successful in yielding the desired DPPZ monointercalators.

2.3.4- Synthesis of phenanthrenequinone diimine complexes:

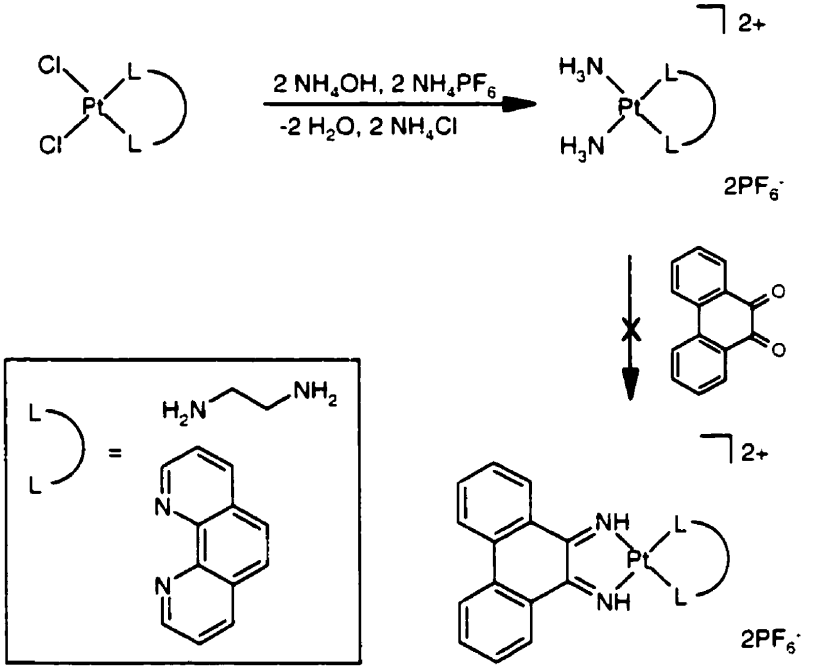

Scheme 37: Synthesis of phenanthrenequinone monomers.

The synthesis of only two phi complexes of platinum was attempted (scheme 37). The strategy involved formation of dichloro precursors[99-100] followed by coordination of ammine ligands.[110] Finally, in a basic medium, 9,10-phenanthrenequinone was added to form phi but these attempts were unsuccessful.[111]

2.4- Pt(II)-Based Molecular Architectures

The next goal of our research consists in the synthesis of platinum-based dimers composed of two DPPZ intercalative ends and of a linking unit. Applications of these dimers are numerous. For example, knowing that the DNA distance between two

histones is approximately 54 bp[14,112] and that DPPZ requires around 1-3 mol of base pair/mol of ligand for its binding stoichiometry,[56] this DNA becomes a potential site of intercalation for dimers. The presence of a bis-intercalator could trigger chromosomic shape modification and perhaps hinder proper separation of the former and newly synthesized chromosomes between the two cells during celluiar division.

Formation of Holliday structures is a known method for DNA repair by recombination.[14] In this process, two DNA duplexes of almost identical sequences are brought into close proximity and exchange parts of DNA strands between them. Bis-intercalating dimers thus become possible ways to bring DNA duplexes in close proximity. Moreover, by controlling the affinity of the intercalation for a precise base sequence, it thus becomes realistic to imagine that two duplexes of DNA of similar sequences could be linked by a dimer. Then, in the presence of recombination enzymes, this could lead to DNA strand exchange and repair of mismatches for example.

The fact that DPPZ intercalates mostly in AT rich regions[60] led to the idea of a more challenging application of bis-intercalating agents. The TATA box is known to be the binding site for transcription factors[113] and consists in the consensus sequence TATAAT located near position -30 of the transcription start site.[114] Transcription factor IIB of RNA polymerase interacts with this portion of DNA to form an initiation complex.[115] Our idea is to mimick the action of a repressor and thus, hinder transcription by RNA polymerase even at high concentration of substrate of the protein coded by this gene. A good example of this kind of process is represented by *E. coli lac* repressor which blocks gene expression at low lactose concentration.[116] *lac* repressor interacts at two sites on the DNA duplex forcing it to form a loop. However, RNA polymerase still

binds to the promoter site as the repressor does not interfere with the binding site and we cannot exclude for now the possibility that intercalation of a dimer would allow binding of the polymerase due to unwinding and lengthening of the DNA around the intercalation site.

2.5- Target Dimer

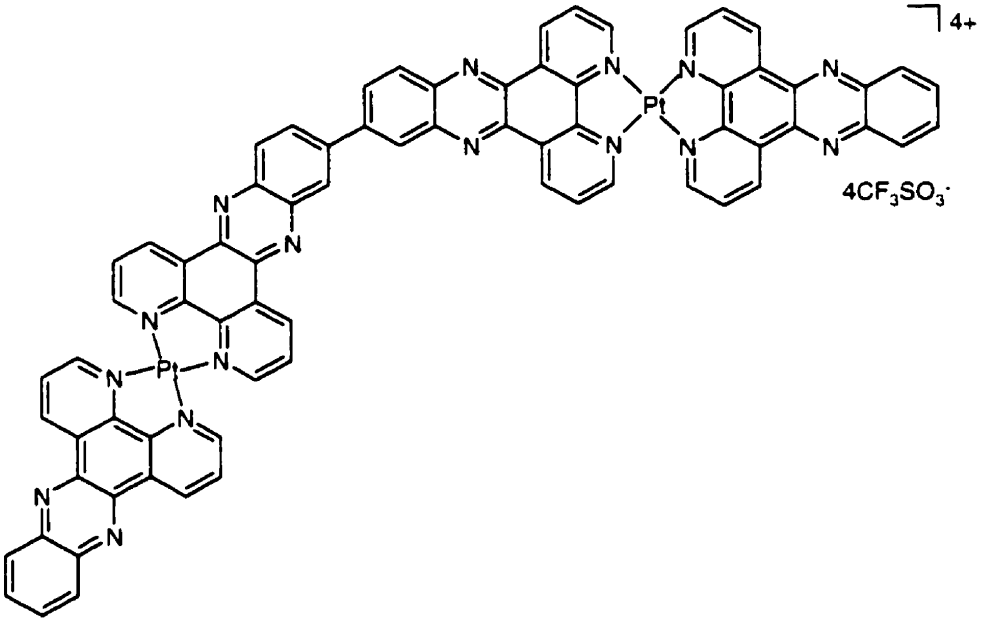

Scheme 38: Target Dimer.

A first dimer has been designed which consists in DPPZ(11-11')DPPZ as the linker (scheme 38). This dimer is not completely rigid as the bond between DPPZ units of the linker allows rotation. However, it can only intercalate its two DPPZ ends by intermolecular cross-linking. This dimer thus becomes an interesting candidate to study the relation between rigidity, flexibility, intramolecular, and intermolecular cross-linking.

2.6- Synthetic Strategy

2.6.1- Synthesis of DPPZ(11-11')DPPZ:

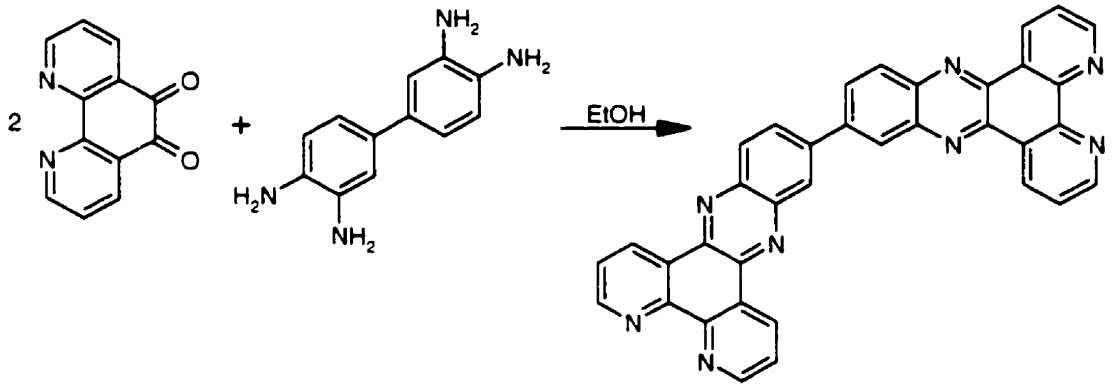

Scheme 39: Synthesis of DPPZ(11-11')DPPZ.

The linker was synthesized using a similar procedure as described for DPPZ (scheme 39).[6] It is the result of a Schiff base formation between 1,10-phenanthroline-5,6-dione and 3,3'-diamonibenzidine.

2.6.2- Synthesis of [(DPPZ)Pt{DPPZ(11-11')DPPZ}Pt(DPPZ)]$(CF_3SO_3)_4$:

Due to the low solubility of DPPZ(11-11')DPPZ, [Pt(phendione)DPPZ]$(CF_3SO_3)_2$ was used as a reagent for the condensation with 3,3'-diaminobenzidine. The reasons for this stepwise strategy will be discussed in the results and discussion section. Scheme 40 shows the successful synthesis of the Pt bis-intercalator.

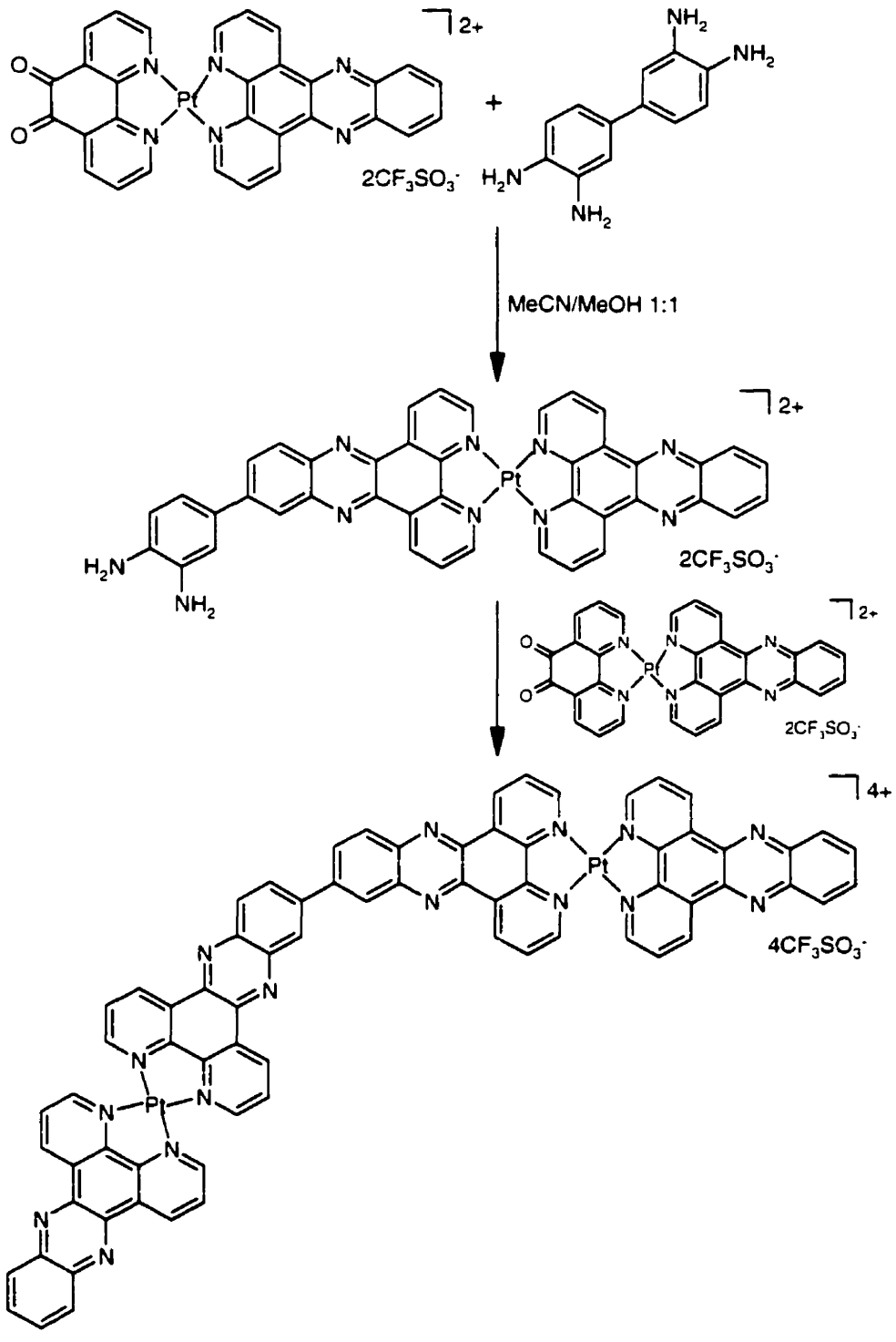

Scheme 40: Synthesis of [(DPPZ)Pt{DPPZ(11-11')DPPZ}Pt(DPPZ)](CF$_3$SO$_3$)$_4$.

Chapter 3. Experimental Section

3.1- Materials and Apparatus

$K_2[PtCl_4]$ was purchased from Pressure Chemicals, Calf Thymus DNA from Sigma, NH_4OH from Fischer, and all other reagents were purchased from Aldrich. ^1H NMR spectra were obtained using a JEOL-270, Mercury 300, and Mercury 400 NMR spectrometers. ^{13}C and ^{19}F NMR spectra were obtained using a Jeol-270 NMR spectrometer. UV-Vis measurements were performed with a CARY 300 Bio spectrophotometer. IR spectra were obtained from a BRUCKNER IFS 48 spectrometer. MALDI-TOF mass spectrometry was carried out using a KOMPACT MALDI III with a dithranol matrix. FAB mass spectra were recorded on a KRATOS MS 25RFA mass spectrometer using 3-nitrobenzyl alcohol as a matrix. Elemental analyses were performed at Quantitative Technologies Inc. Best fittings for binding constants and binding site size were determined using Sigma Plot software.

3.2- Successful Syntheses

Synthesis of 1,10-phenanthroline-5,6-dione:

1,10-phenanthroline-5,6-dione was synthesized as previously described.[102] An ice cold mixture of concentrated H_2SO_4 (40 mL) and HNO_3 (20 mL) was slowly added to the walls of the flask to 4.0 g (0.022 mol) of 1,10-phenanthroline and 4.0 g (0.034 mol) of KBr. The mixture was heated to reflux for 3h. The hot yellow solution was poured over 500 mL of ice and neutralized carefully with 10M KOH until neutral to slightly acidic pH.

Extraction with $CHCl_3$ followed by drying with Na_2SO_4 and removal of solvent gave the expected molecule which was recrystallized from toluene.

Yield: 4.20g (90.9%).

^{1}H NMR (ppm, $CDCl_3$): 9.14 (d, 2H), 8.52 (d, 2H), 7.60 (dd, 2H). ^{1}H NMR (ppm, DMSO-d_6): 9.00 (d, 2H), 8.41 (d, 2H), 7.68 (dd, 4H). IR: 1683.2 cm^{-1} (C=O).

Synthesis of dipyrido[3,2-a:2'-3'-c]phenazine:

Dipyrido[3,2-a:2'-3'-c]phenazine was synthesized as previously described.[6] 1,10-Phenanthroline-5,6-dione (0.50 g, 2.38 mmol) in the minimum amount of ethanol and 0.50g (4.62 mmol) of 1,2-phenylenediamine also in minimum ethanol were mixed and the solution boiled for 5 min. The brown crystals obtained on cooling were collected by vacuum filtration and recrystallized from aqueous ethanol.

Yield: 0.538 g (80.0%).

m.p. 248 °C. ^{1}H NMR (ppm, DMSO-d_6): 9.53 (d, 2H), 9.21 (d, 2H), 8.39 (dd, 2H), 8.08 (dd, 2H), 7.94 (dd, 2H). ^{1}H NMR (ppm, acetone-d_6): 9.63 (d, 2H), 9.21 (d, 2H), 8.40 (dd, 2H), 8.05 (dd, 2H), 7.92 (dd, 2H). UV-Vis (ethanol): λ_{max}= 241, 270, 294, 342, 350, 358, 366, 378 nm.

Synthesis of *cis*-[$Pt(NH_3)_2Cl_2$]:

cis-[$Pt(NH_3)_2Cl_2$] was synthesized as previously described.[98] $K_2[PtCl_4]$ (0.415 g, 1.00 mmol) was dissolved in 7.50 mL of water and 0.25 mL of conc HCl, 0.30 g (5.61 mmol) of NH_4Cl and about 1.00 mL of 3M aqueous ammonia (until neutral to litmus) were then added. An additional 0.68 mL of a 3M ammonia solution was added and the

solution refrigerated until the precipitation of a greenish yellow solid appeared to be complete and the supernatant liquid color has changed from deep red to light yellow (24 to 48h). The precipitate was collected by vacuum filtration and washed with several portions of ice water. The solid was then dissolved in 15 mL of boiling 0.1 N HCl and filtered while hot. The filtrate was then cooled in an ice bath for 2h. The yellow crystals were collected by vacuum filtration, washed with ice water, and dried.

Yield: 0.18 g (59.3%).

^{1}H NMR (ppm, DMSO-d_6): 4.22 (s, 6H).

Synthesis of [Pt(en)Cl_2]:

[Pt(en)Cl_2] was synthesized with slight modifications of a previously described procedure.[99] K_2[$PtCl_4$] (0.30 g, 0.72 mmol) was dissolved in 3 mL of water and 3 mL of a 5% ethylenediamine solution in water were then added. The solution was stirred at room temperature until a yellow solid was observed. The solution was then filtered and more ethylenediamine solution was added to the filtrate. The above steps were continuously carried out over 1h until the pink salt [$Pt(en)_2$][$PtCl_4$] began to separate. The solid collected was then dissolved in boiling 0.1 N HCl solution and filtered while hot. The filtrate was then cooled in an ice bath for 2h. The yellow crystals were collected by vacuum filtration, washed with ice water, and dried.

Yield: 0.20 g (51.6%).

^{1}H NMR (ppm, DMSO-d_6): 5.32 (s, 4H), 2.23 (s, 4H).

Synthesis of [Pt(phen)Cl_2]:

[Pt(phen)Cl_2] was synthesized as previously described.[100] $K_2[PtCl_4]$ (0.40 g, 0.96 mmol) in 50 mL of water, 0.174 g (0.96 mmol) of 1,10-phenanthroline, and 2 mL of 2 N HCl were heated to boiling for five minutes. The solid that formed was collected by vacuum filtration and washed with 0.8 N HCl, diethyl ether, and dried.

Yield: 0.32g (74.6%).

^{1}H NMR (ppm, DMSO-d_6): 9.27 (d, 2H), 8.95 (d, 2H), 8.29 (s, 2H), 8.13 (dd, 2H).

Synthesis of [Pt(Me_2bpy)Cl_2]:

[Pt(Me_2bpy)Cl_2] was synthesized as previously described.[100] $K_2[PtCl_4]$ (0.10 g, 0.24 mmol) in 50 mL of water, 0.46 g (0.24 mmol) of 4,4'-dimethyl-2,2'-bipyridine, and 2 mL of 2 N HCl were heated to boiling for five minutes. The solid that formed was collected by vacuum filtration and washed with 0.8 N HCl, diethyl ether, and dried.

Yield: 0.07 g (65.4%).

^{1}H NMR (ppm, DMSO-d_6): 9.21 (d, 2H), 8.41 (s, 2H), 7.62 (d, 2H), 2.47 (s, 6H).

Synthesis of [Pt(DPPZ)Cl_2]:

[Pt(DPPZ)Cl_2] was synthesized with slight modifications from a previously described procedure.[117] $K_2[PtCl_4]$ (0.20 g, 0.48 mmol) in water and 0.14 g (4.8 mmol) of DPPZ in ethanol were heated to boiling until a brown solid could be observed. The solid was collected by vacuum filtration and washed with ethanol, water, diethyl ether, and then dried.

Yield: 0.18 g (66.7%).

^{1}H NMR (ppm, DMSO-d_6): 9.86 (m, 4H), 8.51 (m, 4H), 8.19 (dd, 2H).

Synthesis of *cis*-[$Pt(NH_3)_2I_2$]:

cis-[$Pt(NH_3)_2I_2$] was synthesized according to two previous literature procedures.[105,106] $K_2[PtCl_4]$ (0.05 g, 0.12 mmol) in water was allowed to react with 0.91g (5.48 mmol) of an excess of KI for 30 min at room temperature. Then, the solution was treated with 2 equivalents of NH_4NO_3 and 2 equivalents of KOH. After 2h, the *cis*-[$Pt(NH_3)_2I_2$] was filtered, washed with hot water and subsequently ice-cold ethanol and ether, and dried.

Yield: 0.0385 g (66.2%).

^{1}H NMR (ppm, acetone-d_6): 3.86 (s, 6H).

Synthesis of [$Pt(en)I_2$]:

[$Pt(en)I_2$] was synthesized as previously described.[107] $K_2[PtCl_4]$ (0.104 g, 0.25 mmol) in water was allowed to react with 0.415 g (2.45 mmol) of an excess of KI for 30 min at room temperature. Addition of a 0.25 mmol solution of ethylenediamine in 1 mL of water resulted in orange-yellow precipitate which was immediately collected by vacuum filtration and washed with water and diethyl ether, and dried.

Yield: 0.082 g (64.7%).

^{1}H NMR (ppm, acetone-d_6): 4.81 (s, 4H), 2.74 (s, 4H).

Synthesis of [Pt(phen)I_2]:

[Pt(phen)I_2] was synthesized with slight modifications from previously described procedures.[105,108] $K_2[PtCl_4]$ (0.10 g, 0.24 mmol) in water was allowed to react with 1.82 g (10.96 mmol) of an excess of KI for 30 min at room temperature. Then, 0.0432 g (0.24 mmol) of 1,10-phenanthroline dissolved in the minimum volume of a slightly acidic HI water (5 mL H_2O, 3 drops conc. HI) solution was added and a greenish yellow precipitate began to form. The suspension was left stirring for 1h at room temperature. The solid was then collected by vacuum filtration, washed with previously prepared HI aqueous solution followed by diethyl ether, and dried.

Yield: 0.104 g (68.9%).

^{1}H NMR (ppm, acetone-d_6): 9.51 (d, 2H), 9.26 (d, 2H), 8.51 (s, 2H), 8.40 (dd, 2H).

Synthesis of [Pt(Me_2bpy)I_2]:

[Pt(Me_2bpy)I_2] was synthesized with slight modifications from previously described procedures.[105,108] $K_2[PtCl_4]$ (0.10 g, 0.24 mmol) in water was allowed to react with 1.82 g (10.96 mmol) of an excess of KI for 30 min at room temperature. Then, 0.0442 g (0.24 mmol) of 4,4'-dimethyl-2,2'-bipyridine dissolved in the minimum volume of a slightly acidic HI water (5 mL H_2O, 3 drops conc. HI) solution was added and a yellowish precipitate began to form. The suspension was left stirring for 1h at room temperature. The solid was then collected by vacuum filtration washed with previously prepared HI aqueous solution followed by diethyl ether, and dried.

Yield: 0.1058 g (69.6%).

^{1}H NMR (ppm, acetone-d_6): 8.75 (d, 2H), 8.54 (s, 2H), 7.64 (d, 2H), 2.62 (s, 6H).

Synthesis of [Pt(phendione)I_2]:

[Pt(phendione)I_2] was synthesized with slight modifications from previously described procedures.[105,108,117] $K_2[PtCl_4]$ (0.10 g, 0.24 mmol) of in water was allowed to react with 1.82 g (10.96 mmol) of an excess of KI for 30 min at room temperature. Then, 0.0504 g (0.24 mmol) of 1,10-phenanthroline-5,6-dione dissolved in methanol was added and the mixture heated to reflux for 5 minutes. A red solid began to separate and more product was obtained by evaporation of methanol. The solid was then collected by vacuum filtration, washed with water and diethyl ether, and dried.

Yield: 0.086 g (54.2%).

^{1}H NMR (ppm, DMSO-d_6): 10.19 (d, 2H), 8.88 (d, 2H), 8.09 (dd, 2H). ^{1}H NMR (ppm, acetone-d_6): 9.10 (d, 2H), 8.49 (d, 2H), 7.75 (dd, 2H). MALDI-TOF: 666.4 [M + Li^+]. UV-Vis (CH_3CN): λ_{max}= 245, 278, 397 nm. IR: 1689.5 cm^{-1} (C=O).

Synthesis of [Pt(DPPZ)I_2]:

[Pt(DPPZ)I_2] was synthesized with slight modifications from previously described procedures.[105,108,117] $K_2[PtCl_4]$ (0.05 g, 0.12 mmol) in water was allowed to react with 0.909 g (5.48 mmol) of an excess of KI for 30 min at room temperature. Then, 0.0339 g (0.12 mmol) of DPPZ dissolved in the minimum amount of a methanol/HI (5 mL MeOH, 3 drops conc. HI) solution was added and the mixture heated to reflux for 10 minutes. The mixture was allowed to cool down and the solid was collected by vacuum filtration, washed with water, methanol, diethyl ether, and dried.

Yield: 0.0632 g (72.0%)

^{1}H NMR (ppm, DMSO-d_6): 10.37 (d, 2H), 9.88 (d, 2H), 8.49 (dd, 2H), 8.34 (dd, 2H), 8.18 (dd, 2H).

Synthesis of *cis*-[$Pt(NH_3)_2(CF_3SO_3)_2$]:

cis-[$Pt(NH_3)_2(CF_3SO_3)_2$] was synthesized as previously described.[108] $AgCF_3SO_3$ (0.053 g, 0.207 mmol) in acetone-d_6 (1.5 mL) was added to a solution of 0.050 g (0.1035 mmol) *cis*-[$Pt(NH_3)_2I_2$] also in acetone-d_6 (1.0 mL) under inert atmosphere. The solution was left stirring for 2h at room temperature with the exclusion of light. AgI formed was removed by centrifugation and the supernatant used for the next step.

^{1}H NMR (ppm, acetone-d_6): 5.01 (s, 6H).

Synthesis of [$Pt(NH_3)_2$DPPZ]($CF_3SO_3)_2$:

[$Pt(NH_3)_2$DPPZ]($CF_3SO_3)_2$ was synthesized with the help of a previously described procedure.[109] DPPZ (0.0292 g, 0.1035 mmol) was dissolved in the minimum volume of acetone (~20 mL) and added to [$Pt(NH_3)_2(CF_3SO_3)_2$] in acetone-d_6 (2.5 mL). The solution was stirred overnight under inert atmosphere. The following day, the solution was centrifuged and the supernatant kept. Acetone was evaporated and the solid washed with CH_2Cl_2. The solid was then dissolved in deionized water, the solution was filtered, and the filtrate containing [$Pt(NH_3)_2$DPPZ]($CF_3SO_3)_2$ evaporated.

Yield: 0.0307 g (36.7%).

^{1}H NMR (ppm, DMSO-d_6): 10.02 (d, 2H), 9.22 (d, 2H), 8.60 (dd, 2H), 8.52 (dd, 2H), 8.30 (dd, 2H), 5.56 (s, 6H). ^{1}H NMR (ppm, acetone-d_6): 10.13 (d, 2H), 9.50 (d, 2H), 8.55 (dd, 2H), 8.48 (dd, 2H), 8.26 (dd, 2H), 5.59 (s, 6H). ^{13}C NMR (ppm, DMSO-d_6): 151.92,

150.67, 142.30, 139.29, 137.55, 133.60, 130.45, 129.78, 128.03, 121,60 (q). ^{19}F NMR (ppm, DMSO-d_6): -77.67. MALDI-TOF: 815.9 [M + Li^+]. UV-Vis (CH_3CN): λ_{max}= 208, 270, 341, 359, 377 nm. Anal. Calcd for $C_{20}H_{16}N_6F_{12}S_2O_6Pt$: C, 29.67; H, 1.99; N, 10.38. Found: C,; H,; N,.

Synthesis of [Pt(en)(CF_3SO_3)$_2$]:

[Pt(en)(CF_3SO_3)$_2$] was synthesized as previously described.[108] $AgCF_3SO_3$ (0.050 g, 0.196 mmol) in acetone-d_6 (1.5 mL) was added to a solution of 0.050 g (9.80×10^{-5} mol) [Pt(en)I_2] also in acetone-d_6 (1.0 mL) under inert atmosphere. The solution was left stirring for 2h at room temperature with the exclusion of light. AgI formed was removed by centrifugation and the supernatant used for the next step.

^1H NMR (ppm, acetone-d_6): 6.11 (s, 4H), 2.79 (s, 4H).

Synthesis of [Pt(en)DPPZ](CF_3SO_3)$_2$:

[Pt(en)DPPZ](CF_3SO_3)$_2$ was synthesized with the help of a previously described procedure.[109] DPPZ (0.0223 g, 7.90×10^{-5} mol) was dissolved in the minimum volume of acetone (~20 mL) and added to [Pt(en)(CF_3SO_3)$_2$] in acetone-d_6 (2.5 mL). The solution was stirred overnight under inert atmosphere. The following day, the solution was centrifuged and the solid was dissolved in deionized water (3 mL), filtered, and the filtrate was kept. Water was then evaporated and the complex dried.

Yield: 0.038 g (46.3%).

^1H NMR (ppm, DMSO-d_6): 9.87 (d, 2H), 9.20 (d, 2H), 8.46 (dd, 2H), 8.44 (dd, 2H), 8.23 (dd, 2H), 7.00 (s, 4H), 2.79 (s, 4H). ^1H NMR (ppm, CD_3CN): 10.01 (d, 2H), 9.01 (d, 2H),

8.53 (dd, 2H), 8.28 (dd, 2H), 8.21 (dd, 2H), 5.64 (s, 4H), 2.95 (s, 4H). ^{13}C NMR (ppm, DMSO-d_6): 153.35, 150.81, 142.51, 139.81, 137.82, 133.60, 130.82, 129.99, 128.51, 121.54 (q), 47.83. ^{19}F NMR (ppm, DMSO-d_6): -77.67. MALDI-TOF: 842.2 [M + Li^+]. UV-Vis (CH_3CN): λ_{max}= 205, 281, 358, 376 nm. Anal. Calcd for $C_{22}H_{18}N_6F_{12}S_2O_6Pt$: C, 31.62; H, 2.17; N, 10.05. Found: C, 31.62; H, 2.07; N, 9.68. MS-FAB : *m/z* (%): 697 [M^{2+} + $CF_3SO_3^-$], 536 [M^{2+}].

Synthesis of [Pt(phen)(CF_3SO_3)$_2$]:

[Pt(phen)(CF_3SO_3)$_2$] was synthesized as previously described.[108] $AgCF_3SO_3$ (0.041 g, 0.158 mmol) in acetone-d_6 (1.5 mL) was added to a solution of 0.0500 g (7.90 x 10^{-5} mol) [Pt(phen)I_2] also in acetone-d_6 (1.0 mL) under inert atmosphere. The solution was left stirring for 2h at room temperature with the exclusion of light. AgI formed was removed by centrifugation and the supernatant used for the next step.

^1H NMR (ppm, acetone-d_6): 9.46 (d, 2H), 9.17 (d, 2H), 8.43 (s, 2H), 8.35 (dd, 2H).

Synthesis of [Pt(phen)DPPZ](CF_3SO_3)$_2$:

[Pt(phen)DPPZ](CF_3SO_3)$_2$ was synthesized with the help of a previously described procedure.[109] DPPZ (0.0223 g, 7.90 x 10^{-5} mol) was dissolved in the minimum volume of acetone (~20 mL) and added to [Pt(phen)(CF_3SO_3)$_2$] in acetone-d_6 (2.5 mL). The solution was stirred overnight under inert atmosphere. The following day, the solution was centrifuged and the supernatant kept Acetone was evaporated and the solid washed with CH_2Cl_2 and deionized water. The solid was then dissolved in distilled acetone, the solution was filtered, and the filtrate containing [Pt(phen)DPPZ](CF_3SO_3)$_2$ evaporated.

Yield: 0.026 g (34.4%).

^{1}H NMR (ppm, DMSO-d_6): 19.66 (d, 2H), 9.27 (m, 4H), 9.04 (d, 2H), 8.33 (dd, 2H), 8.32 (s, 2H), 8.20 (m, 4H), 8.08 (dd, 2H). ^{1}H NMR (ppm, acetone-d_6): 10.06 (d, 2H), 9.52 (d, 2H), 9.45 (d, 2H), 9.18 (d, 2H), 8.53 (dd, 2H), 8.43 (s, 2H), 8.42 (dd, 2H), 8.35 (dd, 2H), 8.17 (dd, 2H). ^{13}C NMR (ppm, DMSO-d_6): 149.81, 148.09, 142.43, 141.99, 141.25, 139.06, 137.75, 137.67, 132.88, 130.02, 129.55, 128.78, 128.00, 127.36, 124.67, 121.50 (q). ^{19}F NMR (ppm, DMSO-d_6): -77.62. MALDI-TOF: 963.9 [M + Li^+]. UV-Vis (CH_3CN): λ_{max}= 207, 270, 358, 377 nm

Synthesis of [Pt(Me_2bpy)(CF_3SO_3)$_2$]:

[Pt(Me_2bpy)(CF_3SO_3)$_2$] was synthesized as previously described.[108] $AgCF_3SO_3$ (0.041 g, 0.158 mmol) in acetone-d_6 (1.5 mL) was added to a solution of 0.050 g (7.90 x 10^{-5} mol) [Pt(dmbp)I_2] also in acetone-d_6 (1.0 mL) under inert atmosphere. The solution was left stirring for 2h at room temperature with the exclusion of light. AgI formed was removed by centrifugation and the supernatant used for the next step.

^{1}H NMR (ppm, acetone-d_6): 9.10 (d, 2H), 8.74 (s, 2H), 7.96 (d, 2H), 2.73 (s, 6H).

Synthesis of [Pt(Me_2bpy)DPPZ](CF_3SO_3)$_2$:

[Pt(Me_2bpy)DPPZ](CF_3SO_3)$_2$ was synthesized with the help of a previously described procedure.[109] DPPZ (0.0223 g, 7.90 x 10^{-5} mol) was dissolved in the minimum volume of acetone (~20 mL) and added to [Pt(Me_2bpy)(CF_3SO_3)$_2$] in acetone-d_6 (2.5 mL). The solution was stirred overnight under inert atmosphere. The following day, the solution was centrifuged and the supernatant kept. Acetone was evaporated and the solid

washed with CH_2Cl_2 and deionized water. The solid was then dissolved in distilled acetone, the solution was filtered, and the filtrate containing $[Pt(Me_2bpy)DPPZ](CF_3SO_3)_2$ evaporated.

Yield: 0.030 g (39.7%).

^1H NMR (ppm, DMSO-d_6): 9.44 (d, 2H), 9.18 (d, 2H), 8.64 (d, 2H), 8.42 (s, 2H), 8.13 (m, 4H), 7.98 (dd, 2H), 7.65 (d, 2H). ^1H NMR (ppm, acetone-d_6): 10.04 (d, 2H), 9.50 (d, 2H), 8.85 (d, 2H), 8.65 (s, 2H), 8.47 (m, 4H), 8.19 (dd, 2H), 7.83 (d, 2H), 2.69 (s, 6H). ^{13}C NMR (ppm, DMSO-d_6): 155.16, 149.99, 147.97, 146.44, 142.14, 141.94, 139.40, 137.44, 132.82, 129.65, 127.93, 127.18, 124.42, 121.49 (q), 21.74. ^{19}F NMR (ppm, DMSO-d_6): -77.65. MALDI-TOF: 966.3 [M + Li^+]. UV-Vis (CH_3CN): λ_{max}= 202, 273, 300, 358, 376. Anal. Calcd for $C_{32}H_{22}N_6F_{12}S_2O_6Pt$: C, 40.05; H, 2.31; N, 8.76. Found: C, 40.54; H, 2.70; N, 8.45. MS-FAB : *m/z* (%): 810 [M^{2+} + $CF_3SO_3^-$], 661 [M^{2+}].

Synthesis of $[Pt(phendione)(CF_3SO_3)_2]$:

$[Pt(phendione)(CF_3SO_3)_2]$ was synthesized as previously described.[108] $AgCF_3SO_3$ (0.039 g, 0.151 mmol) in acetone-d_6 (1.5 mL) was added to a solution of 0.0500 g (7.586 x 10^{-5} mol) $[Pt(phendione)I_2]$ also in acetone-d_6 (1.0 mL) under inert atmosphere. The solution was left stirring for 2h at room temperature with the exclusion of light. AgI formed was removed by centrifugation and the supernatant used for the next step.

^1H NMR (ppm, acetone-d_6): 9.34 (d, 2H), 9.03 (d, 2H), 8.32 (dd, 2H).

Synthesis of [Pt(phendione)DPPZ]$(CF_3SO_3)_2$:

[Pt(phendione)DPPZ]$(CF_3SO_3)_2$ was synthesized with the help of a previously described procedure.[109] DPPZ (0.0214 g, 7.90 x 10^{-5} mol) was dissolved in the minimum volume of acetone (~20 mL) and added to [Pt(phendione)$(CF_3SO_3)_2$] in acetone-d_6 (2.5 mL). The solution was stirred overnight under inert atmosphere. The following day, the solution was centrifuged and the supernatant kept. Acetone was evaporated and the solid washed with CH_2Cl_2 and deionized water. The solid was then dissolved in distilled acetone, the solution was filtered, and the filtrate containing [Pt(phendione)DPPZ]$(CF_3SO_3)_2$ evaporated.

Yield: 0.038g (50.4%).

^{1}H NMR (ppm, DMSO-d_6): 9.72 (d, 2H), 9.28 (d, 2H), 8.97 (d, 2H), 8.42 (dd, 2H), 8.40 (d, 2H), 8.15 (dd, 2H), 8.12 (dd, 2H), 7.68 (dd, 2H). ^{1}H NMR (ppm, acetone-d_6): 10.10 (d, 2H), 9.51 (d, 2H), 9.14 (d, 2H), 8.66 (d, 2H), 8.48 (m, 4H), 8.18 (dd, 2H), 7.93 (dd, 2H). ^{13}C NMR (ppm, DMSO-d_6): 154.58, 150.91, 144.13, 142.27, 140.19, 140.15, 136.56, 136.30, 136.27, 132.51, 129.74, 128.34, 126.92, 126.51, 126.03, 121.50 (q). ^{19}F NMR (ppm, DMSO-d_6): -77.65. MALDI-TOF: 992.8 [M + Li^+]. UV-Vis (CH_3CN): λ_{max}= 201, 272, 357, 376 nm. IR: 1697.6 cm^{-1} (C=O). Anal. Calcd for $C_{32}H_{16}N_6F_{12}S_2O_8Pt$: C,; H,; N,. Found: C,; H,; N,.

Synthesis of [Ru(phen)$_2$DPPZ]$(PF_6)_2$:

[Ru(phen)$_2$DPPZ]$(PF_6)_2$ was synthesized as previousiy described.[53] A mixture of 0.100 g (0.184 mmol) of [Ru(phen)$_2Cl_2$]·$2H_2O$ and 0.0565 g (0.200 mmol) of DPPZ in 30 mL 1:1 methanol/water was refluxed for 4.5h under inert atmosphere.The deep red

solution was concentrated to 10%, diluted with 10 mL of water, boiled for 10 min., cooled in an ice bath, and filtered. NH_4PF_6 (aq.) was then added to precipitate the complex which was collected by vacuum filtration, washed with water and diethyl ether, and dried.

Yield: 2.02 g (75.6%).

^{1}H NMR (ppm, CD_3CN): 9.75 (d, 2H), 8.74 (m, 4H), 8.59 (dd, 2H), 8.39 (s, 4H), 8.34 (d, 2H), 8.28 (dd, 2H), 8.22 (d, 2H), 8.14 (d, 2H), 7.87 (dd, 2H), 7.70 (m, 4H).

Synthesis of $[Pt(NH_3)_2(en)](PF_6)_2$:

$[Pt(NH_3)_2(en)](PF_6)_2$ was synthesized as previously described with some modifications.[110] $[Pt(en)Cl_2]$ (0.0761 g, 0.233 mmol) in water and 0.9 mL of concentrated NH_4OH were boiled for 3h under inert atmosphere with the addition of more concentrated NH_4OH from time to time.The mixture was allowed to cool down, filtered, and the filtrate kept. NH_4PF_6 (aq.) was then added to precipitate the complex which was collected by vacuum filtration, washed with water and diethyl ether, and dried.

Yield: 0.078 g (57.8%).

^{1}H NMR (ppm, DMSO-d_6): 6.21 (s, 4H), 6.01 (s, 6H), 2.59 (s, 4H).

Synthesis of $[Pt(NH_3)_2(phen)](PF_6)_2$:

$[Pt(NH_3)_2(phen)](PF_6)_2$ was synthesized as previously described with some modifications.[110] $[Pt(phen)Cl_2]$ (0.100 g, 0.224 mmol) in water and 0.8 mL of concentrated NH_4OH were boiled for 15 min under inert atmosphere. The solution was allowed to cool down, filtered, and the filtrate kept. NH_4PF_6 (aq.) was then added to

precipitate the complex which was collected by vacuum filtration, washed with water and diethyl ether, and dried.

Yield: 0.087 g (55.6%).

^{1}H NMR (ppm, DMSO-d_6): 9.16 (d, 2H), 9.10 (d, 2H), 8.36 (s, 2H), 8.30 (dd, 2H), 5.46 (s, 6H).

Synthesis of $[Pt(CH_3CN)_2Cl_2]$:

$[Pt(CH_3CN)_2Cl_2]$ was synthesized as previously described.[109] $PtCl_2$ (4.0 g, 0.015 mol) was stirred in refluxing acetonitrile until a clear solution was obtained. The solution was filtered hot and reduced to a small volume. The solid that came out of solution was collected by vacuum filtration, washed with diethyl ether, and dried.

Yield: 2.098 g (84%).

Synthesis of $[Pt(PhCN)_2Cl_2]$:

$[Pt(PhCN)_2Cl_2]$ was synthesized as previously described.[118] Benzonitrile (0.0745 g, 0.723 mmol) was added to an aqueous solution of 0.100 g (0.241 mmol) of $K_2[PtCl_4]$. The solution was allowed to stand at room temperature until the complex crystallized from solution. The complex was then collected by vacuum filtration, washed with water, ethanol and diethyl ether, and dried.

Yield: 0.025 g (21.98%).

^{1}H NMR (ppm, DMSO-d_6): 8.09 (m, 4H), 7.90 (m, 2H), 7.71 (m, 4H).

Synthesis of $[Pt(phen)_2](PF_6)_2$:

$[Pt(phen)_2](PF_6)_2$ was synthesized as previously described.[119] An aqueous suspension of 0.0535 g (0.12 mmol) of $[Pt(phen)Cl_2]$ was heated under inert atmosphere in the presence of a small excess (2.0 mmol) of free 1,10-phenanthroline. The solution was filtered and NH_4PF_6 (aq.) was added to the filtrate. The solid was collected by vacuum filtration, washed with water and diethyl ether, and dried.

Yield: 0.0660 g (78.4%).

^{1}H NMR (ppm, DMSO-d_6): 9.64 (d, 4H), 9.24 (d, 4H), 8.48 (s, 4H), 8.36 (dd, 4H). MALDI-TOF: 705.7 [M + Li^+].

3.3- Synthesis of Pt(II) Dimers

Synthesis of DPPZ(11-11')DPPZ:

DPPZ(11-11')DPPZ was synthesized with the help of a previously described procedure.[6] 3,3'-Diaminobenzidine (0.0287 g, 0.135 mmol) was dissolved in absolute ethanol (8.0 mL). To this solution were added two equivalents (0.0563 g, 0.270 mmol) of 1,10-phenanthroline-5,6-dione also dissolved in absolute ethanol (15.0 mL). The mixture was refluxed for 3.5h under inert atmosphere. The precipitate was collected by vacuum filtration, washed with ethanol, CH_2Cl_2, diethyl ether, and dried.

Yield: 0.0629 g (83.5%).

^{1}H NMR (ppm, acetone-d_6): 10.25 (m, 4H), 9.63 (m, 4H), 9.17 (s, 2H), 8.95 (d, 2H), 8.80 (d, 2H), 8.62 (m, 4H). MALDI-TOF: 568.9 [M + Li^+].

Synthesis of [Pt(DPPZ){11-$(NH_2)_2$PhDPPZ}]$(CF_3SO_3)_2$:

[Pt(DPPZ){11-$(NH_2)_2$PhDPPZ}]$(CF_3SO_3)_2$ was synthesized with the help of previously described procedures.[77,78] [Pt(phendione)DPPZ]$(CF_3SO_3)_2$ (0.0521 g, 5.28 x 10^{-5} mol) and 0.0113 g (5.28 x 10^{-5} mol) of 3,3'-diaminobenzidine were dissolved in 2.5 mL of a 1:1 MeCN-MeOH solution. The mixture was heated at 65 °C for 5h under inert atmonphere. The solution immediately became deep red and a precipitate could be observed. The solid was collected by centrifugation, washed with MeOH, MeCN, and diethyl ether, and dried.

Yield: 0.0385 g (53.7%).

^{1}H NMR (ppm, DMSO-d_6): 9.55 (m, 4H), 9.21 (m, 4H), 8.34 (m, 8H), 7.94 (m, 4H), 7.22 (s, 1H), 7.11 (d, 1H), 6.56 (d, 1H), 4.96 (s, 2H), 4.71 (s, 2H). MALDI-TOF: 1123.1 [M + Li^+].

Synthesis of [(DPPZ)Pt{DPPZ(11-11')DPPZ}Pt(DPPZ)]$(CF_3SO_3)_4$:

[(DPPZ)Pt{DPPZ(11-11')DPPZ}Pt(DPPZ)]$(CF_3SO_3)_4$ was synthesized by dissolving 0.0116 g (8.53 x 10^{-6} mol) of [Pt(DPPZ){11-$(NH_2)_2$PhDPPZ}]$(CF_3SO_3)_2$ and 0.0084 g (8.53 x 10^{-6} mol) of [Pt(phendione)DPPZ]$(CF_3SO_3)_2$ in 2 mL of DMSO. The solution was stirred at room temperature for 4 hours. The solvent was then evaporated and the solid washed with CH_2Cl_2 and deionized water. The solid was then dissolved in dissolved in acetonitrile and filtered. The filtrate was evaporated to dryness.

Yield: 0.014g (77.6%).

^{1}H NMR (ppm, DMSO-d_6): 9.52 (d, 8H), 9.17 (d, 8H), 8.34 (m, 8H), 8.02 (m, 6H), 7.91 (m, 8H). MALDI-TOF: 2114.0 [M].

3.4- Purification of Calf Thymus DNA

Calf thymus DNA has been purified as previously described.[41] Samples of 1-2 mg of DNA/mL of water, dissolved by stirring at 4 °C, were repeatedly shaken with a 1:1 mixture of chloroform-isoamylic acid in order to extract protein. The resulting solution, after centrifugation, was dialyzed against 1 mM phosphate buffer 10 mM NaCl pH 7.0. DNA concentration, expressed in base pair, was calculated spectrophotometrically using an $\varepsilon_{260\,nm}$ value of $1.31 \times 10^{-4}\ M^{-1}\ cm^{-1}$.[115]

3.5-Attempted Syntheses

Synthesis of $[Pt(L\text{-}L)Cl_2]$ (L-L = en, phen, Me_2bpy, DPPZ):

Attempts to synthesize $[Pt(L\text{-}L)Cl_2]$ were done with the help of a previously described procedure.[121] $[Pt(CH_3CN)_2Cl_2]$ was dissolved in minimum acetonitrile and a 50% excess of L also dissolved in minimum acetonitrile added. The solution was heated at 70 °C for 1.5h. The mixture was allowed to cool down and the solid was collected by vacuum filtration.

Synthesis of $[Pt(phendione)Cl_2]$:

An attempt to synthesize $[Pt(phendione)Cl_2]$ was done with the help of a previously described procedure.[122] 0.0250 g (5.29×10^{-5} mol) of $[Pt(PhCN)_2Cl_2]$ was dissolved in 5 mL of CH_2Cl_2. 0.0111 g (5.29×10^{-5} mol) of 1,10-phenanthroline-5,6-dione dissolved in 5 mL of CH_2Cl_2 was added and stirred overnight. The following day, the solid was collected by vacuum filtration.

Synthesis of $[Pt(L\text{-}L)DPPZ]^{2+}$ starting with $[Pt(L\text{-}L)Cl_2]$ (L-L = $2NH_3$, en, phen, Me_2bpy):

-Heating[42]: $[Pt(L\text{-}L)Cl_2]$ was suspended in a 1:1 water/methanol solution and heated under inert atmosphere until dissolution in the presence of a 10 times excess of DPPZ. The solution was then filtered and NH_4PF_6 (aq.) was added to the filtrate to precipitate the $[Pt(L\text{-}L)DPPZ]^{2+}$ complex in the form of a PF_6^- salt.

-Heating[101]: A suspension of $[Pt(L\text{-}L)Cl_2]$ in water with a very slight excess of DPPZ was kept at 50 °C for 18h under inert atmosphere. The solution was allowed to cool down and was filtered. NH_4PF_6 (aq.) was then added to the filtrate to precipitate the $[Pt(L\text{-}L)DPPZ]^{2+}$ complex in the form of a PF_6^- salt.

-$AgCF_3SO_3/CH_3CN$[109]: $[Pt(L\text{-}L)Cl_2]$ was dissolved in acetonitrile under inert atmosphere and twice the stoichiometric amount of $AgCF_3SO_3$ also dissolved in acetonitrile was added. The solution was stirred for 2h at room temperature with the exclusion of light. Precipitated AgCl was removed by vacuum filtration and the stoichiometric amount of DPPZ dissolved in minimum acetonitrile was added to the filtrate. The mixture was stirred overnight. The following day, the solution was filtered and NH_4PF_6 (aq.) was added to the filtrate to precipitate the $[Pt(L\text{-}L)DPPZ]^{2+}$ complex in the form of a PF_6^- salt.

-$AgCF_3SO_3$/DMSO[102]: $[Pt(L\text{-}L)Cl_2]$ was dissolved in DMSO-d_6 with slight warming under inert atmosphere and twice the stoichiometric amount of $AgCF_3SO_3$ also dissolved in DMSO-d_6 was added. The solution was stirred for 1h at 75 °C with the exclusion of light and then filtered to eliminate precipitated AgCl. The stoichiometric amount of

DPPZ dissolved in minimum DMSO-d_6 was added to the filtrate and the mixture was stirred overnight.

-$AgCF_3SO_3$/DMF[103]: $[Pt(L\text{-}L)Cl_2]$ was dissolved in DMF under inert atmosphere and twice the stoichiometric amount of $AgCF_3SO_3$ also dissolved in DMF was added. The solution was allowed to and then filtered to eliminate precipitated AgCl. The stoichiometric amount of DPPZ dissolved in minimum DMF was added to the filtrate and the mixture was stirred overnight.

-CF_3SO_3H[104]: To 2.33 mmol of $[Pt(L\text{-}L)Cl_2]$ were added 4 mL of CF_3SO_3H under inert atmosphere. The mixture was stirred at 100 °C for 2h, removed and cooled in an ice-bath before removing the inert atmosphere. 50 mL of diethyl ether were then added very carefully with strong stirring. The precipitate was collected by vacuum filtration, washed with diethyl ether, and dried. The solid was dissolved in minimum 1:1 CH_2Cl_2/MeCN and the stoichiometric amount of DPPZ dissolved in the minimum amount of the same solvent mixture was added. The solution was left stirring overnight. The following day, the mixture was filtered and NH_4PF_6 (aq.) was added to the filtrate to precipitate the $[Pt(L\text{-}L)DPPZ]^{2+}$ complex in the form of a PF_6^- salt.

Synthesis of $[Pt(L\text{-}L)DPPZ]^{2+}$ starting with $[Pt(DPPZ)Cl_2]$ (L-L = $2NH_3$, en, phen, Me_2bpy):

-Heating[42]: $[Pt(DPPZ)Cl_2]$ was suspended in minimum ethanol and heated under inert atmosphere until dissolution in the presence of a 10 times excess of L-L. The solution

was then filtered and NH_4PF_6 (aq.) was added to the filtrate to precipitate the [Pt(L-L)DPPZ]$^{2+}$ complex in the form of a PF_6^- salt.

-Heating[101]: A suspension of [Pt(DPPZ)Cl_2] in water with a very slight excess of L-L was kept at 50 °C for 18h under inert atmosphere. The solution was allowed to cool down and was filtered. NH_4PF_6 (aq.) was then added to the filtrate to precipitate the [Pt(L-L)DPPZ]$^{2+}$ complex in the form of a PF_6^- salt.

-$AgCF_3SO_3/CH_3CN$[109]: [Pt(DPPZ)Cl_2] was dissolved in acetonitrile under inert atmosphere and twice the stoichiometric amount of $AgCF_3SO_3$ also dissolved in acetonitrile was added. The solution was stirred for 2h at room temperature with the exclusion of light. Precipitated AgCl was removed by vacuum filtration and the stoichiometric amount of L-L dissolved in minimum acetonitrile was added to the filtrate. The mixture was added to the filtrate to precipitate the [Pt(L-L)DPPZ]$^{2+}$ complex in the form of a PF_6^- salt.

-$AgCF_3SO_3$/DMSO[102]: [Pt(DPPZ)Cl_2] was dissolved in DMSO-d_6 with slight warming under inert atmosphere and twice the stoichiometric amount of $AgCF_3SO_3$ also dissolved in DMSO-d_6 was added. The solution was stirred for 1h at 75 °C with the exclusion of light and then filtered to eliminate precipitated AgCl. The stoichiometric amount of L-L dissolved in minimum DMSO-d_6 was added to the filtrate and the mixture was stirred overnight.

-CF_3SO_3H[104]: To 2.33 mmol of [Pt(DPPZ)Cl_2] were added 4 mL of CF_3SO_3H under inert atmosphere. The mixture was stirred at 100 °C for 2h, removed and cooled in an ice-bath before removing the inert atmosphere. 50 mL of diethyl ether were then added very carefully with strong stirring. The precipitate was collected by vacuum filtration, washed with diethyl ether, and dried. The solid was dissolved in minimum 1:1 CH_2Cl_2/MeCN and the stoichiometric amount of L-L dissolved in the minimum amount of the same solvent mixture was added. The solution was left stirring overnight. The following day, the mixture was filtered and NH_4PF_6 (aq.) was added to the filtrate to precipitate the $[Pt(L\text{-}L)DPPZ]^{2+}$ complex in the form of a PF_6^- salt.

Synthesis of $[Pt(DPPZ)_2](PF_6)_2$:

An attempt to synthesize $[Pt(DPPZ)_2](PF_6)_2$ was done with the help of a previously described procedure.[109] $[Pt(CH_3CN)_2Cl_2]$ (0.0174 g, 5.00 x 10^{-5} mol) was dissolved in minimum acetonitrile and 0.0253 g (1.00 x 10^{-4} mol) of $AgPF_6$ also dissolved in acetonitrile was added. The mixture was stirred at room temperature for 2h with the exclusion of light. Precipitated AgCl was removed by vacuum filtration and 0.0282 g (1.00 x 10^{-4} mol) of DPPZ dissolved in minimum CH_2Cl_2/acetonitrile was added to the filtrate. The solution was stirred at room temperature overnight. The following day, the solution was filtered and NH_4PF_6 (aq.) was added to the filtrate to precipitate the complex.

Synthesis of $[Pt(en)phi](PF_6)_2$:

An attempt to synthesize $[Pt(en)phi](PF_6)_2$ was done with the help of a previously

described procedure.[111] $[Pt(NH_3)_2(en)](PF_6)_2$ (0.0207 g, 3.575 x 10^{-5} mol) was dissolved in 100 mL of a 1:1 MeCN/water solution. 0.610 g (1.04 mmol) of NaOH was added and finally 0.008 g (3.575 x 10^{-5} mol) of 9,10-phenanthrenequinone dissolved in 50 mL of acetonitrile was mixed to the previous solution. The mixture was stirred at room temperature for 1 day under inert atmosphere. The following day, the reaction mixture was neutralized with diluted HCl and the volume reduced to approximately 20 mL. The complex was precipitated with NH_4PF_6 (aq.) and collected by vacuum filtration, washed with water and diethyl ether, and dried.

Synthesis of $[Pt(phen)phi](PF_6)_2$:

An attempt to synthesize $[Pt(phen)phi](PF_6)_2$ was done with the help of a previously described procedure.[111] $[Pt(NH_3)_2(phen)](PF_6)_2$ (0.0250 g, 3.575 x 10^{-5} mol) was dissolved in 100 mL of a 1:1 MeCN/water solution. 0.610 g (1.04 mmol) of NaOH was added and finally 0.008 g (3.575 x 10^{-5} mol) of 9,10-phenanthrenequinone dissolved in 50 mL of acetonitrile was mixed to the previous solution. The mixture was stirred at room temperature for 1 day under inert atmosphere. The following day, the reaction mixture was neutralized with diluted HCl and the volume reduced to approximately 20 mL. The complex was precipitated with NH_4PF_6 (aq.) and collected by vacuum filtration, washed with water and diethyl ether, and dried.

Synthesis of $[(DPPZ)Pt\{DPPZ(11\text{-}11')DPPZ\}Pt(DPPZ)](CF_3SO_3)_4$:

An attempt to synthesize $[(DPPZ)Pt\{DPPZ(11\text{-}11')DPPZ\}Pt(DPPZ)](CF_3SO_3)_4$ was done with the help of a previously described procedure.[79]

[Pt(phendione)DPPZ](CF_3SO_3)$_2$ (0.0230 g, 2.33 x 10^{-5} mol) and 0.0025 g (1.17 x 10^{-5} mol) of 3,3'-diaminobenzidine were dissolved in 4.0 mL of a 1:1:1 mixture of deaerated MeCN-thf-HOAc. The solution was heated at 90 °C for 6h. The solid that formed was removed by centrifugation.

Chapter 4. Results and Discussion

4.1- Synthesis of 1,10-phenanthroline-5,6-dione and DPPZ

1,10-phenanthroline-5,6-dione has been known since 1947,[123] but its reported syntheses gave very poor yields.[97] In the procedure described here, 1,10-phenanthroline is oxidized using $H_2SO_4/HNO_3/KBr$ in which bromide is first oxidized to Br_2,[97] and then H_2SO_4 would facilitate the formation of NO_2^+ from HNO_3 which adds to 1,10-phenanthroline (scheme 41).[124] Vigorous conditions of the medium would continue oxidation to the 1,2-diketone form.[6] Theoretical considerations[125-126] as well as experimental observations.[126] strongly support the idea that the 5 and 6 positions of 1,10-phenanthroline are little involved in the delocalized aromatic system. Oxidation at these positions would thus be easier due to the stability of the two other aromatic rings.

One modification was brought to the reported procedure.[97] A recrystallization from toluene instead of ethanol seemed to give a better purification of the product. In fact, the use of ethanol did not allow a proper separation of 1,10-phenanthroline-5,6-dione from its impurity, probably a monoketone product resulting from partial oxidation. The overall yield of 90.9% for this procedure was quite good.

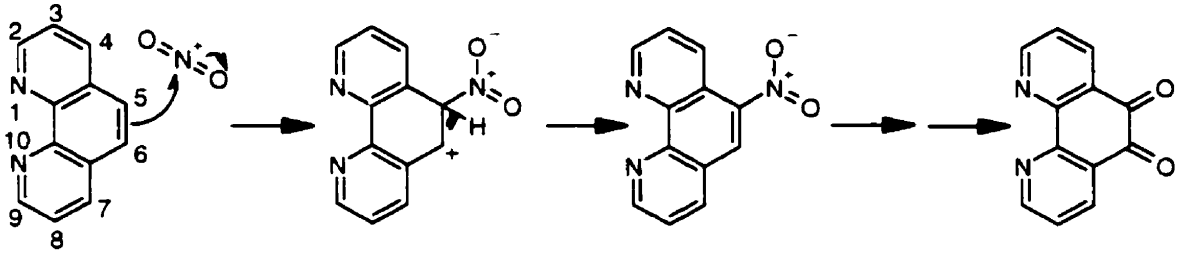

Scheme 41: Mechanism of 1,10-phenanthroline oxidation.

1,10-phenanthroline-5,6-dione reacted quite easily with 1,2-phenylenediamine to give DPPZ[6] in 80.0% yield, a reaction from which only DPPZ has been the isolated product.[127] UV-Vis characterization in ethanol gave identical λ_{max} to previously reported results.[6] Moreover, a melting point of 248 °C (lit.,[6] mp 250 °C) was obtained and ^{1}H NMR spectroscopy using DMSO-d_6 showed 5 peaks with chemical shifts identical to those already published.[53]

4.2- Synthesis of $[Pt(L\text{-}L)DPPZ]^{2+}$ complexes starting from $[Pt(L\text{-}L)Cl_2]$ or $[Pt(DPPZ)Cl_2]$ (L-L = 2 NH_3, en, phen, Me_2bpy, DPPZ)

One platinum complex was initially synthesized, $[Pt(CH_3CN)_2Cl_2]$,[109] and later on another nitrile-based complex, $[Pt(PhCN)_2Cl_2]$,[118] to obtain bidentate dichloride precursors $[Pt(en)Cl_2]$, $[Pt(phen)Cl_2]$, $[Pt(Me_2bpy)Cl_2]$, $[Pt(phendione)Cl_2]$, and $[Pt(DPPZ)Cl_2]$, by ligand substitution.[121-122] Surprisingly, none of these attempts gave the expected result. In using $[Pt(PhCN)_2Cl_2]$ instead of $[Pt(CH_3CN)_2Cl_2]$ in the case of 1,10-phenanthroline-5,6-dione (scheme 42), we relied on a previous literature procedure when the complex, $[Pd(phendione)Cl_2]$ was obtained by reacting $[Pd(PhCN)_2Cl_2]$ and 1,10-phenanthroline-5,6-dione, as a yellow complex in which the α-diimine unit chelates palladium via the nitrogen atom.[122] None of our attempted syntheses with $[Pt(CH_3CN)_2Cl_2]$ or $[Pt(PhCN)_2Cl_2]$ gave the desired products.

Another attempt using a similar approach was directed towards the synthesis of $[Pt(DPPZ)_2](PF_6)_2$ (scheme 43).[109] $[Pt(CH_3CN)_2Cl_2]$ was reacted with two equivalents of $AgPF_6$ in acetonitrile to remove the two chlorides as an AgCl precipitate and to replace

them with solvent molecules, the counteranion becoming PF_6^-. However, no ligand substitution occured when DPPZ (2 molar equivalents) was added to $[Pt(CH_3CN)_4](PF_6)_2$.

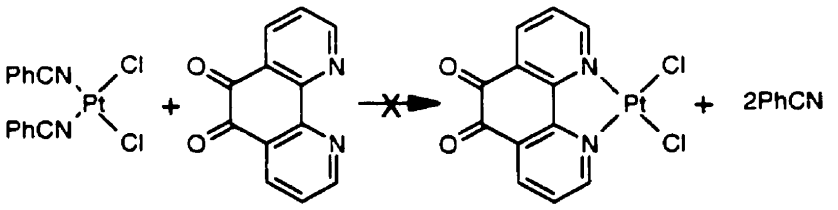

Scheme 42: Synthesis of $[Pt(phendione)Cl_2]$.

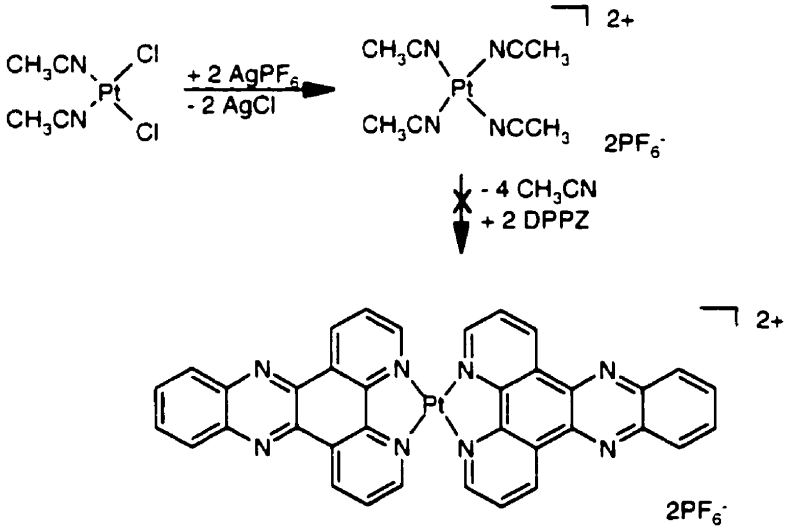

Scheme 43: Attempted synthesis of $[Pt(DPPZ)_2](PF_6)_2$.

Considering these results, a different approach was used to obtain expected dichloro complexes with either the desired ancillary ligands or with the intercalating DPPZ unit. Reported procedures[98-100,117] gave the expected results for *cis*-$[Pt(NH_3)_2Cl_2]$, $[Pt(en)Cl_2]$, $[Pt(phen)Cl_2]$, $[Pt(Me_2bpy)Cl_2]$, and $[Pt(DPPZ)Cl_2]$ (scheme 44). Subsequently, removal of the two remaining chlorides was attempted using six

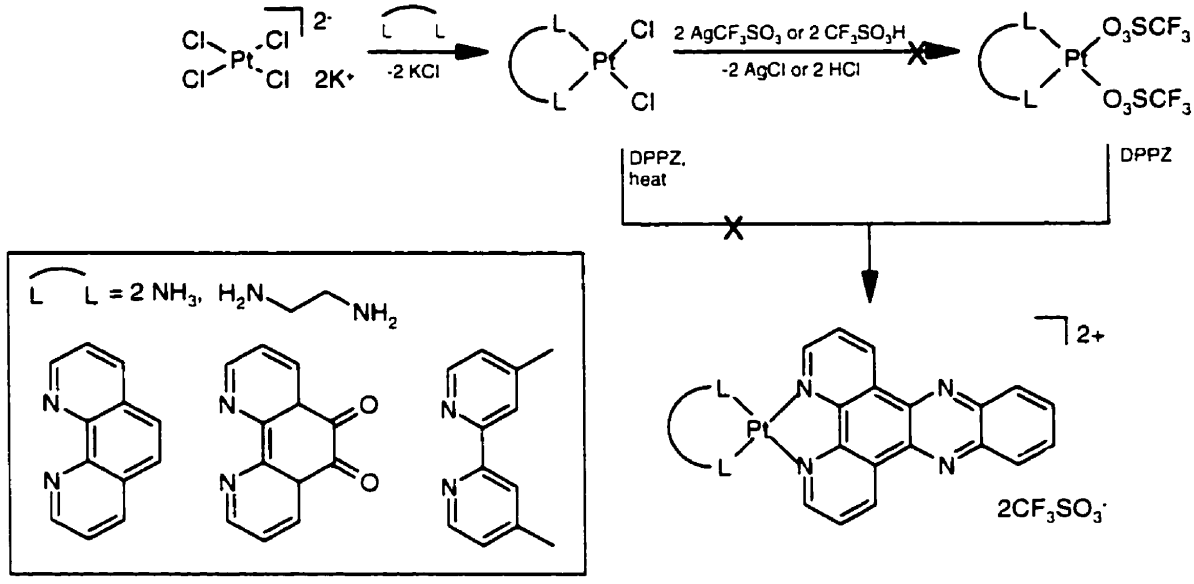

Scheme 44: Synthesis of DPPZ monomers via removal of chlorides.

different methods for all complexes. The two first methods both involved presence of water in the reaction mixture.[47, 101] All dichloro complexes were soluble in hot water except [Pt(DPPZ)Cl_2], probably because of the polyaromaticity of the bidentate ligand increasing its hydrophobicity. Unfortunately, attempts carried out only in water[101] did not allow complete solubilization of one of the reagents and thus did not lead to the expected complexes. Moreover, addition of methanol[47] or ethanol to help solubilize the DPPZ ligand once again did not give the expected ligand substitution. The literature reports on similar platinum complexes suggest that chloride substitution is facile at temperatures near 100 °C, and the synthesis of [Pt(phen)$_2$](PF_6)$_2$ can be successfully carried out in similar conditions.[119] The fact that these attempts did not work with DPPZ could have resulted from the poor solubility of DPPZ in water.

Thus, subsequent attempts were completely carried out in organic solvents such as CH_3CN,[109] DMSO,[102] and DMF.[103] In fact, to avoid too long reaction times and facilitate replacement of chlorides by solvent molecules, two equivalents of $AgCF_3SO_3$ were added to the reaction mixture. The insoluble AgCl formed can thus easily be removed by filtration or centrifugation and is a driving force for ligand substitution. Moreover, free DPPZ is soluble in all three of these solvents at room temperature and its subsequent addition to the filtrate was expected to lead to replacement of weak coordinating $CF_3SO_3^-$ (or loosely bound solvent molecules) ligands by the bidentate intercalator. The same results were expected starting from $[Pt(DPPZ)Cl_2]$ upon addition of silver troflate followed by the proper ancillary ligand. Unfortunately, expected complexes were not obtained. Closer examination of the literature procedures revealed to us that, in most cases, the ligands used were very different in their coordinating abilities from DPPZ (eg. anionic, highly basic, or monodentate ligands).[102,109] Finally, reported formation of $[Pt(bpy)(DMF)_2]^{2+}$ using two equivalents of $AgNO_3$ and its subsequent reaction with cytochrome c led to the coordination of only one cytochrome c, two such molecules probably resulting in serious steric interactions.[103]

A final procedure using more vigorous conditions was then attempted.[104] Anhydrous CF_3SO_3H was added to solid dichloro complexes and the reaction was expected to lead to the replacement of chloride ligands by labile $CF_3SO_3^-$ anion. All attempts lead to the precipitation of a new species upon addition of diethyl ether, but unfortunately its subsequent dissolution in the presence of DPPZ or the appropriate ancillary ligand showed no ligand substitution leading to target complexes.

The fact that the DMF reaction was reported as unsuccessful and especially the reaction time published for the synthesis of $[Pt(bpy)(NCO)_2]$ using DMSO led to the hypothesis that one element would hinder coordination of nitrogen-based ligands in these four procedures. Moreover, previously reported procedures do not contain thorough characterization data of the bis-triflate complexes. Only one report includes the elemental analysis results for *cis*-$[Pt(NH_3)_2(OSO_2CF_3)_2]$.[104] Thus, the reaction of $[Pt(L\text{-}L)Cl_2]$ with $AgCF_3SO_3$ was monitored by ^1H NMR experiments using DMSO-d_6 were performed to assess whether both chlorides are removed under the reaction condition. If complete ligand substitution by $CF_3SO_3^-$ ligands has occured, the resulting platinum complex would be symmetrical and would show 3 peaks by ^1H NMR for the inequivalent aromatic protons (scheme 45 A). However, for an unsymmetrical complex, all protons on the nitrogen-based ligands would be inequivalent (B).

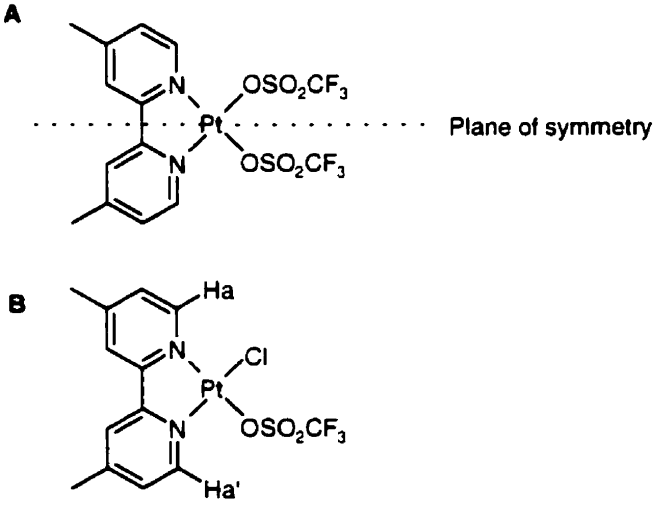

Scheme 45: Symmetrical and dissymmetrical platinum complexes $[Pt(Me_2bpy)(CF_3SO_3)_2]$ and $[Pt(Me_2bpy)(CF_3SO_3)Cl]$.

The results of this study showed that in most complexes only one chloride is removed. NMR analysis of [Pt(Me_2bpy)(CF_3SO_3)Cl] (scheme 46) showed two signals for the ortho protons Ha and Ha' (scheme 36) at 9.43 ppm and 9.12 ppm with a 1:1 ratio. This effect seems to be less significant for meta and para protons as signals overlap at 8.62 ppm and 7.80 ppm respectively giving a 2:2:1:1 para/meta/Ha/Ha' ratio . Subsequent addition of DPPZ to this species does not seem to result in the successful removal of the second chloride.

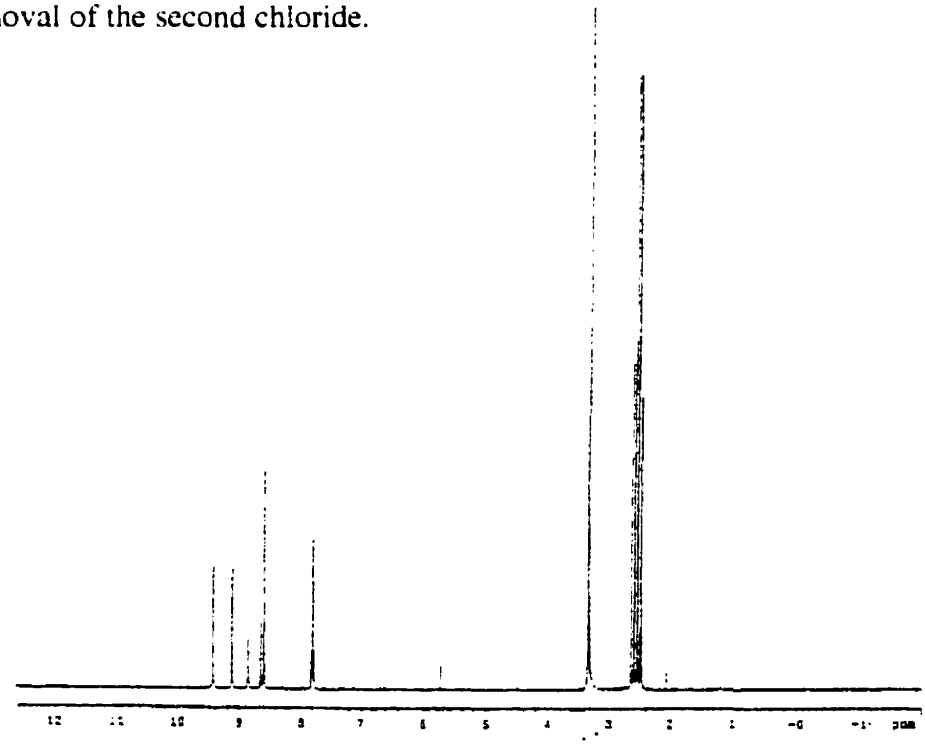

Scheme 46: NMR spectrum of [Pt(Me_2bpy)(CF_3SO_2)Cl] in DMSO-d_6 after addition of two equivalents of $AgCF_3SO_3$.

One more reaction was similarly investigated, namely the unsuccessful results for the CF_3SO_3H reaction. ^1H NMR spectroscopy of the precipitate [Pt(Me_2bpy)(OSO_2CF_3)Cl] in DMSO-d_6 was used to see if the reaction was complete (scheme 47). Surprisingly, even though elemental analysis results were provided in the

literature reported synthesis of *cis*-$[Pt(NH_3)_2(OSO_2CF_3)_2]$, all attempts led to removal of only one chloride and the formation of unsymmetrical species. This would explain why the expected complexes were not obtained as well with this method. Ortho protons of 4,4'-dimethyl-2,2'-bipyridine are split at 9.43 ppm and 9.12 ppm with a 1:1 integration ratio. The NMR spectrum is extremely similar to the one previously obtained following addition of $AgCF_3SO_3$.

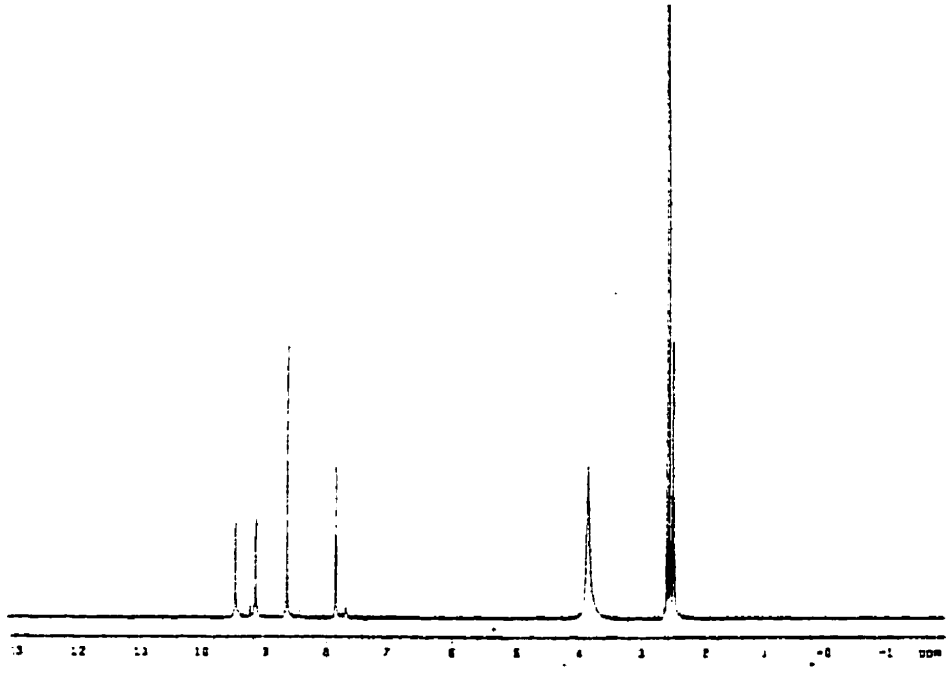

Scheme 47: NMR spectrum of $[Pt(Me_2bpy)(CF_3SO_2)Cl]$ in DMSO-d_6 after addition of two equivalents of CF_3SO_3H.

4.3- Synthesis of $[Pt(L\text{-}L)DPPZ](CF_3SO_3)_2$ complexes starting from $[Pt(L\text{-}L)I_2]$ (L-L = 2 NH_3, en, phen, Me_2bpy, phendione)

Considering the difficulty in removing the second chloride ligand from the coordination sphere of $[Pt(L\text{-}L)Cl_2]$, a new approach was investigated. The starting material $K_2[PtCl_4]$ was converted to its tetrakis iodo species $K_2[PtI_4]$.[98-100] Addition of a

bidentate ligand would lead to the bis iodo complex [Pt(L-L)I_2], and these two iodides are expected to be more easily removed than chlorides.

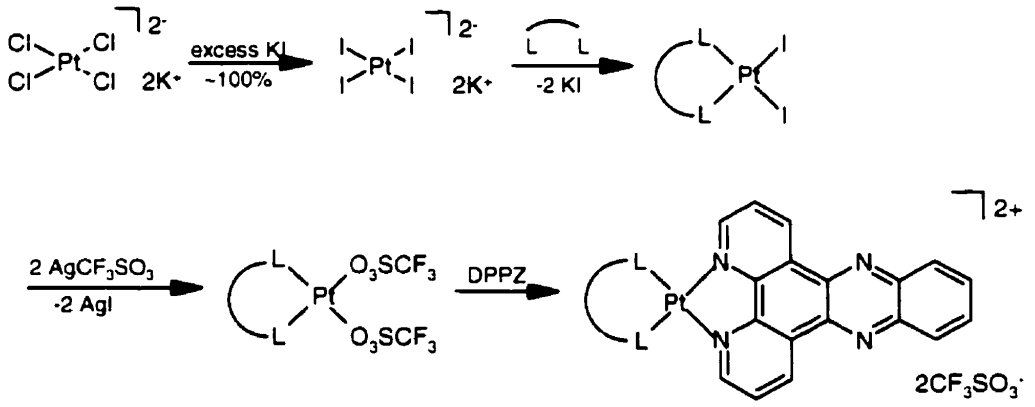

Scheme 48: Synthesis of DPPZ monomers via removal of iodides.

This strategy showed to be successful in removing both iodides and giving the desired products. Reported synthetic procedures for such complexes are similar to those of chlorides (scheme 48).[105,106,108,117] Yields obtained varied between 54.2% and 72.0%. [Pt(DPPZ)I_2] was synthesized but was not used further on due to its low solubility. Moreover, another new complex was synthesized in this research, [Pt(phendione)I_2]. The 1,10-phenanthroline-5,6-dione can chelate platinum in two possible ways. As it is the case for 1,10-phenanthroline, 1,10-phenanthroline-5,6-dione has two chelating nitrogen atoms which can both directly point toward a potential metal center with a favorable site size (scheme 49). However, presence of two adjacent ketones also becomes a potential coordination site due to oxygen lone pairs. In fact, with the low-valent [$Pt(PPh_3)_4$] complex, 1,10-phenanthroline-5,6-dione has been reported to undergo oxidative addition to the two oxygens.[122] This result was confirmed in the literature by the total

disappearance of the C=O IR stretching bands of 1,10-phenanthroline-5,6-dione at 1705 and 1690 cm^{-1}.

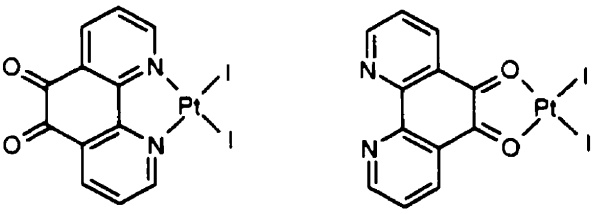

Scheme 49: Coordination of 1,10-phenanthroline-5,6-dione to platinum.

Thus, the synthesis of [Pt(phendione)I_2] was carried in a similar way as for the other iodo complexes except that 1,10-phenanthroline-5,6-dione was previously dissolved in methanol instead of water/HI as was the case for [Pt(phen)I_2], [Pt(Me_2bpy)I_2], and [Pt(DPPZ)I_2]. IR characterization of the deep red solid obtained showed a large stretching band at 1689.5 cm^{-1} which was attributed to C=O. Moreover, the ^{1}H NMR spectrum showed significant downfield chemical shifts for all three protons of chelating 1,10-phenanthroline-5,6-dione compared to the ones of the free molecule, especially for the protons ortho to the coordinationg nitrogen (scheme 50). This peak is shifted donwfield from 8.96 ppm for the free ligand (scheme 50 A) to 10.18 ppm for [Pt(phendione)I_2] (scheme 50 B). These results led to the conclusion that chelation most likely occurs from the nitrogen atoms because the distance between the metal center and the protons would not cause such downfield chemical shifts if coordination would occur from the oxygen atoms.

$AgCF_3SO_3$ was once again used in the following step to remove iodides. A similar ^{1}H NMR experiment as the one previously described was performed using

A B

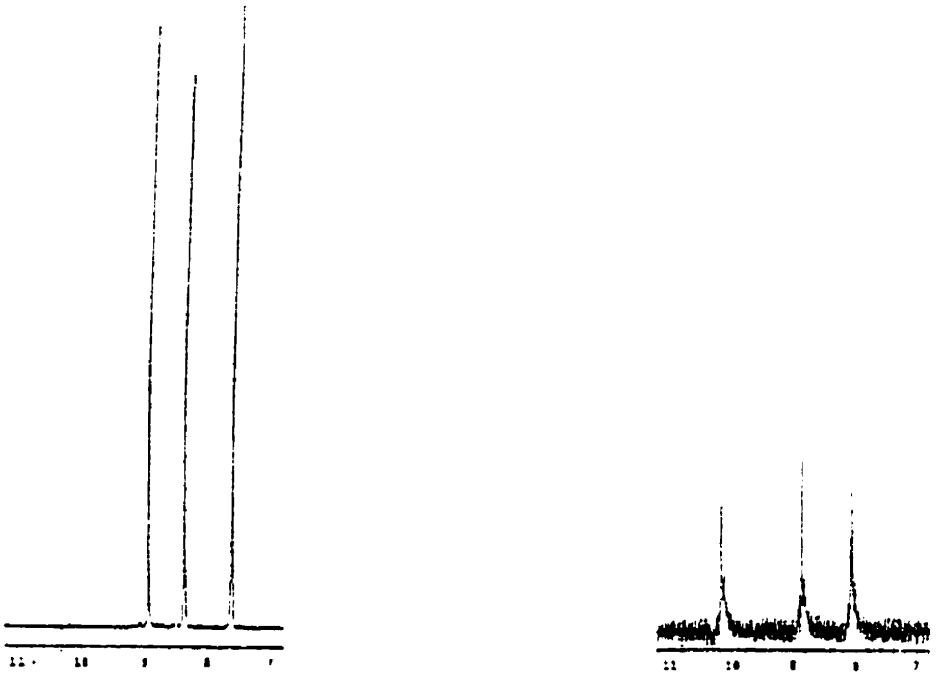

Scheme 50: NMR spectrum of 1,10-phenanthroline-5,6-dione (A) and [Pt(phendione)I_2] (B) in acetone-d_6.

acetone-d_6 to establish if both iodides had been removed in the form of a AgI precipitate. In all attempted cases, the main if not almost exclusive product was [Pt(L-L)$(OSO_2CF_3)_2$] (or [Pt(L-L)(solvent)$_2$]) because signals for a symmetrical complex were obtained (scheme 51). DPPZ dissolved in acetone was then added to all samples and target monomers were all obtained, and characterized by NMR spectroscopy and MALDI-TOF mass spectrometry. In most cases, the complexes remained in acetone at the end of the reaction, except [Pt(en)DPPZ]$(CF_3SO_3)_2$, which came out of solution upon its formation. Moreover, because of its second possible coordination site, an IR spectrum of

[Pt(phendione)DPPZ]$(CF_3SO_3)_2$ showed a C=O stretching band 1697.6 cm^{-1}, establishing that the diketone moiety of phenanthroline dione has remained intact.

A

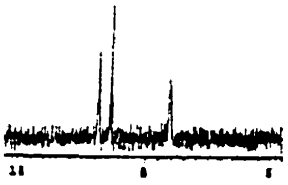

B

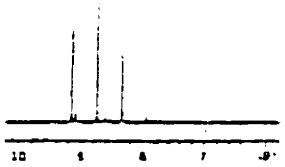

Scheme 51: NMR spectrum of [Pt(Me_2bpy)I_2] (A) and [Pt(Me_2bpy))$(CF_3SO_3)_2$] (B) in acetone-d_6.

4.4- Attempted synthesis of [Pt(en)phi]$(PF_6)_2$ and [Pt(phen)phi]$(PF_6)_2$

Rhodium (III) and ruthenium(II) complexes of phi are usually synthesized according to literature reports, either by coordination of 9,10-diaminophenanthrene to the metal center with subsequent oxidation of the coordinated ligand to the bis-diimine,[111] or, for tris(phi) complexes, by an *in situ* deprotection of bis(trimethylsilyl)phenanthrenequinone diimine in the presence of an appropriate metal precursor.[128] The main drawback of these protocols are their moderate to low yields.[122]

The condensation of amines with aldehydes and ketones is the method of choice to prepare Schiff bases.[129] Thus, a method to synthesize rhodium (III) diimine complexes starting from *o*-quinones and metal complexes with the cis-coordinated amino ligands has been reported to give higher yields thant the above described methods.[111]

Applying this methodology to the synthesis of [Pt(en)phi]$(PF_6)_2$ and [Pt(phen)phi]$(PF_6)_2$, cis-coordinated amino platinum complexes with the proper ancillary

ligand were then synthesized. This reaction which starts from either $[Pt(en)Cl_2]$ or $[Pt(phen)Cl_2]$ led to the successful formation of the bis amino species $[Pt(NH_3)_2(en)](PF_6)_2$ and $[Pt(NH_3)_2(phen)](PF_6)_2$.[110] The last step of the proposed synthetic route takes advantage of the expected higher acidity of amino protons due to coordination of the nitrogen lone pair to platinum (II). Addition of NaOH to the coordinated ammines is thus expected to deprotonate these ligands and facilitate their reaction with 9,10-phenanthrenequinone as previously observed for Rh (III) complexes (scheme 52).

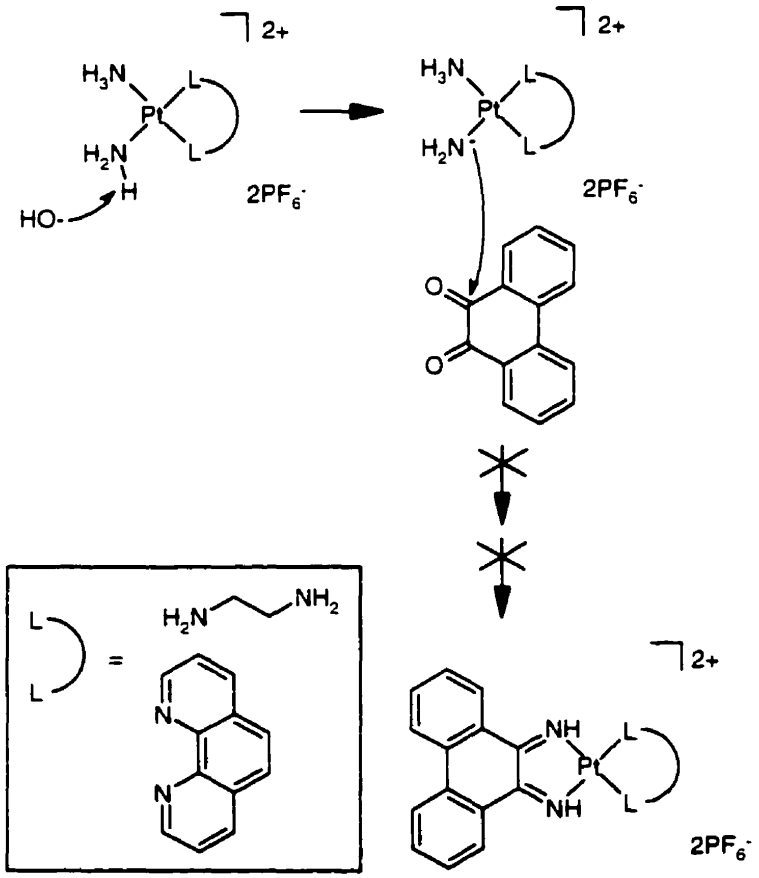

Scheme 52: Proposed mechanism for the synthesis of $[Pt(en)phi](PF_6)_2$ and $[Pt(phen)phi](PF_6)_2$.

Unfortunately, applying the literature method to our synthesis presented here, platinum (II) complexes did not yield the target phi complexes. One explanation involves the empty d_z^2 orbital on Pt(II), which is available for associative ligand substitution processes.[130] The strong base, HO^-, could thus directly attack with the metal center, possibly causing decomposition. This reaction that is unlikely with the literature complexes which contain octahedrally coordinated metal centers such as Rh(III) as their orbitals are all saturated.

4.5- Synthesis of Pt(II) dimers

[Pt(phendione)I_2] and [Pt(phendione)DPPZ]$(CF_3SO_3)_2$ were synthesized for the purpose of obtaining dimers. Synthesis of the free tetradentate ligand DPPZ(11-11')DPPZ was first carried using similar conditions as for the synthesis of DPPZ (scheme 53).[6] A 2:1 ratio of 1,10-phenanthroline-5,6-dione and 3,3'-diaminobenzidine were combined in boiling ethanol and led to the correct molecule as an orange precipitate.

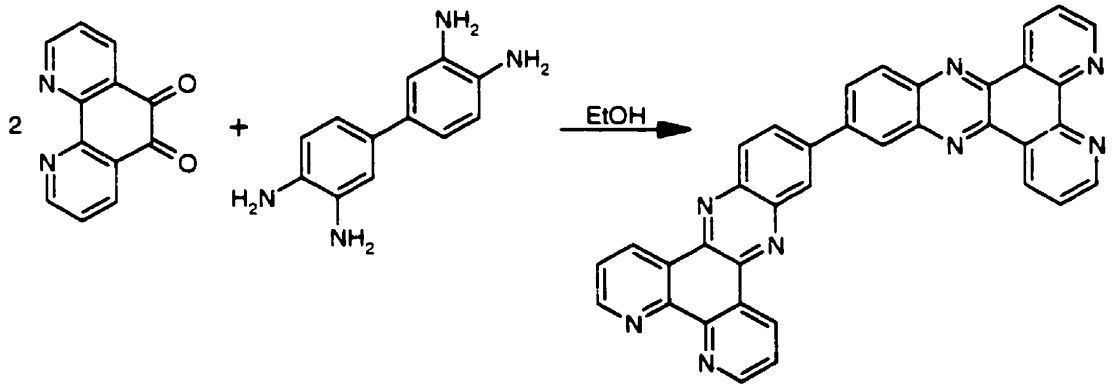

Scheme 53: Synthesis of DPPZ(11-11')DPPZ.

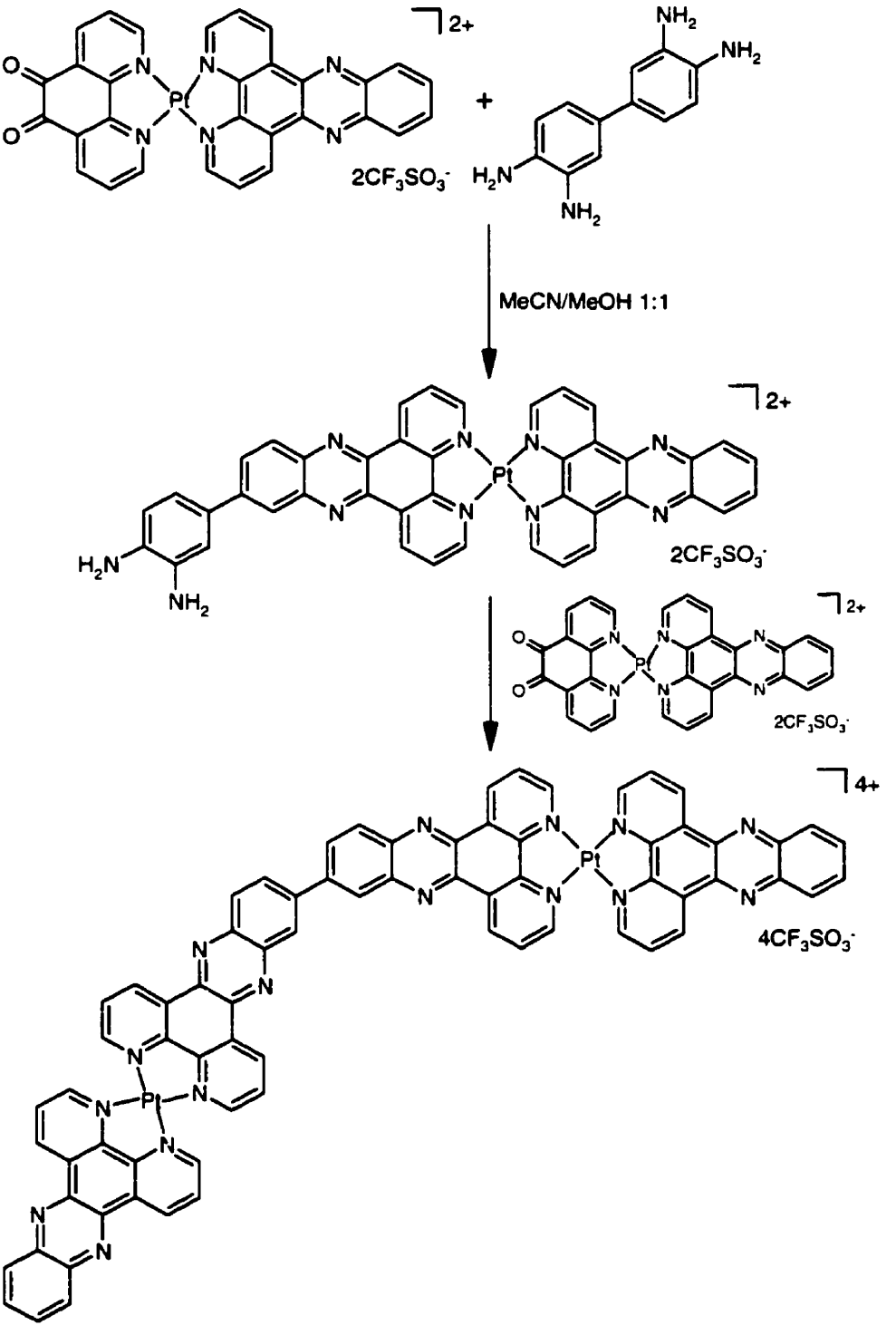

Scheme 54: Synthesis of [(DPPZ)Pt{DPPZ(11-11')DPPZ}Pt(DPPZ)](CF$_3$SO$_3$)$_4$.

Knowing that test reaction works well, a first synthesis of [(DPPZ)Pt{DPPZ(11-11')DPPZ}Pt(DPPZ)]$(CF_3SO_3)_4$ was attempted by reacting [Pt(phendione)DPPZ]$(CF_3SO_3)_2$ with 3,3'-diaminobenzidine in a 1:1:1 mixture of MeCN-thf-HOAc as suggested by Wärnmark et al. for a similar reaction using ruthenium (scheme 54).[93] This acidic medium did not lead to the desired product in the case of platinum dimers, as a white decomposition product came out of solution almost immediately after addition of the reagents. Thus, milder conditions were then used for the second attempt.[82,92] [Pt(phendione)DPPZ]$(CF_3SO_3)_2$ and 3,3'-diaminobenzidine were dissolved in a 1:1 mixture of acetonitrile and methanol and were heated at 65 °C for 5h. Surprisingly, even when using a 2:1 ratio of respectively [Pt(phendione)DPPZ]$(CF_3SO_3)_2$ and 3,3'-diaminobenzidine, the same mono condensed [Pt(DPPZ){11-$(NH_2)_2$PhDPPZ}]$(CF_3SO_3)_2$ complex was obtained as a deep red precipitate. ^{1}H NMR spectroscopy showed the NH_2 groups at 4.96 and 4.71 ppm, MALDI-TOF mass spectrometry gave the correct molecular ion for a 1:1 adduct.

This precipitation was unexpected as previous reported procedures usually involved the addition of a salt such as NH_4PF_6 at the end of the synthesis to encourage precipitation of resulting complexes, even when larger complexes were synthesized.[82, 94-96] Thus, the red precipitate was dissolved in DMSO with one more molar equivalent of [Pt(phendione)DPPZ]$(CF_3SO_3)_2$. This time, the product remained in solution and monitoring the reaction by ^{1}H NMR spectroscopy using DMSO-d_6 (scheme 55) showed quite rapid disappearance of the NH_2 signals and production of water, a side product of Schiff base formation reactions.[129] Obtention of the expected [(DPPZ)Pt{DPPZ(11-

11')DPPZ}Pt(DPPZ)]$(CF_3SO_3)_4$ dimer was then confirmed by MALDI-TOF mass spectrometry.

A

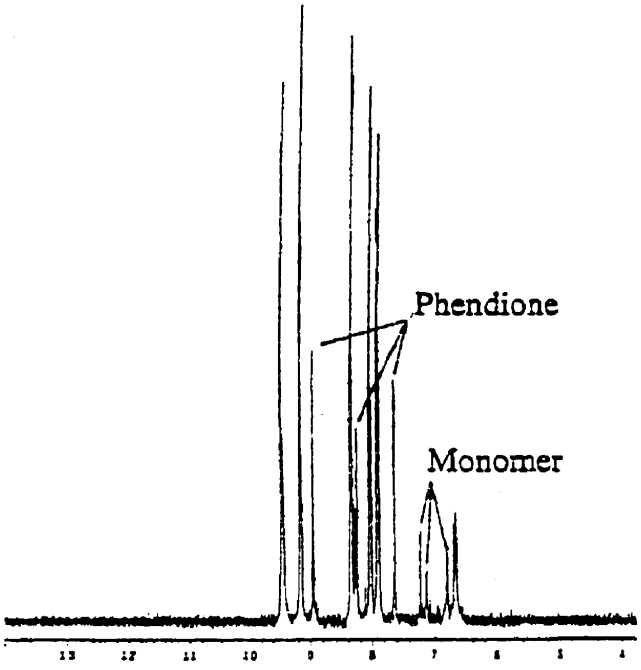

B

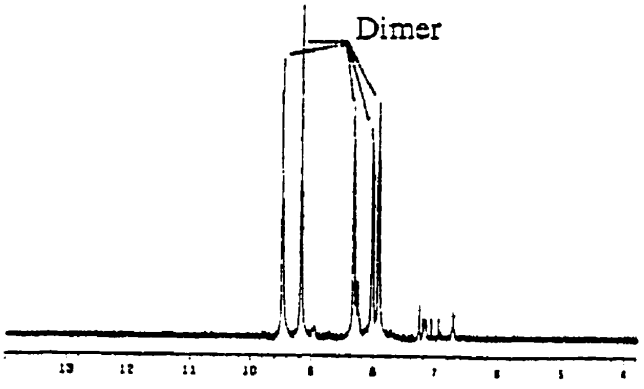

Scheme 55: NMR spectrum in DMSO-d_6 showing the formation of [(DPPZ)Pt{DPPZ(11-11')DPPZ}Pt(DPPZ)]$(CF_3SO_3)_4$ by reaction between [Pt(phendione)DPPZ]$(CF_3SO_3)_2$ and [Pt(DPPZ){11-$(NH_2)_2$PhDPPZ}]$(CF_3SO_3)_2$. (A) time 0; (B) 4 h.

4.6- Absorption spectrum of $[Ru(phen)_2DPPZ](PF_6)_2$ with calf thymus DNA.

The absorption of $[Ru(phen)_2DPPZ](PF_6)_2$ in the visible wavelength region arises from metal-to-ligand charge-transfer (MLCT) transitions at 439 nm and from an intraligand transition of the DPPZ chromophore at 372 nm.[55] Figure 1 shows the behavior of the isotropic absorption spectra of $[Ru(phen)_2DPPZ](PF_6)_2$ upon interaction with calf thymus DNA. The total metal complex concentration was kept constant at 20 μM and, by increasing the DNA concentration, i.e. decreasing the mixing ratio R = [Ru]/[DNA], two phases of events with distinctly different features can be distinguished. Figure 1 A represents the first phase from free complex to R = 0.25. It is characterized by a very pronounced hypochromic effect in the presence of DNA, especially for the intraligand transition at 372 nm. The second phase (figure 1 B) shows a different behavior for mixing ratios smaller than 0.25. The absorption now increases with decreasing mixing ratios. Compared to the spectrum of the unbound metal complex, the MLCT band exhibits no red-shift and only a moderate hypochromicity, whereas the red-shift for the intraligand transition band amounts to 8 nm.

These results are similar to those already published.[55] Reported intrinsic binding constants however differ significantly. Hiort et al. calculated these binding constants to be respectively $1.5 \times 10^7\ M^{-1}$, $6 \times 10^7\ M^{-1}$, and $2.4 \times 10^8\ M^{-1}$ for Λ-$[Ru(phen)_2DPPZ](PF_6)_2$, racemic $[Ru(phen)_2DPPZ](PF_6)_2$, and Δ-$[Ru(phen)_2DPPZ](PF_6)_2$ using the McGhee and von Hippel equation with no cooperativity and n = 2.[55] Haq et al. on the other hand evaluated these binding constants to be $1.7 \times 10^6\ M^{-1}$ and $3.2 \times 10^6\ M^{-1}$ for

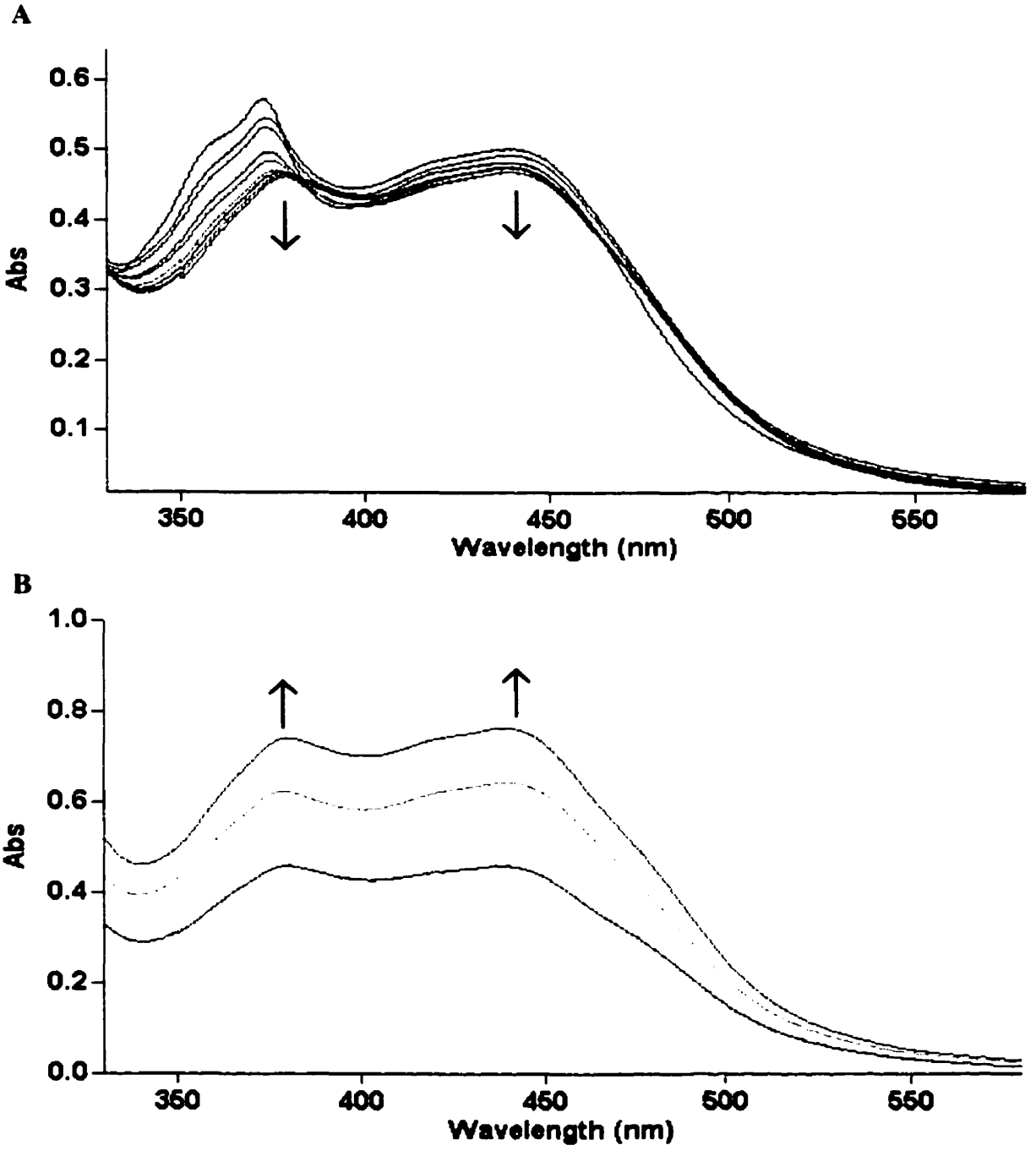

Figure 1: Absorption spectrum of $[Ru(phen)_2DPPZ](PF_6)_2$ in the presence of calf thymus DNA (1×10^{-3} M phosphate, 1×10^{-2} M NaCl, pH 7.0). (A) Mixing ratios [metal complex]/[DNA phosphate], from top to bottom: no DNA, 0.95, 0.89, 0.62, 0.52, 0.42, 0.34, 0.29, 0.25. (B) Mixing ratios: 0.06, 0.13, 0.22. Ru concentration was kept constant at 20 μM.

Λ-[Ru(phen)$_2$DPPZ](PF$_6$)$_2$ and Δ-[Ru(phen)$_2$DPPZ](PF$_6$)$_2$ respectively with binding stoichiometries of 0.7 and 3 mol of base pair/mol of ligand.[56]

This controversy led us to evaluate the binding constant of our racemic [Ru(phen)$_2$DPPZ](PF$_6$)$_2$ using the hypochromicity results obtained (figure 1) and the equation for non luminescent probes .[21] Surprisingly, a binding constant of 3.8 x 10^4 M^{-1} was calculated from the results shown in figure 2. It should however be noted that the determination of binding constants is only a rather crude estimate due to the non linear response at very low [Ru]/[DNA] binding ratios and to the high overall concentrations in the titration when using the McGhee and von Hippel equation.[55] Moreover, with the equation for non luminescent probes, the binding constant is determined from a double-reciprocal plot of the change in the apparent extinction coefficient of the ligand vs. DNA concentration for ratios of bound ligand to DNA base pairs near zero.[21] Thus, in the presence of a strong intercalator such as [Ru(phen)$_2$DPPZ](PF$_6$)$_2$, it becomes difficult to evaluate this binding constant because the ratio of bound ligand to DNA base pairs increases too quickly to allow a proper determination of its binding constant. As the slope $-1/\Delta\varepsilon$ of the plot decreases very fast at these low binding ratios, only a poor lower estimate of the binding constant is obtained because saturation is rapidly obtained (the decrease in absorption is quite small in figure 1).

Non luminescent complex [Ru(NH$_3$)$_4$DPPZ]$^{2+}$ showed a binding constant of only 1.24 x 10^5 M^{-1} using a different equation for non luminescent probes (equation 6)[131] including an estimated binding site size of 0.02.[64] Moreover, a binding constant of 5.1 x 10^6 M^{-1} with a binding site size of 0.6 base pairs was observed by Nair et al. for [Ru(phen)$_2$DPPZ](PF$_6$)$_2$.[64] These reported results thus become a good basis to explain

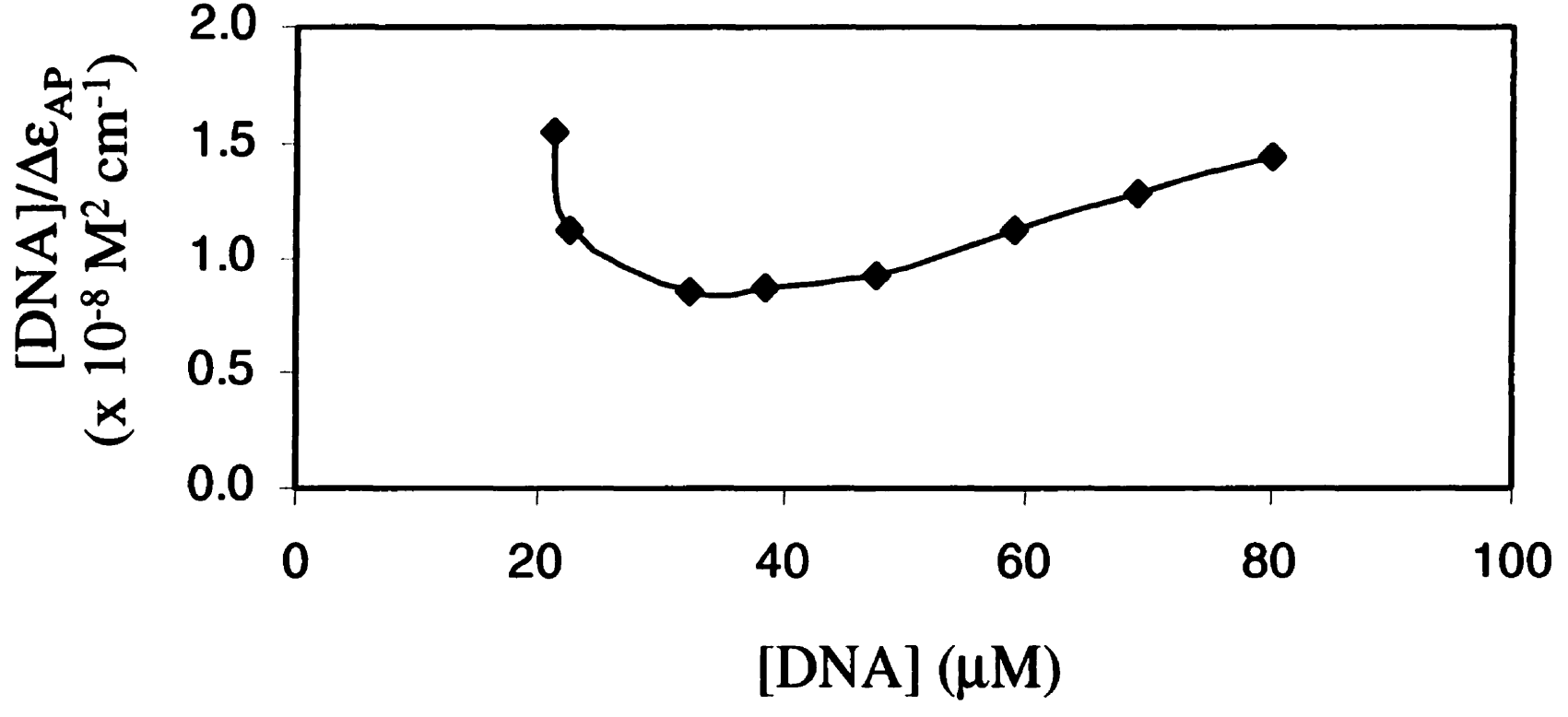

Figure 2: Absorption titration results of $[Ru(phen)_2DPPZ](PF_6)_2$ using equation 4 (page 7).

that binding constants are estimates. $[Ru(NH_3)_4DPPZ]^{2+}$ exists as only one isomer, its NH_3 ancillary ligands are less bulky than 1,10-phenanthroline, and they can hydrogen bond. It has been suggested that the NH_3 face of $[Ru(NH_3)_4DPPZ]^{2+}$ competes with the DPPZ face for DNA binding. This difference may be due to direct hydrogen bonding between the NH_3 ligands to the oxygens and nitrogens of bases as well as to neighboring phosphate groups of the DNA. Therefore, considering that the McGhee and von Hippel equation must need a site size parameter (n) which is only estimated, whereas binding constant determination by hypochromicity is based on observed extinction coefficient changes, this can lead to major differences as seen in our case for $[Ru(phen)_2DPPZ]^{2+}$.

Equation 6: $$(\varepsilon_A - \varepsilon_F)/(\varepsilon_B - \varepsilon_F) = \frac{b - (b^2 - 2K^2C_t[DNA]/s)^{1/2}}{2KC_t}$$

$$b = 1 + KC_t + K[DNA]/2s$$

ε_A = extinction coefficient observed at particular DNA concentration

ε_F = extinction coefficient for the complex free in solution

ε_B = extinction coefficient of fully bound species

C_t = total concentration of the metal complex

[DNA] = DNA concentration

K = binding constant of the complex for DNA (M^{-1})

s = binding site site (base pairs) (estimated)

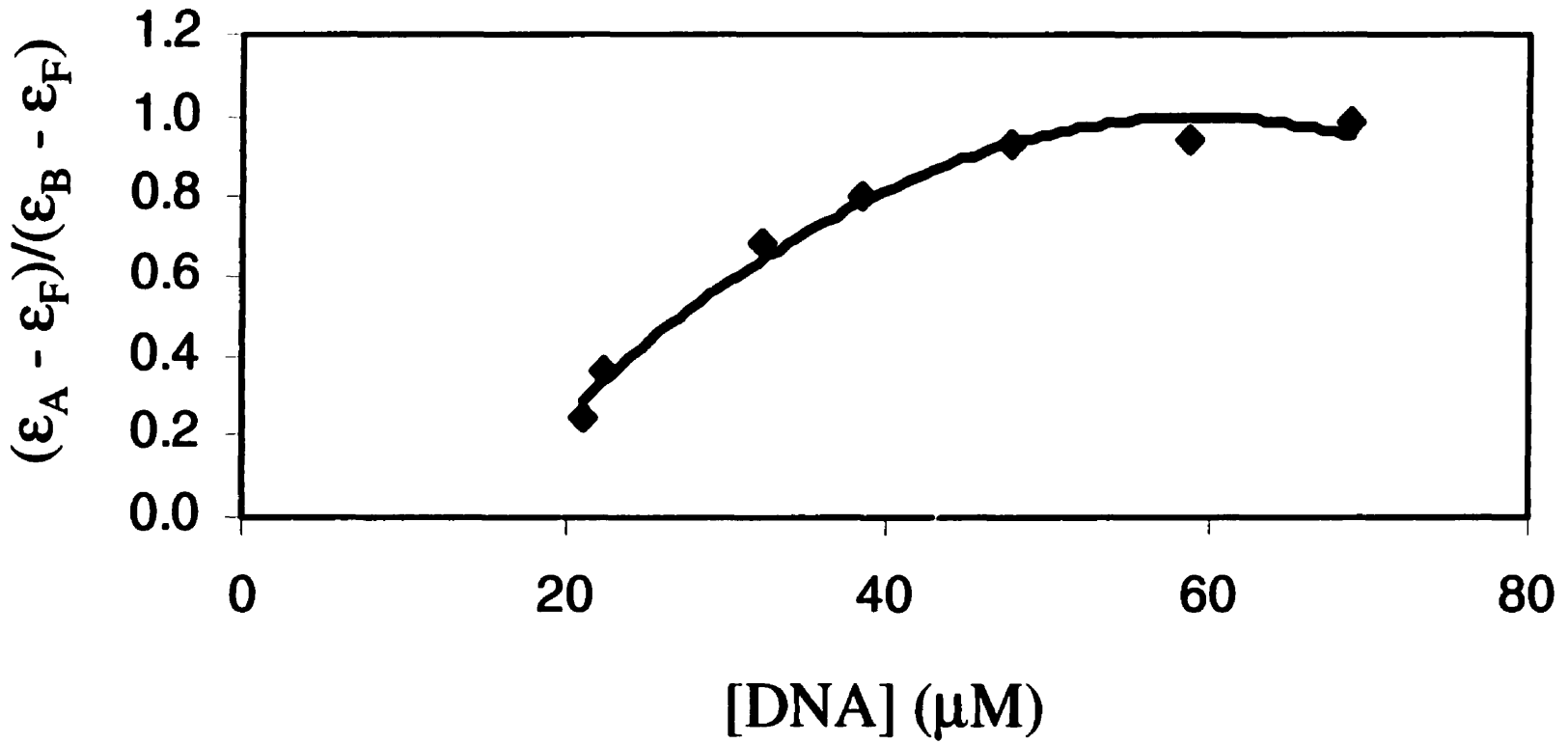

Figure 3: Fits of equation 6 (page 89) to absorption titration of $[Ru(phen)_2DPPZ](PF_6)_2$.

We did also evaluate the binding constant of $[Ru(phen)_2DPPZ](PF_6)_2$ with equation 6 considering our data (figure 3). Fitting gave a binding constant of 2.55 x 10^7 M^{-1} and a binding site size of 1.29 base pairs. This result is quite comparable to reported results. However, it should be noted that this best fitting method can lead to major differences in K and s values.

To moreover explain this difference, it should be mentioned that the binding affinity varies sometimes to a large extent by changing the salt concentration and the DNA sequence. For example, ethidium bromide showed a binding constant of 2 x 10^5 M^{-1} with calf thymus DNA ($[Na^+]$ = 0.075 M),[132] but only 4.2 x 10^4 M^{-1} with a Na^+ concentration of 1.0 M.[85] Moreover, this binding constant drops to 2.0 x 10^4 M^{-1} with (dG-dC)•(dG-dC) and to 2 x 10^3 M^{-1} with dA•dT, $[Na^+]$ = 1.0 M. Thus, considering these factors and also the fact that the equation for non luminescent probes was used for binding constant determination of reported platinum complexes,[46-49,65] this equation was applied for our platinum complexes to obtain further results.

4.7- $[Pt(NH_3)_2DPPZ](CF_3SO_3)_2$ and $[Pt(en)DPPZ](CF_3SO_3)_2$: binding constants to calf thymus DNA

Binding constant determination of $[Pt(en)DPPZ](CF_3SO_3)_2$ was initially carried out following the method of Hiort et al.[55] and Che et al.[69] The complex appears to be stable in the phosphate buffer as no major change was observed over 2h30. Two maximum absorption wavelengths can be observed at 361 nm and 379 nm. Upon addition of DNA, two phases can be observed as seen for parent $[Ru(phen)_2DPPZ]^{2+}$

complex.[55] A decrease in absorption is obtained for mixing ratios ([complex]/[DNA]) from no DNA to 0.34 (figure 4 A). The 361 nm and 379 nm bands undergo no apparent red shift upon DNA addition. However, at lower binding ratios (0.25 - 0.06), an increase in absorption is observed and red shift for both bands can be seen (figure 4 B).

The apparent binding constant was then evaluated using the decreasing absorption ratios (0.95 – 0.34) (figure 5). [Pt(en)DPPZ]$(CF_3SO_3)_2$ would bind quite strongly to DNA with a binding constant of 1.18 x 10^4 M^{-1}. This result is not tremendously different from those obtained from parent [Pt(DPPZ)(tN^C)](CF_3SO_3) (1.3 x 10^4 M^{-1}), [Pt(DPPZ)(Meim-1)]$(CF_3SO_3)_2$ (1.1 x 10^4 M^{-1}), and [Pt(DPPZ)$(NH_2py\text{-}4)_2$]$(CF_3SO_3)_2$ (1.2 x 10^4 M^{-1}) complexes reported by Che et al.[69] However, comparing this binding constant to other platinum complexes, it becomes a bit surprising to realize that $[Pt(bpy)(en)]^{2+}$ shows a slightly higher binding constant of 1.45 x 10^4 M^{-1},[45] and that complexes such as $[Pt(bpy)(py)_2]^{2+}$ and $[Pt(4,4'\text{-}\ Ph_2bpy)(py)_2]^{2+}$ also present higher binding constants (16.2 x 10^4 M^{-1} and 16.7 x 10^6 M^{-1} respectively).[47] The presence of attached phenyl groups would thus enhance the binding strength more than having a polyaromatic extended ligand.

As a comparison, equation 6 was used with our data (figure 6). Our results were extremely different as a binding constant of 2.17 x 10^8 M^{-1} and a s value of 1.87 bp were obtained. It should however be noted that to our knowledge, binding constant determination of platinum complexes has never been reported using this equation. Moreover, the correlation coefficients were better using the non luminescent probes equation. More experiments such as equilibrium dialysis need to be carried out to confirm these binding constants.

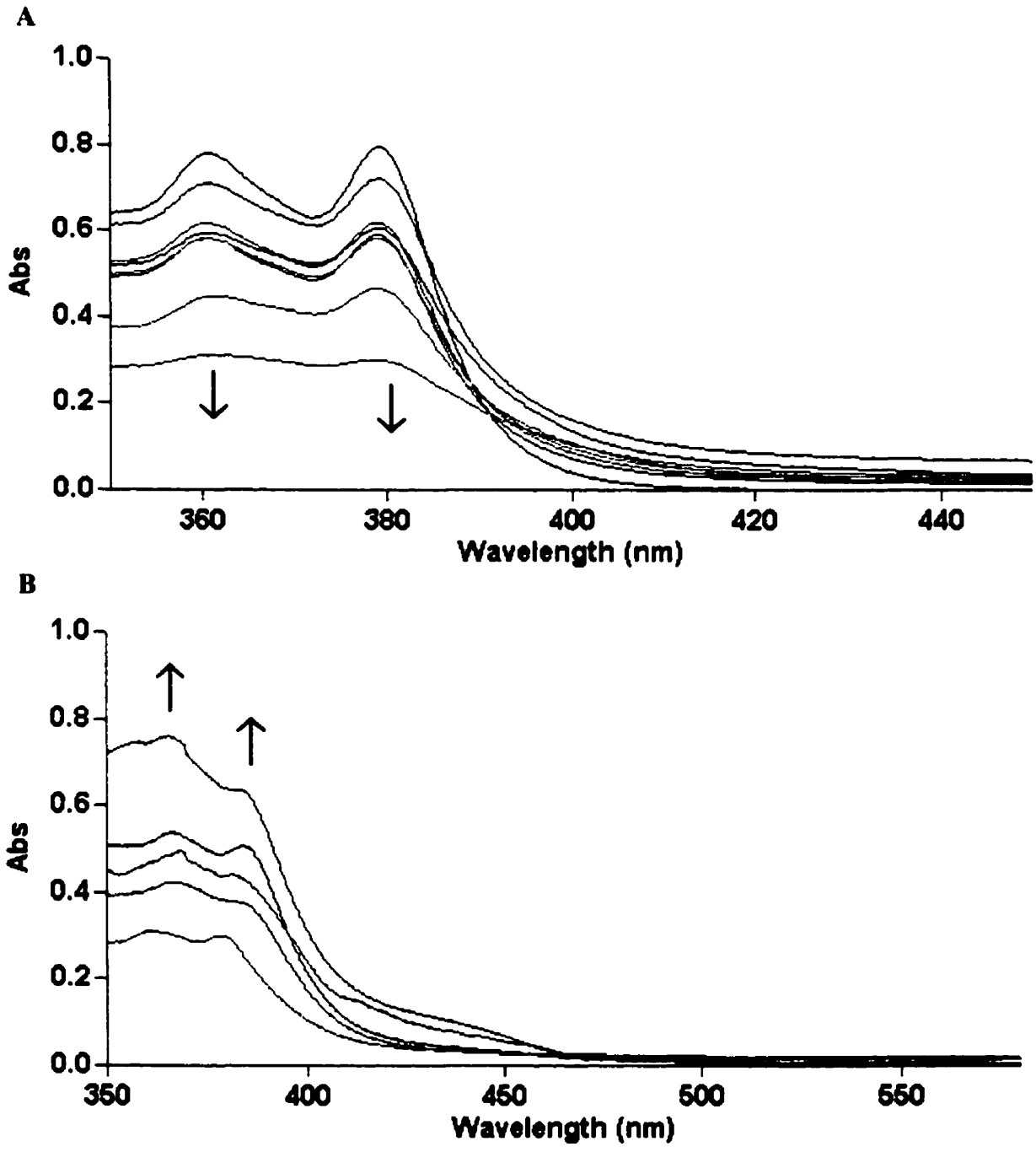

Figure 4: Absorption spectrum of [Pt(en)DPPZ]$(CF_3SO_3)_2$ in the presence of calf thymus DNA (1 x 10^{-3} M phosphate, 1 x 10^{-2} M NaCl, pH 7.0). (A) Mixing ratios [metal complex]/[DNA phosphate], from top to bottom: no DNA, 0.95, 0.89, 0.83, 0.72, 0.62, 0.42, 0.34. (B) Mixing ratios: 0.06, 0.13, 0.22, 0.25, 0.29. Pt concentration was kept constant at 20 μM.

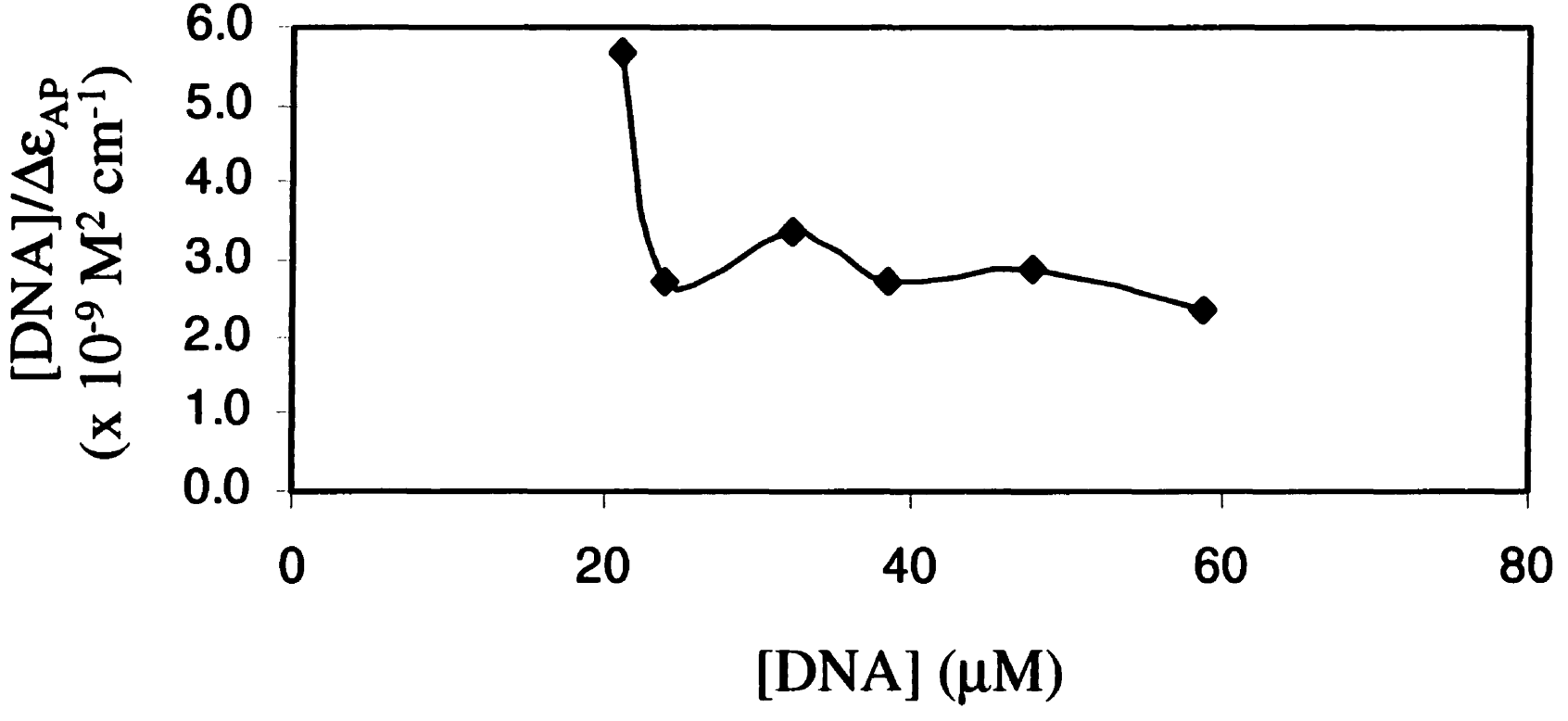

Figure 5: Absorption titration results of $[Pt(en)DPPZ](CF_3SO_3)_2$ using equation 4 (page 7).

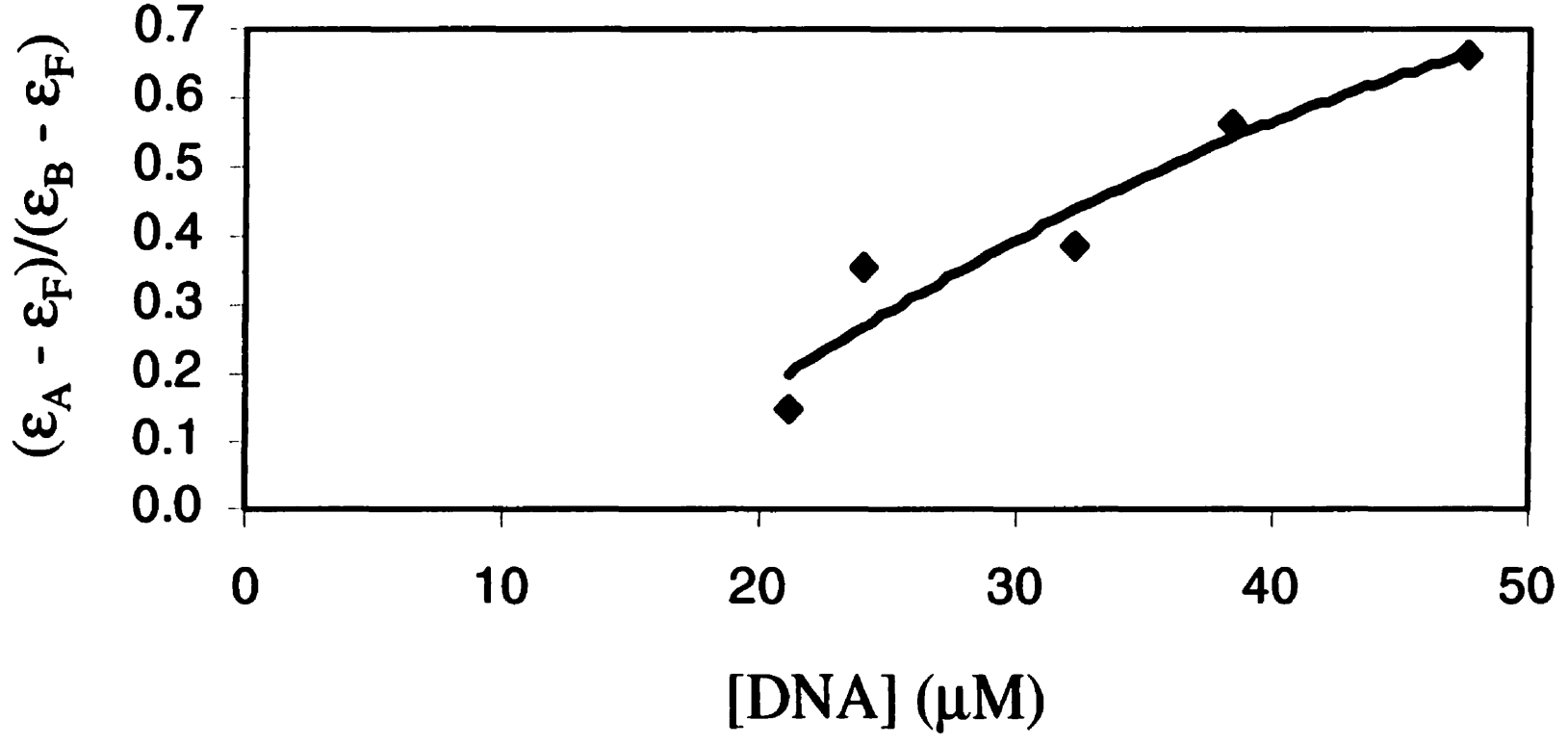

Figure 6: Fits of equation 6 (page 89) to absorption titration of Pt(en)DPPZ]$(CF_3SO_3)_2$.

$[Pt(NH_3)_2DPPZ](CF_3SO_3)_2$ was also stable in the phosphate buffer over 2h30 but it behaved very differently from $[Pt(en)DPPZ](CF_3SO_3)_2$. Strong hypochromicity is observed after addition of calf thymus DNA (figure 7 A) until that decrease in absorption stabilizes for both the 361 nm and 380 nm bands. Then, an increase in absorption is observed at lower binding ratios (figure 7 B). The binding constant calculated from these data, 2.58 x 10^4 M^{-1}, is close to two fold higher than for $[Pt(en)DPPZ](CF_3SO_3)_2$. This higher binding constant could result from the hydrogen bonding capacity of the ancillary ligands with the phosphate backbone or with oxygens and nitrogens of bases as proposed by Nair et al.[64] and from the smaller steric hindrance caused by NH_3 ligands compared to ethylenediamine.

4.8- $[(DPPZ)Pt\{DPPZ(11\text{-}11')DPPZ\}Pt(DPPZ)](CF_3SO_3)_4$: binding constants to calf thymus DNA

Due to the low solubility of the dimer in aqueous buffer, a small amount of DMSO was added to keep the complex in solution. $[(DPPZ)Pt\{DPPZ(11\text{-}11')DPPZ\}Pt(DPPZ)](CF_3SO_3)_4$ appears to remain stable in solution as seen for $[Pt(NH_3)_2DPPZ](CF_3SO_3)_2$ and $[Pt(en)DPPZ](CF_3SO_3)_2$. In the absence of calf thymus DNA, two maximum absorption wavelengths can be observed at 360 nm and 378 nm (figure 8). Upon addition of DNA, hypochromicity occurs as expected and a red shift of 3-4 nm is observed for both bands.

Considering these results, an estimated binding constant of 1.44 x 10^5 M^{-1} was obtained (figure 9). This binding constant is higher than those estimated previously for

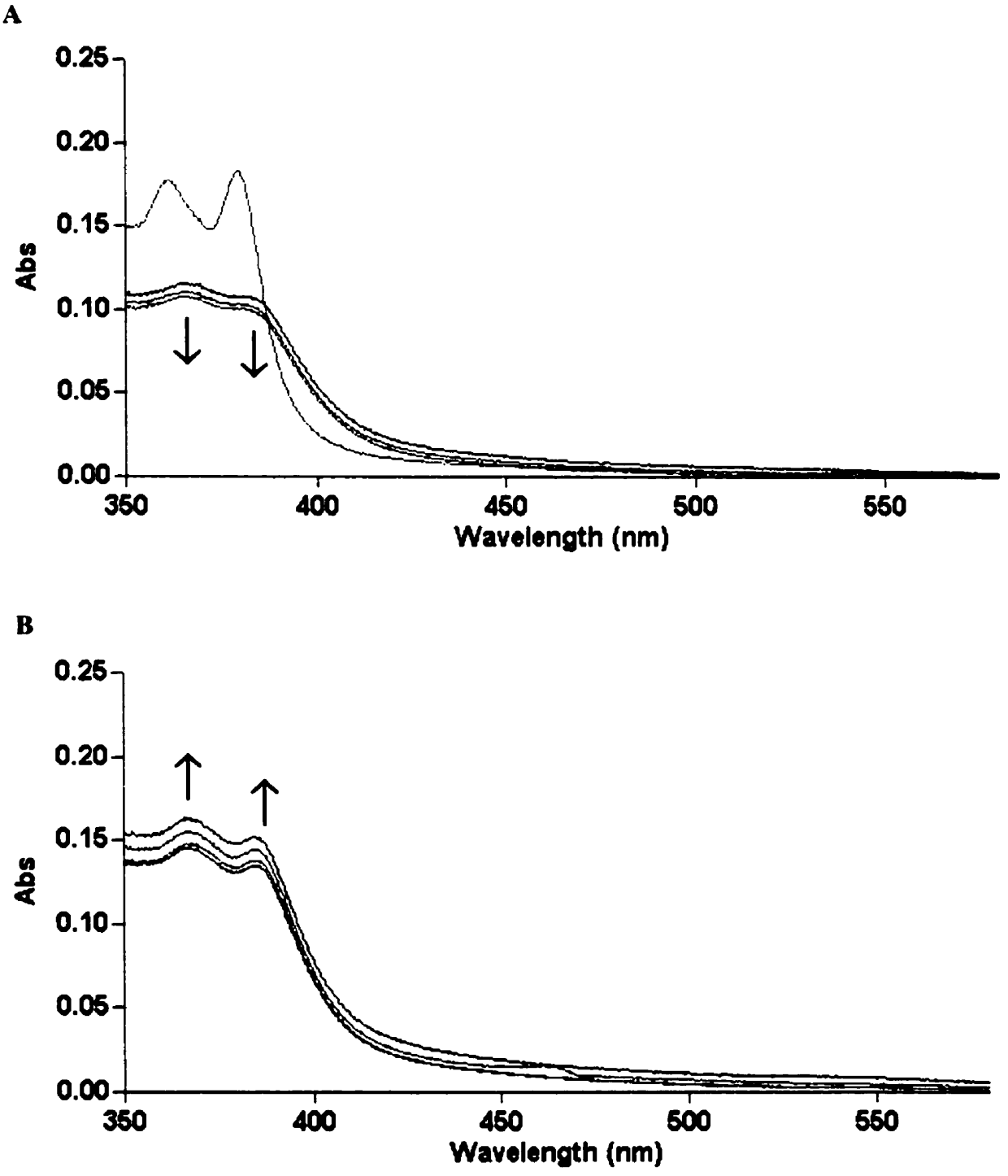

Figure 7: Absorption spectrum of $[Pt(NH_3)_2DPPZ](CF_3SO_3)_2$ in the presence of calf thymus DNA (1×10^{-3} M phosphate, 1×10^{-2} M NaCl, pH 7.0). (A) Mixing ratios [metal complex]/[DNA phosphate], from top to bottom: no DNA, 4.95, 4.90, 4.80. (B) Mixing ratios: 0.30, 0.65, 1.10, 1.25. Pt concentration was kept constant at 100 μM.

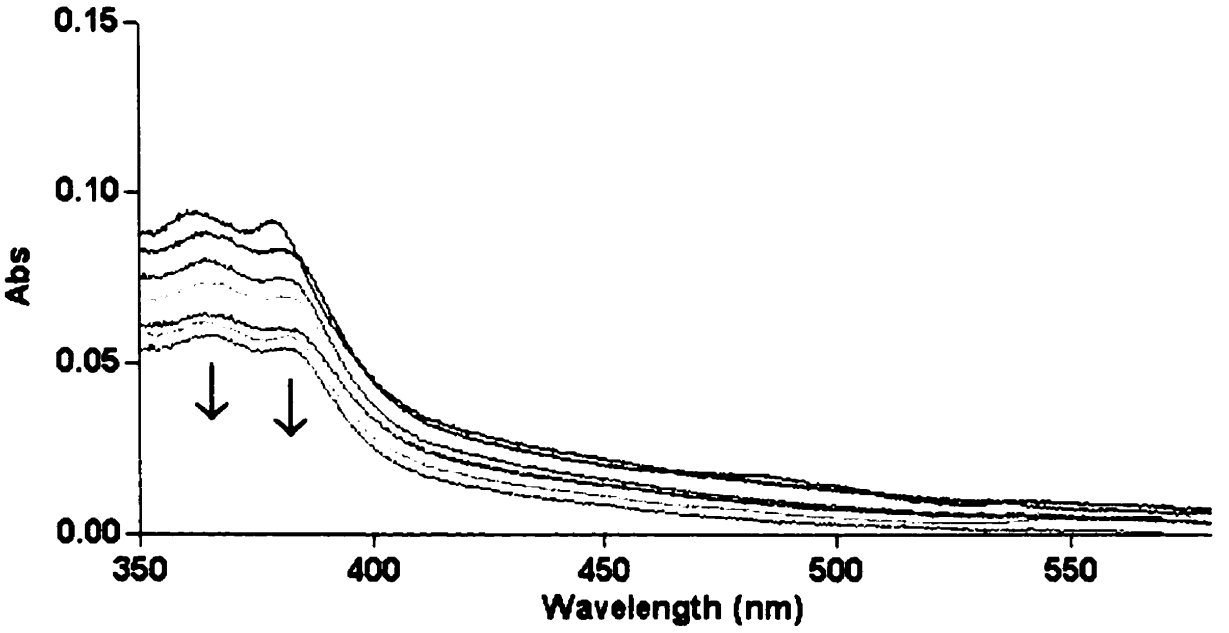

Figure 8: Absorption spectrum of [(DPPZ)Pt{DPPZ(11-11')DPPZ}Pt(DPPZ)]$(CF_3SO_3)_4$ in the presence of calf thymus DNA (1 x 10^{-3} M phosphate, 1 x 10^{-2} M NaCl, 2.4% DMSO, pH 7.0). Mixing ratios [metal complex]/[DNA phosphate], from top to bottom: no DNA, 5.00, 4.00, 3.00, 2.50, 2.00, 1.25. Pt concentration was kept constant at 200 μM.

$[Pt(NH_3)_2DPPZ](CF_3SO_3)_2$ and $[Pt(en)DPPZ](CF_3SO_3)_2$. This result was expected considering the two intercalative DPPZ ends. When comparing this affinity to the ethidium bromide dimer ~10^{11} M^{-1} binding constant,[85] a major difference is observed. However, it should be noted that ethidium bromide showed an higher affinity (10^5 M^{-1}) for calf thymus DNA than $[Pt(NH_3)_2DPPZ](CF_3SO_3)_2$ and $[Pt(en)DPPZ](CF_3SO_3)_2$ complexes. Thus, enhanced affinity should be observed for ethidium bromide bis-intercalator and this increase should be more pronounced than between platinum DPPZ complexes and [(DPPZ)Pt{DPPZ(11-11')DPPZ}Pt(DPPZ)]$(CF_3SO_3)_4$. Moreover,

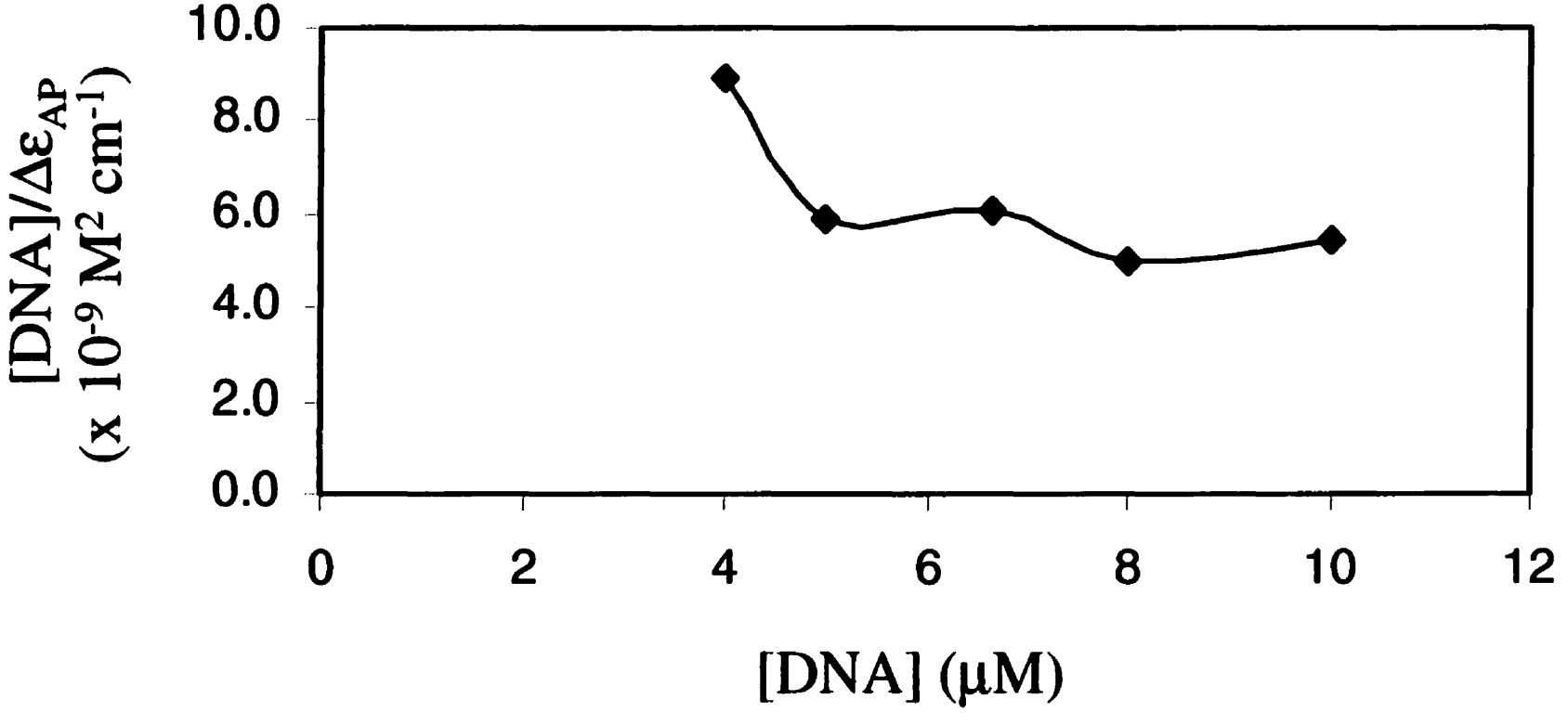

Figure 9: Absorption titration results of [(DPPZ)Pt{DPPZ(11-11')DPPZ}Pt(DPPZ)]$(CF_3SO_3)_4$ using equation 4 (page 7).

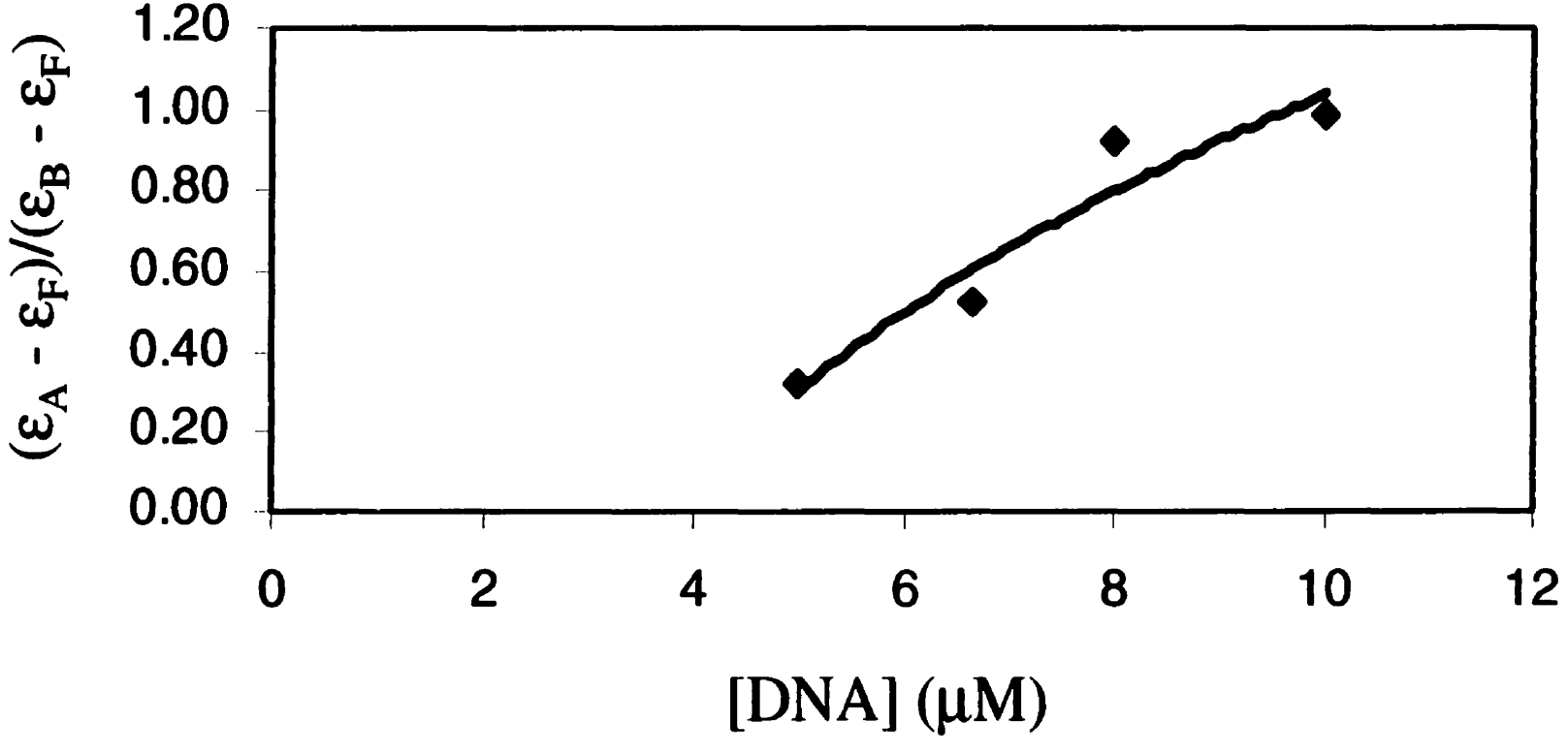

Figure 10: Fits of equation 6 (page 89) to absorption titration of [(DPPZ)Pt{DPPZ(11-11')DPPZ}Pt(DPPZ)]$(CF_3SO_3)_4$.

experimental conditions in this case were different due to the addition of DMSO. The medium is thus less hydrophilic and this could lead to a smaller affinity for intercalation of the platinum dimer. Therefore, a higher binding constant should be expected for this complex in a completely aqueous medium, if complete dissolution of the dimer were possible.

Once again, we did apply equation 6 to our results (figure 10). As seen previously, a higher binding constant of 2.58 x 10^7 M^{-1} was obtained with a binding site size of 0.27. Surprisingly, this binding constant is smaller than those observed for $[Pt(NH_3)_2DPPZ](CF_3SO_3)_2$ and $[Pt(en)DPPZ](CF_3SO_3)_2$. The explanation comes from the different experimental conditions as DMSO was added to solubilize the dimer as mentioned previously.

Conclusions

Transition-metal complexes have been extensively used to probe DNA and they tend to interact with the host molecule either via electrostatic interactions or by intercalation. Planar heteroaromatic ligands insert themselves between the DNA bases and have proved to block gene transcription and DNA replication. These small complexes thus become important as probes to study how genetic information is expressed.

Here have been presented the successful syntheses of five DPPZ complexes of platinum (II), and the attempted syntheses of $[Pt(en)phi](PF_6)_2$ and $[Pt(phen)phi](PF_6)_2$. The best synthetic strategy for DPPZ complexes involved the conversion of $K_2[PtCl_4]$ into $K_2[PtI_4]$, followed by substitution of two iodides by the appropriate ancillary ligand. Addition of $AgCF_3SO_3$ and subsequent reaction with DPPZ resulted in the expected $[Pt(NH_3)_2DPPZ](CF_3SO_3)_2$, $[Pt(en)DPPZ](CF_3SO_3)_2$, $[Pt(phen)DPPZ](CF_3SO_3)_2$, $[Pt(Me_2bpy)DPPZ](CF_3SO_3)_2$, and $[Pt(phendione)DPPZ](CF_3SO_3)_2$ complexes. Unfortunately, phi complexes were not obtained, probably because of the basic conditions used in the last synthetic step.

$[Pt(en)DPPZ](CF_3SO_3)_2$ has shown to be extremely easy to synthesize as it precipitated out of acetone and was soluble in water. $[Pt(NH_3)_2DPPZ](CF_3SO_3)_2$ was also soluble in water but showed an higher solubility in acetone than $[Pt(en)DPPZ](CF_3SO_3)_2$. $[Pt(phen)DPPZ](CF_3SO_3)_2$ and $[Pt(Me_2bpy)DPPZ](CF_3SO_3)_2$ were almost insoluble in water.

The binding constants to calf thymus DNA of $[Pt(NH_3)_2DPPZ](CF_3SO_3)_2$ and $[Pt(en)DPPZ](CF_3SO_3)_2$ were respectively estimated to be 2.58 x 10^4 M^{-1} and 1.18 x 10^4 M^{-1} by hypochromism. These two values do compare with other reported results for similar platinum complexes.

$[Pt(phendione)DPPZ](CF_3SO_3)_2$ was synthesized in the goal of forming $[(DPPZ)Pt\{DPPZ(11\text{-}11')DPPZ\}Pt(DPPZ)](CF_3SO_3)_4$. The synthetic strategy involved formation of a Schiff base by addition of one molar equivalent of 3,3'-diaminobenzidine to $[Pt(phendione)DPPZ](CF_3SO_3)_2$. The complex then obtained was mixed with one more molar equivalent of $[Pt(phendione)DPPZ](CF_3SO_3)_2$. The binding constant of this dimer was estimated to be 1.44 x 10^5 M^{-1}. This result is higher than the binding constants showed by the monomers due to the bis-intercalative DPPZ ends.

This research makes a new advance in the field of bis-intercalators as only one other metal-based bis-intercalating dimer has been reported. Knowing the success of this synthetic strategy, many other linkers can be designed with variable lengths and geometries. This will provide a greatly enhanced opportunity to study and influence close-packaged DNA.

References

1- Erkkila, K.E.; Odom, D.T.; Barton, J.K. *Chem. Rev.* **1999**, *99*, 2777-2795.

2- Rosenberg, B.; Van Camp, L.; Trosko, J.E.; Mansour, V.H. *Nature* **1969**, *222*, 385-386.

3- Rosenberg, B.; Van Camp, L. *Cancer Res.* **1970**, *30*, 1799-1802. Kociba, R.J.; Sleight, S.D.; Rosenberg, B. *Cancer Chemother. Rep.* **1970**, *54*, 325-328.

4- Jennette, K.W.; Lippard, S.J.; Vassiliades, G.A.; Bauer, W.R. *Proc. Natl. Acad. Sci. U.S.A.* **1974**, *71*, 3839-3843.

5- Long, E.C.; Barton, J.K. *Acc.Chem. Res.* **1990**, *23*, 273-279.

6- Dickeson, J.E.; Summers, L.A. *Aust. J. Chem.* **1970**, *23*, 1023-1027.

7- Belser, P.; von Zelewsky, A.; Zehnder, M. *Inorg. Chem.* **1981**, *20*, 3098-3103.

8- Lerman, L.S. *J. Mol. Biol.* **1961**, *3*, 18-30.

9- Barton, J.K. *Science* **1986**, *233*, 727-734.

10- Berman, H.M.; Young, P.R. *Annu. Rev. Biophys. Bioeng.* **1981**, *10*, 87-114.

11- Dougherty, G.; Pigram, W.J. *CRC Crit. Rev. Biochem.* **1982**, *12*, 103-132.

12- Waring, M. *J. Mol. Biol.* **1970**, *54*, 247-279.

13- Fisher, L.M.; Kuroda, R.; Sakai, T.T. *Biochemistry* **1985**, *24*, 3199-3207.

14- Lodish, H.; Baltimore, D.; Berk, A.; Zipursky, S.L.; Matsudaira, P.; Darnell, J. *Molecular Cell Biology*, 3rd ed.; Scientific American Books: New York, 1996.

15- Gao, X.; Patel, D.J. *Q. Rev. Biophys.* **1989**, *22*, 93-138. Patel, D.J. *Acc. Chem. Res.* **1979**, *12*, 118-125.

16- Norden, B.; Tjernald, F. *Biophys. Chem.* **1976**, *4*, 191-198.

17- Fritzsche, H.; Triebel, H.; Chaires, J.B.; Dattagupta, N.; Croters, D.M. *Biochemistry* **1982**, *21*, 3940-3946.

18- Kumar, C.V.; Barton, J.K.; Turro, N.J. *J. Am. Chem. Soc.* **1985**, *107*, 5518-5523.

19- Scatchard, G. *Ann. N.Y. Acad. Sci.* **1949**, *51*, 660-672.

20- McGhee, J.D.; von Hippel, P.H. *J. Mol. Biol.* **1974**, *86*, 469-489.

21- Wolfe, A.; Shimer, G.H.J.; Meehan, T. *Biochemistry* **1987**, *26*, 6392-6396.

22- Rosenberg, B.; Van Camp, L.; Krigas, T. *Nature* **1965**, *205*, 698-699.

23- Lippard, S.J. *Science* **1982**, *218*, 1075-1082.

24- Lippard, S.J. *Acc. Chem. Res.* **1978**, *11*, 211-217.

25- Bosl, G.J.; Motzer, R.J. *N. Engl. J. Med.* **1997**, *337*, 242-253.

26- Jamieson, E.R.; Lippard, S.J. *Chem. Rev.* **1999**, *99*, 2467-2498.

27- Hathway, D.E.; Kolar, G.F. *Chem. Soc. Rev.* **1980**, *9*, 241-264. Wing, R.M.; Pjura, P.; Drew, H.R.; Dickerson, R.E. *EMBO J.* **1984**, *3*, 1201-1206. Johnson, N.P.; Mazard, A.M.; Escalier, J.; Macquet, J.P. *J. Am. Chem. Soc.* **1985**, *107*, 6376-6380.

28- Eastman, A. *Biochemistry* **1985**, *24*, 5027-5032.

29- Fichtinger-Schepman, A.M.J.; Lohman, P.H.M.; Reedijk, J. *Nucl. Acids Res.* **1982**, *10*, 5345-5356.

30- Pasini, A.; Zunino, F. *Angew. Chem., Int. Ed. Engl.* **1987**, 26, *615-624.*

31- Bancroft, D.P.; Lepre, C.A.; Lippard, S.J. *J. Am. Chem. Soc.* **1990**, *112*, 6860-6871. Johnson, N.P.; Hoeschele, J.D.; Rahn, R.O. *Chem. Biol. Interact.* **1980**, *30*, 151-169. Barnham, K.J.; Berners-Price, S.J.; Krenkiel, T.A.; Frey, U.; Sadler, P.J. *Angew. Chem., Int. Ed. Engl.* **1995**, *34*, 1874-1877.

32- Fichtinger-Schepman, A.M.J.; van der Veer, J.L.; den Hartog, J.H.J.; Lohman, P.H.M.; Reedijk, J. *Biochemistry* **1985**, *24*, 707-713.

33- van der Veer, J.L.; van den Elst, H.; Reedijk, J. *Inorg. Chem.* **1987**, *26*, 1536-1540.

34- Miller, S.K.; Marzilli, L.G. *Inorg. Chem.* **1985**, *24*, 2124-2425.

35- Cohen, G.L.; Bauer, W.R.; Barton, J.K.; Lippard, S.J. *Science* **1979**, *203*, 1014-1016. Macquet, J.P.; Butour, J.L. *Biochimie* **1978**, *60*, 901-914. Scovell, W.M.; Kroos, L.R. *Biochem. Biophys. Res. Commun.* **1982**, *104*, 1597-1603.

36- Maeda, Y.; Nunomura, K.; Ohtsubo, E. *J. Mol. Biol.* **1990**, *215*, 321-329. Nunomura, K.; Maeda, Y.; Ohtsubo, E. *J. Gen. Appl. Microbiol.* **1991**, *37*, 207-214. Kagemoto, A.; Takagi, H.; Naruse, K.; Baba, Y. *Thermochim. Acta* **1991**, *190*, 191-201. Naser, L.J.; Pinto, A.L.; Lippard, S.J.; Essigmann, J.M. *Biochemistry* **1988**, *27*, 4357-4367.

37- Kozelka, J.; Petsko, G.A.; Lippard, S.J.; Quigley, G.J. *J. Am. Chem. Soc.* **1985**, *107*, 4079-4081.

38- Harder, H.C.; Smith, R.G. *Cancer Res.* **1976**, *36*, 3821-3829. Pinto, A.L.; Lippard, S.J. *Proc. Natl. Acad. Sci. U.S.A.* **1985**, *82*, 4616-4619. Ciccarelli, R.B.; Solomon, M.J.; Varshavsky, A.; Lippard, S.J. *Biochemistry* **1985**, *24*, 7533-7540.

39- Corda, Y.; Job, C.; Anin, M.F.; Leng, M.; Job, D. *Biochemistry* **1991**, *30*, 222-230. Corda, Y.; Anin, M.F.; Leng, M.; Job, D. *Biochemistry* **1992**, *31*, 1904-1908. Corda, Y.; Job, C.; Anin, M.F.; Leng, M.; Job, D. *Biochemistry* **1993**, *32*, 8582-8588.

40- Sorenson, C.M.; Eastman, A. *Cancer Res.* **1988**, *48*, 4484-4488. Sorenson, C.M.; Eastman, A. *Cancer Res.* **1988**, *48*, 6703-6707.

41- Wong, E.; Giandomenico, C.M. *Chem. Rev.* **1999**, *99*, 2451-2466.

42- Hayes, D.M.; Cvitkovic, E.; Golbey, R.B.; Scheiner, E.; Helson, L.; Krakoff, I.H. *Cancer* **1977**, *39*, 1372-1381.

43- Weiss, R.B.; Christian, M.C. *Drugs* **1993**, *46*, 360-377. Lebwohl, D.; Canetta, R. *Eur.J. Cancer* **1998**, *34*, 1522-1534.

44- Basch, H.; Krauss, M.; Stevens, W.J.; Cohen, D. *Inorg. Chem.* **1986**, *25*, 684-688. Sundquist, W.I.; Ahmed, K.J.; Hollis, L.S.; Lippard, S.J. *Inorg. Chem.* **1987**, *26*, 1524-1528.

45- Liu, M.Q.; Peng, S.M.; Che, C.M. *J.Chem Soc., Chem. Commun.* **1995**, 509-510.

46- Cusumano, M.; Giannetto, A. *J. Inorg. Biochem.* **1997**, *65*, 137-144.

47- Cusumano, M.; Pietro, M.L.; Giannetto, A.; Nicolo, F.; Rotondo, E. *Inorg. Chem.* **1998**, *37*, 563-568.

48- Cusumano, M.; Di Pietro, M.L.; Giannetto, A. *Inorg. Chem.* **1999**, *38*, 1754-1758.

49- Cusumano, M.; Di Pietro, M.L.; Giannetto, A.; Romano, F. *Inorg. Chem.* **2000**, *98*, 50-55.

50- Pyle, A.M.; Rehmann, J.P; Meshoyrer, R; Kumar, C.V.; Turro, N.J.; Barton, J.K. *J. Am. Chem. Soc.* **1989**, *111*, 3051-3058.

51- Chambron, J.C.; Sauvage, J.P.; Amouyal, E.; Koffi, P. *New J. Chem.* **1985**, *9*, 527-529.

52- Hartshorn, R.M.; Barton, J.K. *J. Am. Chem. Soc.* **1992**, *114*, 5919-5925.

53- Amouyal, E.; Homsi, A.; Chambron, J.C.; Sauvage, J.P. *J. Chem. Soc., Dalton Trans.* **1990**, 1841-1845.

54- Friedman, A.E.; Chambron, J.C.; Sauvage, J.P.; Turro, N.J.; Barton, J.K. *J. Am. Chem. Soc.* **1990**, *112*, 4960-4962.

55- Hiort, C.; Lincoln, P.; Norden, B. *J. Am. Chem. Soc.* **1993**, *115*, 3448-3454.

56- Haq, I.; Lincoln, P.; Suh, D.; Norden, B.; Chowdhry, B.Z.; Chaires, J.B. *J. Am. Chem. Soc.* **1995**, *115*, 4788-4796.

57- Dupureur, C.M.; Barton, J.K. *Inorg. Chem.* **1997**, *36*, 33-43.

58- Friedman, A.E.; Kumar, C.V.; Turro, N.J.; Barton, J.K. *Nucl. Acids Res.* **1991**, *19*, 2595-2602. Norden, B.; Tjerneld, F. *FEBS Lett.* **1976**, *67*, 368-370. Barton, J.K.; Goldberg, J.M.; Kumar, C.V.; Turro, N.J. *J. Am. Chem. Soc.* **1986**, *108*, 2081-2088. Satyanarayana, S.; Dabrowiak, J.C.; Chaires, J.B. *Biochemistry* **1992**, *31*, 9319-9324. Hiort, C.; Norden, B.; Rodger, A.. *J. Am. Chem. Soc.* **1990**, *112*, 1971-1982. Eriksson, M.; Leijon, M.; Hiort, C.; Norden, B.; Graslund, A. *J. Am. Chem. Soc.* **1992**, *114*, 4933-4934.

59- Chambron, J.C.; Sauvage, J.P. *Chem. Phys. Lett.* **1991**, *182*, 603-607.

60- Holmlin, R.E.; Stemp, E.D.A.; Barton, J.K. *Inorg. Chem.* **1998**, *37*, 29-34.

61- Jenkins, Y.; Barton, J.K. *J. Am. Chem. Soc.* **1992**, *114*, 8736-8738.

62- Dupureur, C.M.; Barton, J.K. *J. Am. Chem. Soc.* **1994**, *116*, 10286-10287.

63- Tuite, E.; Lincoln, P.; Norden, B. *J. Am. Chem. Soc.* **1997**, *119*, 239-240.

64- Nair, R.B.; Teng, E.S.; Kirkland, S.L.; Murphy, C.J. *Inorg. Chem.* **1998**, *37*, 139-141.

65- Che, C.M.; Yang, M.; Wong, K.H.; Chen, H.L.; Lam, W. *Chem. Eur. J.* **1999**, *5*, 3350-3356.

66- Arounaguiri, A.; Maiya, B.G. *Inorg. Chem.* **1999**, *38*, 842-843. Arounaguiry, A.; Maiya, B.G. *Inorg. Chem.* **2000**, *39*, 4256-4263. Arounaguiry, A.; Maiya, B.G. *Inorg. Chem.* **2000**, *39*, 4264-4272.

67- Collins, J.G.; Sleeman, A.D.; Aldrich-Wright, J.R.; Greguric, I.; Hambley, T.W. *Inorg. Chem.* **1998**, *37*, 3133-3141.

68- Moucheron, C.; Kirsch-De Mesmaeker, A.; Choua, S. *Inorg. Chem.* **1997**, *36*, 584-592. Campagna, S.; Serroni, S.; Bodige, S.; MacDonnell, F.M. *Inorg. Chem.* **1999**, *38*, 692-701.

69- Holmlin, R.E.; Yao, J.A.; Barton, J.K. *Inorg. Chem.* **1999**, *38*, 174-189.

70- Ghosh, P.K.; Bard, A.J. *J. Phys. Chem.* **1984** *88*, 5519-5526. Krenske, D.; Abdo, S.; Van Damme, H.; Cruz, M.; Fripiat, J.J. *J. Phys. Chem.* **1980**, *84*, 2447-2457.

71- Pyle, A.M.; Barton, J.K. *Inorg. Chem.* **1987**, *26*, 3820-3823.

72- Pyle, A.M.; Long, E.C.; Barton, J.K. *J. Am. Chem.Soc.* **1989**, *111*, 3051-3058.

73- Pyle, A.M.; Chiang, M.Y.; Barton, J.K. *Inorg. Chem.* **1990**, *29*, 4487-4495.

74- Sitlani, A.; Long, E.C.; Pyle, A.M.; Barton, J.K. *J. Am. Chem. Soc.* **1992**, *114*, 2303-2312.

75- Pyle, A.M.; Long, E.C.; Barton, J.K. *J. Am. Chem. Soc.* **1989**, *111*, 4520-4522.

76- Chow, C.S.; Barton, J.K. *J. Am. Chem. Soc.* **1990**, *112*, 2839-2841.

77- Hudson, B.P.; Dupureur, C.M.; Barton, J.K. *J. Am. Chem. Soc.* **1995**, *117*, 9379-9380.

78- Hudson, B.P.; Barton, J.K. *J. Am. Chem. Soc.* **1998**, *120*, 6877-6888.

79- Terbrueggen, R.H.; Johann, T.W.; Barton, J.K. *Inorg. Chem.* **1998**, *37*, 6874-6883.

80- Pabo, C.O.; Sauer, R.T. *Annu. Rev. Biochem.* **1992**, *61*, 1053-1095. Pavletich, N.L.; Pabo, C.O. *Science* **1991**, *252*, 809-817.

81- Jackson, B.A.; Barton, J.K. *J. Am. Chem. Soc.* **1997**, *119*, 12986-12987.

82- Onfelt, B.; Lincoln, P.; Norden, B. *J. Am. Chem. Soc.* **1999**, *121*, 10846-10847.

83- Huang, C.H.; Mirabelli, C.K.; Mong, S.; Crooke, S.T. *Cancer Res.* **1983**, *43*, 2718-2724.

84- Carlsson, C.; Jonsson, M.; Akerman, B. *Nucl. Acids Res.* **1995**, *23*, 2413-2420.

85- Becker, M.M.; Dervan, P.B. *J. Am. Chem. Soc.* **1979**, *101*, 3664-3666.

86- Annan, N.K.; Cook, P.R.; Mullins, S.T.; Lowe, G. *Nucl. Acids Res.* **1992**, *20*, 983-990.

87- Peek, M.E.; Lipscomb, L.A.; Bertrand, J.A.; Gao, Q.; Roques, B.P.; Garbay-Aureguiberry, C.; Williams, L.D. *Biochemistry* **1994**, *33*, 3794-3800.

88- Jacobsen, J.P.; Pedersen, J.B.; Hansen, L.F.; Wemmer, D.E. *Nucl. Acids Res.* **1995**, *23*, 753-760. Spielmann, H.P.; Wemmer, D.E.; Jacobsen, J.P. *Biochemistry* **1995**, *34*, 8542-8553. Hansen, L.F.; Jensen, L.K.; Jacobsen, J.P. *Nucl. Acids Res.* **1996**, *24*, 859-867. Petersen, M.; Hamed, A.A.; Pedersen, E.B.; Jacobsen, J.P. *Bioconj. Chem.* **1999**, *10*, 66-74.

89- Winter, S.; Lober, G. *J. Biomed. Opt.* **1997**, *2*, 125-130.

90- Stellwagen, N. *Biopolymers* **1985**, *24*, 2243-2255. Nielsen, P.E.; Zhen, W.; Henriksen, U.; Buchardt, O. *Biochemistry* **1988**, *27*, 67-73. Crater, G.D.; Gregg, M.R.; Holzwarth, G. *Nucl. Acids Res.* **1989**, *10*, 310-315. Reese, H.R. *Biopolymers* **1994**, *34*, 1349-1358.

91- Crothers, D.M. *Biopolymers* **1968**, *6*, 575-584.

92- Bolger, J.; Gourdon, A.; Ishow, E.; Launay, J.P. *J. Chem. Soc., Chem, Commun.* **1995**, 1799-1800.

93- Warnmark, K.; Thomas, J.A.; Heyke, O.; Lehn, J.M. *Chem Commun.* **1996**, 701-702.

94- Warnmark, K.; Heyke, O.; Thomas, J.A.; Lehn, J.M. *Chem Commun.* **1996**, 2603-2604.

95- Lowe, G.; Droz, A.S.; Park, J.J.; Weaver, G.W. *Bioorg. Chem.* **1999**, *27*, 477-486.

96- Lincoln, P.; Norden, B. *Chem. Commun.* **1996**, 2145-2146.

97- Paw, W.; Eisenberg, R. *Inorg. Chem.* **1997**, *36*, 2287-2293.

98- Kauffman, G.B.; Cowan, D.O. *Inorg. Synth.* **1963**, *7*, 239-245.

99- Basolo, F.; Bailar, J.C.J.; Tarr, B.R. *J. Am. Chem. Soc.* **1950**, *72*, 2433-2438.

100- Morgan, G.T.; Burstall, F.H. *J. Chem. Soc.* **1934**, 965-971.

101- Bielli, E.; Gidney, P.M.; Gillard, R.D.; Heaton, B.T. *J. Chem. Soc., Dalton Trans.* **1974**, 2133-2139.

102- Coyer, M.J.; Herber, R.H. *Inorg. Chim. Acta* **1990**, *175*, 47-55.

103- Peerey, L.M.; Kostic, N.M. *Inorg. Chem.* **1987**, *26*, 2079-2083.

104- Diver, C.; Lawrance, G.A. *J. Chem. Soc., Dalton Trans.* **1988**, 931-934.

105- Dhara, S.C. *Ind. J. Chem.* **1970**, *8*, 193-194.

106- Hollis, L.S.; Stern, E.W.; Amunsden, A.R.; Miller, A.V.; Doran, S.L. *J. Am. Soc. Chem.* **1987**, *109*, 3596-3602.

107- Kratochwil, N.A.; Zabel, M.; Range, K.J.; Bednarski, P.J. *J. Med. Chem.* **1996**, *39*, 2499-2507.

108- Cerasino, L.; Williams, K.M.; Intini, F.P.; Cini, R.; Marzilli, L.G.; Natile, G. *Inorg. Chem.* **1997**, *36*, 6070-6079.

109- Hartley, F.R.; Murray, S.G.; McAuliffe, C.A. *Inorg. Chem.* **1979**, *18*, 1394-1397.

110- Kukushkin, Y.N.; Dhara, S.C. *Ind. J. Chem.* **1970**, *8*, 184-185.

111- Murner, H.; Jackson, B.A.; Barton, J.K. *Inorg. Chem.* **1998**, *37*, 3007-3012.

112- Arents, G.; Moudrianakis, E.N. *Proc. Natl. Acad. Sci. U.S.A.* **1993**, *90*, 10489-10493.

113- Davison, B.L.; Egly, J.M.; Mulvihill, E.R.; Chambon, P. Nature **1983**, *301*, 680-686. Parker, C.S.; Topol, J. *Cell* **1984**, *36*, 357-369. Sawadogo, M.; Roeder, R.G. *Cell* **1985**, *43*, 165-175. Berk, A.J.; Boyer, T.G.; Kapanidis, A.N.; Ebright, R.H.; Kobayashi, N.N.; Horn, P.J.; Sullivan, S.M.; Koop, R.; Surby, M.A.; Triezenberg, S.J. *Cold Spring Harbor Symp. Quant. Biol.* **1998**, *63*, 243-252.

114- Reinberg, D.; Orphanides, G.; Ebright, R.; Akoulitchev, S.; Carcamo, J.; Cho, H.; Cortes, P.; Drapkin, R.; Flores, O.; Ha, I.; Inostroza, J.A.; Kim, S.; Kim, T.K.; Kumar, P.; Lagrange, T.; LeRoy, G.; Lu, H.; Ma, D.M.; Maldonado, E.; Merino, A.; Mermelstein, F.; Olave, I.; Sheldon, M.; Shiekhattar, R.; Stone, N.; Sun, X.; Weis, L.; Yeung, K, Zawei, L. *Cold Spring Harbor Symp. Quant. Biol.* **1998**, *63*, 83-103.

115- Ebright, E. *Cold Spring Harbor Symp. Quant. Biol.* **1998**, *63*, 11-20. Oleknovich, I.N.; Kadner, R.J. *J. Bacteriol.* **1999**, *181*, 7266-7273.

116- Horton, R.H.; Moran, L.A.; Ochs, R.S.; Rawn, J.D.; Scrimgeour, K.G. *Principe de Biochimie*; DeBoeck Université, Brussels, 1994.

117- Kato, M.; Kosuge, C.; Yano, S.; Kimura, M. *Acta Crystallogr. Sect. C* **1998**, *54*, 621-623.

118- Walton, R.A. *Spectrochim. Acta* **1965**, *21*, 1795-1801.

119- Little, W.A.; Lorentz, R. *Inorg. Chim. Acta* **1976**, *18*, 273-278. Erickson, L.E. *J. Am. Chem. Soc.* **1969**, *91*, 6284-6290. Erickson, L.E.; Sarneski, J.E.; Reilley, C.N. *Inorg. Chem.* **1975**, *14*, 3007-3017.

120- Wells, R.D.; Larson, J.E.; Grant, R.C.; Shortle, B.E.; Cantor, C.R. *J. Mol. Biol.* **1970**, *54*, 465-497.

121- Miskowski, V.M.; Houlding, V.H.; Che, C.M.; Wang, Y. *Inorg. Chem.* **1993**, *32*, 2518-2524.

122- Girgis, A.Y.; Sohn, Y.S.; Balch, A.L. *Inorg. Chem.* **1975**, *14*, 2327-2331.

123- Smith, G.F.; Cagle, F.W.J. *J. Org. Chem.* **1947**, *12*, 781-784.

124- Vollhardt, K.P.C.; Schore, N.E. *Traité de Chimie Organique*, 2nd ed.; DeBoeck Université: Brussels, 1995.

125- Hanazaki, I.; Nagakura, S. *Inorg. Chem.* **1969**, *8*, 648-654.

126- Kaim, W. *J. Am. Chem. Soc.* **1982**, *104*, 3833-3837.

127- Nyquist, E.B.; Jouille, M.M. *J. Heterocycl. Chem.* **1967**, *4*, 539-545.

128- Schlosser, K.; Hower, E.Z. *Anorg. Allg. Chem.* **1972**, *387*, 91-106.

129- March, J. *Advanced Organic Chemistry*, 4th ed.; John Wiley & Sons: New York, 1992.

130- Collman, J.P.; Hegedus, L.S.; Norton, J.R.; Finke, R.G. *Principles and Applications of Organotransition Metal Chemistry*; University Science Books, Mill Valley, 1987.

131- Smith, S.R.; Neyhart, G.A.; Kalsbeck, W.A.; Thorp, H.H. *New J. Chem.* **1994**, *18*, 397-406. Carter, M.T.; Rodrigues, M.; Bard, A.J. *J. Am. Chem. Soc.* **1989**, *111*, 8901-8911.

132- LePecq, J.B.; Paoletti, C. *J. Mol. Biol.* **1967**, *27*, 87-106.